

Hydraulic Resistance due to Emergent Wetland Vegetation

Candice Dawn Piercy

Dissertation submitted to the faculty of the Virginia Polytechnic Institute and State University in
partial fulfillment of the requirements for the degree of

Doctor of Philosophy

In

Biological Systems Engineering

Theresa Wynn

Brian Benham

W. Lee Daniels

Panos Diplas

W. Cully Hession

March 26, 2010

Blacksburg, Virginia

Keywords: wetlands, vegetated flow, hydraulic resistance, vegetation, modeling

Copyright 2010 by Candice D. Piercy unless otherwise stated

Hydraulic Resistance due to Emergent Wetland Vegetation

Candice D. Piercy

Abstract

Models to estimate hydraulic resistance due to vegetation in emergent wetlands are crucial to wetland design and management. Hydraulic models that consider vegetation rely on an accurate determination of a resistance parameter such as a friction factor or a bulk drag coefficient. At low Reynolds numbers typical of flows in wetlands, hydraulic resistance is orders of magnitude higher than fully turbulent flows and resistance parameters are functions of the flow regime as well as the vegetation density and structure. The exact relationship between hydraulic resistance, flow regime and vegetation properties at low-Reynolds number flows is unclear. The project goal was to improve modeling of emergent wetlands by linking vegetation and flow properties to hydraulic resistance. A 12.2-m x 1.2 m vegetated flume was constructed to evaluate seven models of vegetated hydraulic resistance through woolgrass (*Scirpus cyperinus* (L.) Kunth), a common native emergent wetland plant. Measurements of vegetation geometry and structure were collected after each set of flume runs. Study results showed at low stem-Reynolds numbers (<100), the drag coefficient is inversely proportional to the Reynolds number and can vary greatly with flow conditions. Empirical models that were developed from data collected in natural wetlands predicted flow velocity most accurately. Using data from this flume study, regression models were developed to predict hydraulic resistance. Results indicated stem Reynolds number, stem diameter, and vegetation area per unit volume were the best predictors of friction factor. Vegetation flexibility and water depth were also important parameters but to a lesser extent. The spatial distribution of hydraulic resistance was estimated in a small floodplain wetland near Stephens City, VA using the regression models developed from the flume data. MODFLOW was used to simulate a 4-hour flood event through the wetland. The vegetated open water surface was modeled as a highly conductive aquifer layer. On average, MODFLOW slightly underpredicted the water surface elevation. However, the model error was within the range of survey error. MODFLOW was not highly sensitive to small changes in the estimated surface hydraulic conductivity caused by small changes in vegetation properties, but large decreases in surface hydraulic conductivity dramatically raised the elevation of the water surface.

Funding Acknowledgements

Funding for this research was provided by a Society of Wetland Scientists Student Research Grant, the Piedmont Wetlands Research Program, administered by Wetland Studies and Solutions, Inc. and the Peterson Family Foundation, and the Chesapeake Bay Targeted Watershed Grants Program administered by the National Fish and Wildlife Foundation in cooperation with the Chesapeake Bay Program and the CSREES Mid-Atlantic Regional Water Quality Project.

dedicated to my parents: who always told me I could be whatever I wanted to be

Acknowledgments

I would like to thank my advisor Tess Wynn for all her help the last seven years, helping me transition from undergraduate researcher to graduate student and (hopefully) into the postgraduate world. I would also like to thank my committee: Brian Benham, Lee Daniels, Panos Diplas, and Cully Hession.

I am indebted to Laura Teany for all of her help with every aspect of data collection. She's been there to lend a helpful hand with everything from flume construction, to flume measurements to fixing the obstinate pump whenever it decided to stop working. I'd like to thank my awesome field help, Andrew Frock and Aaron Bowman, as well all of the graduate students who came out to help move plants or help me collect data.

I'd really like to thank Andrea Ludwig for letting me participate in collecting data during the epic AOE's at the Hedgebrook Farm wetland and for sharing her dissertation data with me so I could finally achieve a working model. A special thanks goes to everyone who helped out before, during, and after the AOE's: Jim Lawrence, Laura Teany, Heather Knepe, Mike Nassry, Jonathan Resop, and Durelle Scott.

I also want to thank my cheerleading section: Leslie Hopkinson, Barb Utley, Danielle Gift, and Cami Charonko. A special thanks goes to Jess Kozarek for always being there with a sympathetic ear and sometimes a cookie exactly when I needed it. Another special thanks also goes to Paul Anderson who always was there with a swift kick in the butt precisely when I needed some motivation. And finally, thanks to my best friend, Buckley, because sometimes no amount of advice or encouragement can match a wagging tail and a kiss on the nose.

Table of Contents

List of Figures	x
List of Tables	xii
Notation.....	xiii
Chapter 1 Introduction	1
1.1 Introduction.....	1
1.2 Goals and Objectives	3
1.3 Overall Study Design.....	4
Chapter 2 Literature Review.....	5
2.1 What are wetlands?.....	5
2.2 Wetland values.....	6
2.3 Wetland loss.....	7
2.4 Wetland legislation	8
2.5 Wetland restoration, enhancement, and creation	9
2.6 Wetland hydrology.....	10
2.7 Hydraulic resistance due to vegetation	12
2.8 Predicting hydraulic resistance due to vegetation.....	15
2.8.1 Vegetative drag	18
2.8.1-1 Measuring drag coefficient.....	24
2.8.1-2 Drag coefficient and friction factor	25
2.8.2 Vegetative parameters that affect hydraulic resistance.....	26
2.9 Modeling wetland hydrology	31
Chapter 3 Flume methods	35
Chapter 4 Vegetation-induced roughness in low-Reynolds number flows	39

4.1 Introduction.....	39
4.2 Methods.....	39
4.2.1 Flume Methods	39
4.2.2 Data Analysis.....	40
4.3 Results.....	41
4.3.1 General Results	41
4.3.2 Model Fit.....	43
4.3.3 Relative Error Analysis.....	46
4.4 Discussion.....	54
4.4.1 Fit of individual models.....	54
4.4.2 Overall trends in model fit.....	56
4.5 Conclusions.....	59
Chapter 5 The relationship between friction factor and vegetation properties in emergent vegetated flows	61
5.1 Introduction.....	61
5.2 Methods.....	62
5.2.1 Flume methods.....	62
5.2.2 Regression techniques.....	62
5.2.3 Regression Validation.....	64
5.3 Results and discussion	64
5.3.1 Robust regression.....	65
5.3.1-1 maa Regressions	65
5.3.1-2 maa regressions with tailgate indicator variables.....	68
5.3.1-3 A_f Regressions	71
5.3.1-4 Regression coefficient sensitivity.....	74

5.3.1-5 Comparing regression coefficients	76
5.3.2 Validation.....	77
5.3.2-1 Validation results	77
5.3.2-2 Model lack of fit	81
5.4 Conclusions.....	82
Chapter 6 Modeling surface water flow through emergent vegetation in a small floodplain wetland.....	84
6.1 Introduction.....	84
6.2 Application of MODFLOW to surface-flow systems.....	85
6.3 Methods.....	87
6.3.1 Site Description.....	87
6.3.2 Field methods.....	89
6.3.3 Modeling	91
6.4 Results.....	92
6.4.1 Measured results	92
6.4.2 Modeling results.....	94
6.4.3 Model sensitivity analysis.....	98
6.4.3-1 MODFLOW sensitivity	98
6.4.3-2 K-prediction sensitivity	100
6.5 Discussion.....	101
6.6 Conclusions.....	103
Chapter 7 Summary and Conclusions.....	104
7.1 Objective 1: Identify, fit, and assess the usefulness of existing models applicable to low-Reynolds number flows	104
7.2 Objective 2: Determine the relationship between friction factor and measurable properties of natural vegetation	105

7.3 Objective 3: Model wetland surface water flow through a small constructed wetland	107
7.4 Study implications	108
7.5 Limitations and future work.....	109
Chapter 8 References	111
Appendix A1: Flume data.....	119
Appendix A2: AOE May Event Data	123
Appendix A3: MODFLOW Iteration ArcGIS Toolbox Script.....	125

List of Figures

Figure 3.1 Flume experimental setup.....	35
Figure 3.2 Point gage measurements of the flume water depth and water surface.....	36
Figure 3.3 Diagram describing photo imaging technique for measuring streamwise frontal area of vegetation.....	37
Figure 4.1 Boxplots of measured hydraulic grade slope (S_g), friction slope (S_f), cross-sectionally averaged velocity (V), stem Reynolds number (Re_{stem}), and depth (h) by tailgate height (n=43).....	42
Figure 4.2 Goodness of fit statistics for the six best-performing models. Models include a drag coefficient predictor and a flow model.	45
Figure 4.3 Relative error plots for the six best-performing models.....	48
Figure 4.4 Interaction between relative error and average stem diameter.....	51
Figure 4.5 Interaction between relative error and blockage factor.	53
Figure 4.6 Interaction between relative error and MEI	54
Figure 4.7 Drag coefficient versus Re_{stem} for the <i>Harvey et al.</i> [2009] drag coefficient prediction relationship (HR).	56
Figure 4.8 Model relative error by tailgate height.....	58
Figure 5.1 Relative error distribution for regressions a. 2M, b. 3Ma, c. 3Mb, and d. 4M shaded by tailgate height.....	67
Figure 5.2 Relative error distribution for regressions a. 2MI, b. 3MIa, and c. 3MIb shaded by tailgate height.....	68
Figure 5.3 Relative error distribution for regressions a. 2F, b. 2FIa, and c. 2FIb shaded by tailgate height.....	73
Figure 5.4 Regression 2M model fit using data collected by <i>Harvey et al.</i> [2009] for ridge conditions.....	75
Figure 5.5 Regression 2M model fit using data collected by <i>Harvey et al.</i> [2009] for ridge conditions.....	75
Figure 5.6 Regression 2M model residuals and relative error using data collected by <i>Harvey et al.</i> [2009] for ridge conditions.	78

Figure 5.7 Regression 2M model relative error over time using data collected by <i>Harvey et al.</i> [2009] for ridge conditions.	79
Figure 6.1 Regional location of the Opequon Creek watershed and the Hedgebrook Farm wetland site.	88
Figure 6.2 Map of Hedgebrook Farm wetland site topography piezometer nest locations, staff gage transects, and subsurface hydraulic conductivity.	89
Figure 6.3 Measured water surface slope a. interpolated using triangulated irregular network (TIN) interpolation and b. trend surface analysis.	93
Figure 6.4 Hedgebrook Farm spatial distribution of vegetation.	95
Figure 6.5 MODFLOW error a. absolute error, b. error scaled by elevation drop from the inlet to the outlet, and c. error scaled by water depth.	96
Figure 6.6 Predicted, measured, triangulated irregular network (TIN), and trend surface (TS) water surface at the five measurement transects.	98

List of Tables

Table 2.1. Area coefficient definitions for drag coefficient models.	21
Table 2.2 Summary of drag coefficient predictors.	23
Table 2.3 Summary of bulk drag coefficient predictors.	24
Table 2.4 Vegetation parameters relevant to predict hydraulic resistance from vegetation.....	27
Table 2.5 Comparison of wetland water budget model components.....	34
Table 4.1 Summary of significant relative error interactions for the six best-performing models by tailgate height.....	49
Table 5.1 Summary of regression models for emergent vegetated flows using the area coefficient based on the unit momentum absorbing area (<i>maa</i>).	65
Table 5.2 Summary of regression models for emergent vegetated flows using the area coefficient based on the unit momentum absorbing area (<i>maa</i>) with the addition of a tailgate height indicator variable for the 0.2-m tailgate height.....	70
Table 5.3 Comparison of mean relative error between unit momentum absorbing area (<i>maa</i>) regression models with and without tailgate height indicator variables.	71
Table 5.4 Summary of regression models for emergent vegetated flows using the area coefficient based on the vegetation frontal area per unit volume (A_f) with and without the addition of a tailgate height indicator variable for the 0.2-m tailgate height.	72
Table 6.1 MODFLOW sensitivity to changes in the surface hydraulic conductivity (K).	100
Table 6.2 Sensitivity of surface hydraulic conductivity (K) to changes in vegetation properties and the estimated velocity.....	101
Table A1. 1 Summary of flume flow data.	119
Table A1. 2 Summary of flume vegetation data.....	120
Table A1. 3 Derived parameters from flume data	121
Table A2. 1 May 20, 2009 Artificial Overbank Event (AOE) steady-state water depths	123
Table A2. 2 Hedgebrook Farm wetland vegetation data by community	124
Table A2. 3 Hedgebrook Farm wetland vegetal area coefficient by community	124

Notation

a	projected streamwise plant area per unit volume as defined by <i>Nepf</i> [1999] (L^2/L^3)
a_g	vegetation density – ratio between the plant diameter and the horizontal area of influence of each plant (L^{-1})
a_x	longitudinal stem spacing (L)
a_y	lateral stem spacing (L)
A	Manning constant for units (1.49 for English units, 1 for metric)
A_d	cross-sectional area of porous media (L^2)
A_s	bed area covered by stems (L^2)
A_f	frontal area – measured projected plant area per unit volume (L^{-1})
A_r	reference area – the characteristic area of a drag coefficient (L^2)
A_s'	area of bed occupied by stems (L^2)
A_u	unit bed area (L^2)
A_x	cross-sectional flow area (L^2)
b	cross-sectional width (L)
BF	blockage factor – proportion of the flow area blocked by vegetation
BH	board height above the ground (L)
C_d	drag coefficient
C_d'	bulk drag coefficient (L^{-1})
$C_{d\infty}$	drag coefficient of a single cylinder in an ideal 2-D flow
d	stem diameter (L)
d_4	stem diameter measured at a height $z_v/4$ above the ground (L)
dh/dl	hydraulic head gradient (L/L)
E	modulus of elasticity ($M/L-T^2$)
ET	evapotranspiration (L^3/T)

f	friction factor
F_{45}	force required to bend vegetation to 45° (M·L/T ²)
h	water depth (L)
G	<i>Turner and Chanmeesri</i> [1984] coefficient of roughness
g	acceleration due to gravity (L/T ²)
G_i	groundwater inflow (L ³ /T)
G_o	groundwater outflow (L ³ /T)
I	2 nd area moment of inertia (L ⁴)
K	hydraulic conductivity (L/T)
K_a	<i>Kadlec</i> [1990] premultiplier parameter
m	<i>Turner and Chanmeesri</i> [1984] depth coefficient
MAA	momentum absorbing area – one-sided plant area of vegetation (L ²)
maa	unit momentum absorbing area – MAA per unit volume (L ⁻¹)
MEI	flexural rigidity (M·L ³ /T ²)
N	number of stems per unit bed area
n	Manning's coefficient – Manning's roughness parameter
p	fluid pressure (M/L·T ²)
P_n	net precipitation (L ³ /T)
q	flowrate (L ³ /T)
Q/W	volumetric flow per unit width (L ³ /L·T)
R	hydraulic radius (L)
Re_{stem}	stem Reynolds number
Re_{depth}	depth Reynolds number
S	unspecified slope (L/L)

S_b	bed slope (L/L)
S_f	friction slope – slope attributed to shear (L/L)
S_g	hydraulic grade slope (L/L)
S_i	surface inflow (L ³ /T)
S_o	surface outflow (L ³ /T)
S_w	water surface slope (L/L)
Δs	average stem spacing (L)
T	tidal inflow or outflow (L ³ /T)
u'	instantaneous velocity in the streamwise direction (L/T)
$ u $	average streamwise velocity (L/T)
v'	instantaneous velocity in the spanwise direction (L/T)
V	cross-sectionally averaged velocity (L/T)
v	velocity per unit cross-sectional area (L/T)
$\Delta V/\Delta t$	change in wetland water storage volume per unit time (L ³ /T)
x	streamwise distance (L)
z_b	elevation of the bed (L)
z_v	elevation of top of stems relative to the bed (L)
α	<i>Kadlec</i> [1990] slope exponent
β	<i>Kadlec</i> [1990] depth exponent
λ	area coefficient – streamwise projected plant area per volume (L ⁻¹)
ε	flow porosity – volume of void space per unit volume (L ³ /L ³)
ρ	density of fluid (M/L ³)
θ	angle of shear plane
τ	shear stress (M/L·T ²)

μ

fluid viscosity (M/L·T)

Chapter 1 Introduction

1.1 Introduction

Wetlands are historically hard to define; over 50 definitions exist globally [Dugan, 1993]. Some common terms for wetlands throughout the world are swamp, slough, marsh, bog, billabong, fen, mire, and moor [Mitsch and Gosselink, 2000]. Though there are many types of wetlands, they do provide similar functions that are environmentally and socio-economically valuable. Wetlands make up between 4 to 6 percent of the earth's land area [Mitsch and Gosselink, 2000]. However, they play a vital role, providing habitat, fish and shellfish production, water storage, erosion control, and improved water quality.

Despite the value of wetlands, large portions of wetland areas have been lost worldwide. The loss has not been well documented but some researchers estimate that over 50% of the world's original wetland area has been lost [Dugan, 1993]. Between the mid-1780s and the mid-1980s, the U.S. lost 53% of the original wetland acreage [Dahl, 1990].

Wetland restoration, enhancement, and creation has become of interest in past years to help recover environmental and socio-economic values lost due to wetland loss and degradation [Mitsch and Gosselink, 2000]. While constructed wetlands are a way to facilitate the "no net loss" goal, the wetlands restored or created may not necessarily possess the same functions and values as the original wetland that was converted or destroyed [Mitsch and Wilson, 1996]. Recreating wetland hydrology can be a difficult task.

Many created wetlands are too wet, resulting in open water; these wetlands most likely do not function as the wetlands they were designed to replace [Cole and Brooks, 2000]. Constructed wetlands that are too wet can lead to the development unintended vegetation communities (herbaceous emergent species growing instead of trees or open water instead of herbaceous emergent species). Wetland designers may intentionally underestimate wetland water balance outputs to be certain the jurisdictional hydrologic criteria are satisfied. However, natural wetlands periodically dry out. The most common and serious mistake in constructed wetland plans is the paucity of detail concerning the hydrology [Garbisch, 2002]. To restore wetland

function and not just wetland acreage, the created wetland must be hydrologically equivalent to the wetland it was designed to replace [Bedford, 1996].

To improve wetland mitigation science, prediction models are required that can connect the structural aspects of a wetland to its functions [Mitsch and Wilson, 1996]. Since hydrology is thought of as the driving force behind the establishment and maintenance of wetlands and wetland functions [Mitsch and Gosselink, 2000], hydrologic processes in wetlands are a logical starting point for the development of wetland stage prediction models.

Water storage in wetlands is dynamic, depending on the rate of inputs and outputs. Surface inflows and outflows are often extremely important to the wetland water budget [Mitsch and Gosselink, 2000]. Outflow in wetlands depends on a number of conditions. Wetland outlet controls should be designed with sufficient capacity to remove excess water in wetlands fed by groundwater and surface runoff [Garbisch, 2002]. During high-water events, a slope will develop on the water surface towards the water elevation control structure. Once this slope develops, hydraulic resistance will affect the water depth. In flow-through wetlands, outflow is often estimated, at least in part, using the hydraulic resistance within the wetland [Kadlec, 1990].

The primary source of hydraulic resistance in wetland flow is vegetation. Hydraulic resistance from vegetation depends on properties of the flow and vegetation. Vegetation can affect flow, both in wetlands and channels, in a number of ways. Flow velocities decrease as water moves through vegetated zones, affecting flow even outside of vegetated zones [Bennett, 2004].

Previous studies that have modeled hydraulic resistance using vegetation properties were based on rigid and/or simplified vegetation models such as wooden dowels over a uniform bed [Nepf, 1999]. Few studies have focused on how vegetation properties, such as structure, size, or flexibility, directly contribute to changes in drag, whether it be for a single stem or a stand [Sand-Jensen, 2003]. Regardless of the scarcity of knowledge as to how dense vegetation affects flow, numerous empirical and analytical models have been proposed to describe flow through vegetation [Kadlec, 1990; Fathi-Moghadam and Kouwen, 1997; Bolster and Saiers, 2002; James et al., 2004].

Since wetland flows often fall outside the conditions for which many of these models were developed, roughness parameters are often inflated to accommodate the low-energy flows through very dense vegetation. Plants bend and streamline with increasing flow power, decreasing the drag from the vegetation [Sand-Jensen, 2003]; drag can be assumed to be near its maximum in the slow laminar to transitional flows of wetlands. At low Reynolds numbers typical of shallow flows through emergent vegetation, hydraulic resistance is orders of magnitude higher than fully turbulent flows and resistance parameters are functions of the flow regime and water depth, as well as the vegetation density and structure. Any resistance model that simply involves an increase in the resistance to accommodate dense wetland vegetation may not accurately simulate wetland flow dynamics [Krause, 1999].

A resistance model is needed that can predict hydraulic resistance in laminar to transitional flows through emergent natural vegetation based on measureable properties of the vegetation such as size, density, or flexibility. The ideal resistance model could be used by wetland designers to predict water depth during theoretical surface-flow events for wetland design.

1.2 Goals and Objectives

The goal of this research was to determine how emergent herbaceous vegetation affects hydraulic resistance in laminar to transitional flows typically observed in wetland systems. To achieve this goal, three main objectives were completed:

1. Identify and assess the usefulness of existing models applicable to low-Reynolds number flows typical of low-gradient, densely-vegetated wetlands. (Chapter 4);
2. Determine the relationship between friction factor and measureable properties of natural vegetation, including the streamwise projected vegetation area including and neglecting vegetation overlap, stem density, stem diameter, vegetation spacing, and flexibility (Chapter 5); and,
3. Model wetland surface-water flow through a small constructed wetland using properties of the wetland emergent vegetation to determine the hydraulic resistance using the results from Objective 2 (Chapter 6).

1.3 Overall Study Design

A large outdoor flume was constructed and planted with woolgrass (*Scirpus cyperinus* (L.) Kunth), a native herbaceous emergent species commonly found in mitigation wetlands in Virginia. Flume experiments were conducted to determine if existing vegetative resistance models predicted flow velocity through dense emergent natural vegetation. The flume vegetation was measured to determine what properties were most important in the prediction of hydraulic resistance and goodness-of-fit of existing hydraulic resistance models was assessed. Regression models were developed to predict hydraulic resistance through dense emergent vegetation based on properties of the flow and vegetation. The regression models developed from data collected in the flume system were then used to predict hydraulic resistance during a simulated flow event through a small, recently-constructed wetland using an existing finite difference model.

Chapter 2 Literature Review

2.1 What are wetlands?

Wetlands are historically hard to define; over 50 definitions exist globally [Dugan, 1993]. Some common terms for wetlands throughout the world are swamp, slough, marsh, bog, billabong, fen, mire, and moor [Mitsch and Gosselink, 2000]. Some wetlands, like coastal marshes and cypress (*Taxodium distichum* (L.) Rich.) – tupelo (*Nyssa* L.) swamps, are easy to recognize. However, not all jurisdictional wetlands are as easily identifiable. In general, wetlands satisfy three conditions: the presence of water for a significant portion of the growing season, soils that exhibit signs of saturation and differ from upland soils, and the presence of vegetation adapted to wet conditions. The key characteristic is the regularity with which these areas are saturated [Dugan, 1993]. The Food Security Act of 1985 defined wetlands in a legal respect. Title 16 § 3801 (a)(18) states

The term “wetland”, except when such term is part of the term “converted wetland”, means land that—

- (A) has a predominance of hydric soils;
- (B) is inundated or saturated by surface or groundwater at a frequency and duration sufficient to support a prevalence of hydrophytic vegetation typically adapted for life in saturated soil conditions; and
- (C) under normal circumstances does support a prevalence of such vegetation.

For purposes of this Act, and any other Act, this term shall not include lands in Alaska identified as having high potential for agricultural development which have a predominance of permafrost soils.

While the strict legal definition of a wetland tends to define land area into regions of wetland and non-wetland, wetlands do not have well-defined boundaries. The transition from upland to wetland is often more of a gradient and defining a legal boundary can be challenging.

2.2 Wetland values

Despite the different types of wetlands, they do provide similar functions that are environmentally and socio-economically valuable. Wetlands only make up between 4 to 6 percent of the earth's land area [*Mitsch and Gosselink, 2000*]. However, they play a vital role, providing habitat, fish and shellfish production, water storage, erosion control, and improved water quality. Wetlands such as swamps and marshlands are among the most productive communities in the world with a net primary productivity between 800 and 3,500 t/km² [*Townsend et al., 2003*].

Wetlands provide critical habitat for any number of species such as waterfowl, amphibians, reptiles, and plants. Estimates from the United States Fish and Wildlife Service (US FWS) indicate that 43% of endangered species in the U.S. depend on wetlands for survival either directly or indirectly. According to the U.S. Environmental Protection Agency (US EPA), almost 50% of North American bird species utilize wetlands areas for food, shelter, or reproduction.

Wetlands are also valuable to fish and shellfish production. Some 75% of commercially important fish species depend on wetlands for food and/or habitat. Ninety % of recreationally important fish species depend on wetlands. In the southeastern region, 96% of commercially valuable fish and shellfish species depend on wetlands. Commercial fishing in the U.S. is a \$2 billion per year industry. Wetlands are critical in the support of the industry.

Wetlands also provide critical storage for floodwater. The removal of wetlands in upland areas contributes to the increase in peak flow in streams. This function is economically very valuable. The U.S. Army Corps of Engineers (US ACE) estimates the protection of 3,400 ha of wetlands along the Charles River corridor near Boston, Massachusetts saved \$17 million in flood damage [*EPA, 2001*]. Minnesota estimates replacing the floodwater storage of 2023 ha of wetlands with manmade structures costs about \$1.5 million annually.

Coastal wetlands help prevent shoreline erosion due to flooding and wave action. The wetland vegetation dampens the force of waves from hurricanes and floods. The root systems hold the sediments in place, further preventing erosion. The United Kingdom predicted that sea walls built behind a protective salt water marsh zone would be 20 times cheaper than walls built without the protection of salt marsh [*Dugan, 1993*].

Wetlands act as a filter for the water that passes through them. As water enters a wetland, it slows down, allowing suspended solids to settle out of the water, reducing the turbidity and the concentration of sediment-bound pollutants of the water leaving. Anaerobic conditions result in chemical precipitations and denitification, removing soluble nitrogen from the system. The numerous plants also help to remove excess nutrients, helping to prevent eutrophication and algal blooms downstream of the wetland. The build-up of organic matter in wetlands as vegetation dies can bind organic toxins, limiting their mobility out of the system. This contribution to water quality has a significant economic contribution [*Mitsch and Gosselink, 2000*].

2.3 Wetland loss

Despite the value of wetlands, large portions of wetland areas have been lost worldwide. The loss has not been well-documented but some researchers estimate that over 50% of the world's original wetland area has been lost [*Dugan, 1993*]. Effort has been made in the U.S. to document wetland loss over the course of the country's history. In the 1780s, it was estimated that 89.4 million ha of wetlands existed in the lower 48 states [*Dahl, 1990*]. In the 1980's, the estimate was 42.1 million ha. This corresponds to a 53% loss of wetland acreage. However, some areas were more affected than others; the most severe losses (greater than 2 million ha) have occurred in Florida, Texas, Louisiana, Arkansas, Illinois, Minnesota, Mississippi, Michigan, and North Carolina. More recent trends in wetland losses across the U.S. have been documented by the U.S. FWS National Wetlands Inventory Group. *Tiner Jr.* [1984] estimated that around 4.5 million ha of wetlands were destroyed from the period beginning in the mid-1950's until the mid-1970's.

While wetlands continue to be lost across the U.S., the rate of loss has consistently slowed in the last decades. However, it was not until the creation of the National Wetlands Inventory (NWI) in 1974 that wetland loss has been documented and compiled in a meaningful way. Estimated wetland loss rates from the second half of the 21st century ranged from 185,000 ha lost per year to 24,500 ha lost per year [*Tiner Jr.*, 1984; *Dahl*, 1990; *Dahl et al.*, 1991; *Frayser et al.*, 1993; *Dahl*, 2000].

Higher rates of wetland loss occurred before 1950s. The period between the mid-1800s to the early 1900s after the passage of the Swamp Land Acts of 1849, 1850, and 1860 is considered to be the time during which the majority of U.S. wetlands were destroyed. The Swamp Land Acts of 1849, 1850, and 1860 encouraged Alabama, Arkansas, California, Florida, Illinois, Indiana, Iowa, Louisiana, Michigan, Minnesota, Mississippi, Missouri, Ohio, Oregon, and Wisconsin to drain wetlands by constructing levees and drainage ditches [*Tiner Jr.*, 1984; *Dahl*, 1990; *Dahl et al.*, 1991; *Frayser et al.*, 1993; *Dahl*, 2000].

The magnitude of wetland loss between the 1780's and the 1980's has threatened both environmental and socio-economic values such as habitat, fish and shellfish production, water storage, erosion control, and water quality [*Dahl*, 1990]. The further loss since the 1980's has most certainly further threatened these values.

2.4 Wetland legislation

While wetlands are valuable to the society as a whole, the values rarely apply to individual stakeholders. For instance, a landowner stands to gain more economically by selling his wetland areas to a developer than by retaining and maintaining the wetlands. For this reason, wetlands continue to be destroyed. Federal legislation has been implemented to help protect and restore wetlands in the U.S. The Clean Water Act of 1972 was the first piece of legislation designed to specifically improve water quality [*Votteler and Muir*, 2002]. A 1977 amendment to the legislation specified that wetlands were included in the waters of the U.S. Section 404 of the Clean Water Act mandated that the U.S. ACE, with the aid of the U.S. EPA, develop regulations concerning wetlands [*Votteler and Muir*, 2002]. The U.S. ACE was also authorized to issue or deny permits that deposit dredge or fill material in the waters of the U.S., which is the means by

which most wetlands are converted to other land uses. The U.S. EPA has the authority to review and deny any permits issued by the U.S. ACE.

Other legislation related to wetlands is the 1985 Food Security Act, also known as Swampbuster. Swampbuster applied to the conversion of wetlands to agricultural activity and so was somewhat limited in scope [*Votteler and Muir, 2002*]. The Act denied Federal farm benefits for the year from any farmer who converted wetland acreage to another use. Producers who restored any lost wetlands would reinstate their farm benefit eligibility. The Food, Agriculture, Conservation, and Trade Act of 1990 strengthened the Food Security Act by denying Federal farm benefits for subsequent years after wetland conversion [*Votteler and Muir, 2002*]. The Act also set up the mitigation banking program, allowing farmers to convert wetland acreage as long as an equal acreage was restored, enhanced, or created in another location.

2.5 Wetland restoration, enhancement, and creation

Wetland restoration, enhancement, and creation have become of interest in past years to help regain environmental and socio-economic values lost due to wetland loss and degradation. These pieces of legislation have created a foundation for the rehabilitation and restoration of impaired and filled wetlands as well as the construction of wetlands where no wetland existed before. With the authority to grant dredge and fill permits, the U.S. ACE has the responsibility to require any applicants to avoid wetland areas or minimize impacts to comply with the Clean Water Act [*Losses, 2001*]. The U.S. EPA with the U.S. ACE has developed guidelines to conduct the permitting process in cooperation with the Clean Water Act Section 404(b)(1) [*Votteler and Muir, 2002*]. In these guidelines, habitat restoration or development to minimize the impact of any destroyed habitat is mentioned as a possible condition for permit approval, forming the legal basis for wetland mitigation. However, the U.S. ACE considers compensatory wetland mitigation as a last resort. Applicants must avoid wetland areas if at all possible. The next step is to minimize any impacts. If impact cannot be avoided or minimized, compensatory mitigation is required either through wetland restoration, enhancement or creation.

While constructed wetlands are a way to facilitate the “no net loss” goal, the wetlands restored or created may not necessarily possess the same functions and values as the original wetland that

was converted or destroyed [*Mitsch and Wilson, 1996*]. Most successful projects have been restoration projects that occur on sites where wetlands once existed. The topography that is conducive to wetlands already exists on these sites so the restoration of wetland function can be as simple as eliminating man-made drainage and monitoring the site for the return of wetland function.

Recreating the hydrology of wetlands is a difficult task. Many created wetlands are too wet, allowing open water; these wetlands most likely do not function as the wetlands they were designed to replace [*Cole and Brooks, 2000*]. Some of this may be due to caution by the designer to satisfy the jurisdictional hydrologic criteria. However, natural wetlands can periodically dry out. The most common and serious mistake in constructed wetland plans is the paucity of detail concerning the hydrology [*Garbisch, 2002*]. Not all wetlands are identical and when cookie-cutter approaches are used to restore or establish hydrology, failures can occur. *Galatowitsch and VanderValk [1996]* found that while most restored prairie potholes had hydrology satisfactorily reestablished (60%), some 20% of the sites had massive hydrologic failures. To restore wetland function and not just wetland acreage, the created wetland must be hydrologically equivalent to the wetland it was designed to replace [*Bedford, 1996*].

Mitsch and Wilson [1996] state the need for further research, developing wetland mitigation into a science. This requires the development of prediction models that can connect the structural aspects of a wetland to its functions. Constructed wetlands for wastewater treatment suffer similar problems; the assumption that flow in wetlands is uniform and steady can lead to design failures during significant input fluxes such as strong storm events [*Buchberger and Shaw, 1995*]. Since hydrology is thought of as the driving force behind the establishment and maintenance of wetlands and their functions [*Mitsch and Gosselink, 2000*], hydrologic processes in wetlands are a logical starting point for the development of wetland stage prediction models.

2.6 Wetland hydrology

Each wetland has a unique hydrologic regime: depth, duration, and frequency of flooding varies with wetland location and type [*Dugan, 1993*]. To adequately describe wetland hydrology, an

appropriate water budget must be estimated. Mitsch and Gosselink [2000] mathematically describe a generalized wetland water budget as follows:

$$\frac{\Delta V}{\Delta t} = P_n + S_i + G_i - ET - S_o - G_o \pm T \quad [2.1]$$

where $\Delta V/\Delta t$ is the change in volume of water storage in wetland per unit time (L^3/T), P_n is net precipitation (L^3/T), S_i is surface inflow (L^3/T), including flooding streams, G_i is groundwater inflow (L^3/T), ET is evapotranspiration (L^3/T), S_o is surface outflow (L^3/T), G_o is groundwater outflow (L^3/T), and T is tidal inflow (+) or outflow (-). From this water budget, the average water depth (h) (L) of the wetland can be estimated through continuity.

While the water budget seems simple, values such as the wetland surface area can be difficult to measure or calculate. Wetlands, especially herbaceous wetlands, can be very densely vegetated, adding a degree of difficulty to defining the surface area.

The water budget is also defined in terms of a change in storage volume per unit time. Water storage is dynamic, depending on the rate of inflow and outflow. Surface inflows and outflows are often extremely important to the wetland water budget [Mitsch and Gosselink, 2000]. The residence time of water in a wetland system affects pollutant removal; for instance, the longer the residence time, the more suspended sediment will settle out [Raisin and Mitchell, 1995]. Surface flows also require a great deal of data to adequately estimate. For wetlands systems associated with riverine systems, or other such systems that are defined by channelized inflows and/or outflows, flows can be estimated using continuity of flow.

While inflow and outflow velocities for existing wetlands can be measured using a variety of instruments such as weirs and flow meters, sites that are to be enhanced, restored or created often do not offer such an *a priori* luxury. Inflow can be estimated using any number of runoff estimation techniques or, in the case of a stream-fed wetland, existing stream flows can be measured. However, outflow will depend on any number of conditions. Garbisch [2002] recommended designing a control for high-water elevation with sufficient capacity to remove excess water in wetlands fed by groundwater and surface runoff. During high-water events, a hydraulic resistance in the wetland will cause the development of a water surface slope towards

the water elevation control structure, affecting the wetland depth. In flow-through wetlands, outflow is often estimated, at least in part, using the hydraulic resistance within the wetland [Kadlec, 1990].

2.7 Hydraulic resistance due to vegetation

A principal source of hydraulic resistance in wetland flow is vegetation [Kadlec, 1990]. In systems in which outflow is an important component of the wetland water budget, the outlet elevation in part determines water depth in the wetland. For a wetland under design consideration, outflow may be the primary component of the water budget the designer can control so it is crucial to accurately estimate the relationship between outflow and water depth. If vegetation is sufficiently dense, hydraulic resistance from vegetation can elevate the wetland water surface beyond the outlet elevation [Kadlec, 1990].

Water depth is especially crucial in emergent herbaceous wetlands since overtopping of vegetation can essentially short-circuit the system. The portion of the flow overtopping the vegetation will move faster than the portion of the flow moving through the vegetation [Jarvela, 2005]. Vegetation overtopping can lead to significant portion of the flow with a shorter residence time in the wetland and a significant portion of the outflow not undergoing any of the beneficial processes that occur during the residence time in a wetland [Holland *et al.*, 2004].

Flow through vegetation can be classified in six different regimes depending on the flow power [Roig, 1994]. The regimes are identified by the reaction of the vegetation to the flow and are as follows:

- (1) Lowest power, vegetation stationary, no deflection;
- (2) Vegetation stationary with stems and leaves oriented downstream;
- (3) Stiff vertical stems vibrate, oblique or elongated horizontal stems movement;
- (4) Stiff stems deflected, submerged leaves oriented with flow, loss of dead parts of vegetation;

- (5) Stiff stems becoming prone or compacted, surface leaves submerged; and,
- (6) Highest power, severe damage or loss of parts or entire plant.

The regimes of consequence to the majority of wetland flow are (1) and (2) [Roig, 1994]. Plants bend and streamline with increasing flow power, decreasing the drag [Sand-Jensen, 2003]. Therefore, drag can be assumed to be near its maximum in the slow laminar to transitional flows of wetlands. In a laboratory flume study, Järvelä [2002a] found that maximum values of friction factor for grasses, sedges and willows were obtained when Reynolds number or flow velocity was at its lowest. The opposite is also true: velocity is inversely proportional to the projected plant area so the depth at which the projected plant area is at a minimum is the area of maximum velocity [Lightbody and Nepf, 2006].

Vegetation can affect flow, both in wetlands and channels, in a number of ways. Bennett [2004] found that flow velocity decreased as it moved through vegetated zones of an experimental channel populated with emergent wooden dowels. The total flow averaged over the experimental channel was affected, even outside the vegetated zones. Flow resistance in the entire channel increased, with increasing density of simulated vegetation leading to an increase in flow depth, a decrease in the mean flow velocity, and an increase in mean boundary drag coefficient (C_d).

The presence of vegetation within flow also affects the vertical distribution of shear stress. Christiansen *et al.* [2000] found that the vertical shear stress distribution was more uniform within a tidal salt marsh vegetation canopy than for unobstructed flow. The salt marsh vegetation reduced the turbulence of the flow either preventing the formation of, or reducing the size of, eddies.

A key distinction to make when describing hydraulic resistance due to vegetation is whether the vegetation is submerged or unsubmerged. At low flows when vegetation is unsubmerged, hydraulic resistance increases with flow depth [Wu *et al.*, 1999; Carollo *et al.*, 2002]. As flows increase, hydraulic resistance depends less on flow depth and approaches a constant value. Once the vegetation begins to become submerged, hydraulic resistance increases slightly before

substantially dropping. *Copeland* [2000] found the same pattern in a laboratory flume experiment for shrubs and woody plants. The transition between unsubmerged flow and submerged flow appeared to occur when the flow depth reached about 80% of the undeflected plant height.

Few studies have focused on how properties of vegetation such as the structure, size, or flexibility directly contribute to changes in drag, whether it be for a single stem or a stand [*Sand-Jensen*, 2003]. However, through the years, many physical characteristics of vegetation have been found to affect flow. *Dudley et al.* [1998] found an increase in the frontal area of vegetation or woody debris projected on a plane perpendicular to the flow resulted in an almost proportional increase in the resistance coefficient of an experimental channel (Manning's n).

Green [2005a] measured velocity and turbulence distributions in and around lotic macrophytes using a two-dimensional electromagnetic current meter (EMCM). Species with a high shooting density appear to have a more pronounced affect on flows than low shooting density species [*Green*, 2005a]. Flow velocities decreased to a constant low value within a few cm of the planted section of the experimental channel.

Järvela [2002b] found the vegetal drag coefficient for leafless willows was insensitive to Reynolds number, while for leafy willows, the vegetal drag coefficient was inversely proportional to Reynolds number. A two-fold increase in the density of leafy willows corresponded to a two-fold increase in vegetal drag coefficient.

Sand-Jensen [2003] studied five structurally-different macrophytes and found that species characterized by bushy shoots and large, broad leaves generated greater drag forces than long, flexible species. Higher velocities resulted in more bending of both natural and simulated vegetation and resulted in a subsequent reduction in drag.

Vegetation drag varies seasonally and diurnally with changing conditions. The greatest resistance values are found during the mid-summer when plants are the most rigid [*Haslam*, 1978]. Plant rigidity decreases during the night and increases during the day due to an increase in buoyancy from oxygen production due to photosynthesis [*Powell*, 1978]. The mean rigidity of plant stems

occurs around 9 am. Fluctuations in plant buoyancy are thought to be negligible except in high vegetation densities, as in wetlands [Green, 2005b].

2.8 Predicting hydraulic resistance due to vegetation

Hydraulic resistance models fall into different categories based on their intended uses; systems in which vegetation resistance is important include vegetated streams, vegetated floodplains, overland flow, vegetated waterways, and wetlands, both high energy tidal systems and low energy freshwater systems [Kouwen and Li, 1980; Kadlec, 1990; Abdelsalam et al., 1992; Kouwen and Fathi-Moghadam, 2000; Green, 2005a]. The assumptions associated with each model vary depending on the intended use.

Flows in streams and on banks and floodplains are often in the turbulent range and the vegetation can range from sparsely populated woody streams and shrubs to dense grasses of various heights to lotic macrophytes [Kouwen and Fathi-Moghadam, 2000; Green, 2005a]. Flows may be emergent or submerged depending on the vegetation type and stream stage. Overland flows can also be emergent or submerged depending on the vegetation type and the flow in question. Flow can occur through short, mowed grass or through tall vegetation such as crops. Vegetated waterways in agricultural systems often utilize overland flow models. Overland flow through tall vegetation appears similar to wetland flow. However, overland flow models, while adequate for very shallow flows over vegetated surfaces, are limited as predictive tools in wetland flow simulation [Bolster and Saiers, 2002].

Few pure wetland models exist. It is important to consider the type of wetland for which the model was developed since wetlands vary so dramatically. There are two distinct categories of models describing flow through wetland vegetation: those that assume turbulent flow and those that are valid for the transition to laminar flows found in wetlands [Kadlec, 1990]. High energy tidal systems can have flows ranging from turbulent to the transition range while lower energy freshwater systems are often in the transition to laminar range [Kadlec, 1990]. Low energy freshwater systems also vary with vegetation type: forested systems have a lower density of drag-creating elements than herbaceous systems.

One of the most common estimates of hydraulic resistance is Manning's equation. Manning's equation was developed for open channel, fully-turbulent flow with the primary hydraulic resistance coming from the channel boundary. The coefficient describing the channel boundary resistance is known as Manning's n .

$$V = \frac{A}{n} R^{2/3} S_w^{1/2} \quad [2.2]$$

where V is the average velocity (L/T), A is a constant (1.49 for English units, 1 for SI units), n is the Manning's coefficient, R is the hydraulic radius (L), and S_w is the slope of water surface (L/L).

Extensive tables of Manning's n values have been developed for a variety of bed materials. However, picking a value from compiled tables of average values assumes the site conditions are representative of the range of conditions from which the average n values were compiled. The strict use of Manning's equation is not applicable for wetland flow through dense vegetation. Manning's n values must be recalculated for each set of conditions using an iteration scheme; the values cannot be tabulated and used as a constant.

Many authors have cited the inadequacy of Manning's equation in describing overland flow through grasses and crops [Smith *et al.*, 1990]. Abdelsalam *et al.* [1992] determined that Manning's equation was inadequate for describing flow in wide irrigation canals. Viscosity may be a significant component of hydraulic resistance in shallow overland flows [Maheshwari, 1992]. In contrast, Beuselinck *et al.* [2002] found that Manning's equation adequately fit data collected from laboratory flume experiments simulating overland flow conditions despite the fact that the flows were in the laminar to transition range and a constant value for Manning's n was used.

Even with the difficulties involved with successfully selecting a value for Manning's n [Green, 2005a], the equation is still used currently to model flows in vegetated channels [Brookes *et al.*, 2000] and salt marshes [Lawrence *et al.*, 2004]. The roughness coefficient, Manning's n , has also been used in large scale spatial management models for the Mississippi River delta in which a Manning's n is assigned to a 100-km² cell [Martin *et al.*, 2000].

In addition to the problems in accurately determining a value for Manning's n , none of the conditions for which values of Manning's n have been developed mimic conditions found in wetland systems [Kadlec, 1990]. In the laminar to transitional flow range, Manning's n is not a constant; it varies with depth and discharge. This can introduce additional problems with accurately estimating n .

Kadlec [1990] argued that the use of Manning's equation for the estimation of hydraulic resistance in wetlands is inherently flawed. Wetland flow does not satisfy the necessary assumptions for Manning's equation to be valid. Wetland flow is not fully turbulent; it is often in the laminar to transition range due to the low slope and the shallow depths. Reynolds number (Re_{depth}) in constructed wetlands can range from 1 to 1000 [Kadlec, 1990]. Additionally, hydraulic resistance due to the boundary is negligible compared to the resistance due to the vegetation. Manning's equation is valid for wetland conditions only if n is allowed to vary with Re (stem or depth), which introduces additional complexity since Re varies spatially within a channel [Tsihrintzis and Madiedo, 2000].

The issues in modeling flow in wetlands associated with Manning's n are not limited to Manning's equation alone. Any stage-discharge relation that simply involves an increase in the resistance to accommodate dense wetland vegetation may not accurately simulate the flow dynamics of wetlands [Krause, 1999]. Technically, Manning's equation is a special case of a power-law function. A more general form of the power law can be used to accommodate a wider range of conditions. Turner and Chanmeesri [1984] proposed an alternate form of a resistance equation that describes flow through broad shallow channels.

$$q = \frac{1}{G} h^m S^{1/2} \quad [2.3]$$

where q is the inflow rate, G is the coefficient of roughness independent of slope, h is expressed in mm, and m is the exponent reflecting the degree of mixing in the flow.

Equation [2.2] has been used to describe hydraulic resistance due to wetland vegetation in the wetland flow model WETFLOW [Feng and Molz, 1997]. Feng and Molz [1997] describe the

Turner and Chanmeesri [1984] model as “diffusion-based” due to the fact that it was developed for low velocity flows through relatively dense vegetation.

Kadlec [1990] proposed a more general form of the power law expression to describe hydraulic resistance in wetlands due to vegetation. Although this equation also used a form of the power law like Manning’s equation, the assumptions made are consistent with wetland flow.

$$\frac{Q}{W} = K_a h^\beta S_f^\alpha \quad [2.4]$$

Q/W is the volumetric flow per unit width ($L^3/L \cdot T$), K_a is the pre-multiplier, S_f is the friction slope (L/L), α is the slope exponent, and β is the depth exponent. The value of α depends on the type of flow that is occurring; α is 0.5 for turbulent flow and 1.0 for laminar flow. Typical values for β range from 2 to 4 [Kadlec, 1990]. The value for K_a is site-specific; values of K_a for different data sets range from 0.37×10^8 to 28.5×10^8 .

Equation [2.4] is probably the most commonly used model for describing hydraulic resistance through wetland vegetation [Bolster and Saiers, 2002]. It has been used to successfully model a dynamic wetland water budget using a modified version of the power law [Walton et al., 1996] and flow through tidal wetlands using the California tidal wetland modeling system (CalTWiMS) [Arega and Sanders, 2004]. Kadlec’s determination of drag force has also been used in a 2-D numerical model used to demonstrate the importance of vegetation layout within constructed wetlands [Jenkins and Greenway, 2005] and in the MODFLOW Wetland Package [Restrepo et al., 1998].

2.8.1 Vegetative drag

Hydraulic resistance due to vegetation is not simple to quantify; it is a result of many forms of drag and frictional losses. Four resistance mechanisms are at work in wetlands: (1) form drag due to the difference in hydrodynamic pressure around an object or stem; (2) skin drag due to shear stresses from contact of flow with surfaces; (3) wave drag due to the deformation of the water surface where stems penetrate; and, (4) energy losses from turbulence and viscosity [Rouse, 1965; Roig, 1994].

Drag is an opposing force of a submerged or emergent object in the direction opposite of flow (F_d). The drag force, assuming form drag is dominant, is the integral of the forces in the x-direction, the sum of the fluid pressure and shear stress distribution applied to the object by the fluid.

$$F_d = \int dF_x = \int p \cos \theta dA_r + \int \tau \sin \theta dA_r = \frac{1}{2} \rho C_d A_r V^2 \quad [2.5]$$

where F_x is the resultant force in the x-direction ($M \cdot L/T^2$), p is the fluid pressure ($M/L \cdot T^2$), θ is the angle of the shear plane, and τ is the shear stress ($M/L \cdot T^2$). The reference area (A_r) (L^2) is the characteristic area of the object (similar to the Re characteristic length), which is usually assumed to be the projected frontal area (A_f) (L^2) of the object but may also be defined as the planform area (A_b) (L^2) or the total momentum absorbing area (MAA) (L^2), for example. The drag coefficient (C_d) and the average upstream velocity (V) (L/T) can be used in place of the pressure and shear stress distributions.

For gradually varied flow, typical of flow through natural vegetation, the drag force is equal to the gravitational force (F_g) ($M \cdot L/T^2$) of the flowing water per unit bed area:

$$F_g = \rho g h S \quad [2.6]$$

where ρ is the fluid density (M/L^3), g is the acceleration due to gravity (L/T^2), h is the flow depth (L), and S is the unspecified slope (L/L). The slope may be represented as the bed slope (S_b), the energy grade slope (S_g), or S_f . The slope used in a hydraulic model is at times unclear. For steady, uniform flow, S_f , S_g , and S_b are equivalent; however, flow in densely vegetated natural systems is not uniform. Local variations in bed topography and plant density make the uniform flow assumption invalid; instead flows are better characterized as gradually varied. Depending on the formulation, the unit bed area may include or exclude stems. Combining [2.5] and [2.6], a general formulation for flow through vegetation can be obtained:

$$ghS = \frac{1}{2} C_d \frac{A_r}{A_*} V^2 \rightarrow gS = \frac{1}{2} C_d \lambda V^2 \quad [2.7]$$

In the second formulation, the area coefficient (λ) (L^{-1}) is A_r per unit volume ($h \cdot A_*$) (L^3), where A_* is the bottom area (L^2).

A number of models have been developed using basic force, energy or momentum balances to describe flow through vegetation, real or simulated. The models differ in the definition of λ and consequently may have different C_d . Equation [2.8] has been rearranged in the form below so each model can be compared:

$$V = \sqrt{\frac{2gS}{\lambda C_d}} \quad [2.8]$$

Table 2.1. presents a summary of the various forms of λ . The differences in λ between models are nuanced; however, depending on the vegetation architecture, small differences in A_r and A_* definitions can result in great differences in the final value of λ . The difference between the *Fathi-Moghadam and Kouwen* [1997], *Nepf* [1999], *Stone and Shen* [2002], and *Kadlec* [1990] definitions of λ will be examined as an example.

The *Fathi-Moghadam and Kouwen* [1997] A_r is defined as the momentum absorbing area (*MAA*) (L^2). *MAA* is the one-sided area of a stand of vegetation. The *Fathi-Moghadam and Kouwen* [1997] A_* is the total bed area covered by stems for the stand of vegetation, A_s . The *Fathi-Moghadam and Kouwen* [1997] λ is the one-sided area of a stand of vegetation divided by the submerged volume of the stand of vegetation.

The *Nepf* [1999] λ is defined as a , the projected streamwise stem area per unit volume. The *Stone and Shen* [2002] λ is the projected streamwise stem area per unit bed volume. The *Nepf* [1999] and *Stone and Shen* [2002] A_r is calculated by multiplying h by the stem density, N , and the stem diameter, d . The *Nepf* [1999] A_* is the unit bottom area, A_u , (stem area + bed area) while

the *Stone and Shen* [2002] A_* is the unit bed area only (stem area removed). The *Nepf* [1999] and *Stone and Shen* [2002] A_r definitions are similar to the *Fathi-Moghadam and Kouwen* [1997] A_r definition; the A_r definition is theoretically identical for cylindrical vegetation. However, for leafy vegetation, only the leaf area that is oriented in the streamwise direction will be included in the *Nepf* [1999] A_r while the entire one-sided leaf area will be included in the *Fathi-Moghadam and Kouwen* [1997] A_r .

Table 2.1. Area coefficient definitions for drag coefficient models.

Flow Model	Vegetal Area Coefficient, λ (L ⁻¹) ¹
<i>Lindner</i> [1982] (as presented by <i>Järvelä</i> [2004])	$\lambda = \frac{d}{\Delta s^2}$
<i>Kadlec</i> [1990]	$\lambda = A_f$
<i>Fathi-Moghadam and Kouwen</i> [1997]	$\lambda = \frac{MAA}{h \cdot A_b}$
<i>Nepf</i> [1999]	$\lambda = a$
<i>Stone and Shen</i> [2002] and <i>James et al.</i> [2004]	$\lambda = \frac{N \cdot d}{\left(1 - \frac{A_s}{A_u}\right)}$
<i>Hoffman</i> [2004]	$\lambda = \frac{1 - \varepsilon}{\varepsilon \cdot d \left(\sqrt{\frac{\pi}{4}} - \sqrt{1 - \varepsilon}\right)^2}$

¹ d is the stem diameter (L), Δs is the stem spacing (L), A_f is the projected frontal area (L²), MAA is the momentum absorbing area (L²), h is the flow depth (L), A_b is the drag bottom area (L²), a is the projected plant area per unit volume (L⁻¹), A_f is the frontal area per unit volume (L⁻¹), N is the stem density, A_s is the area of stems (L²), A_u is the unit bottom area (L²), ε is the flow porosity

The *Kadlec* [1990] λ is the vegetation frontal area per unit volume (A_f) (L⁻¹) and excludes vegetation that is hidden behind upstream stems; consequently, the *Kadlec* [1990] λ is much

smaller than the *Fathi-Moghadam and Kouwen* [1997] and *Nepf* [1999] λ for large stem densities. For cylindrical vegetation that does not overlap, the *Fathi-Moghadam and Kouwen* [1997], *Nepf* [1999], and *Kadlec* [1990] A_r are identical.

Drag coefficients can be quantified in three ways: the drag coefficient for a single isolated element, the drag coefficient for a single element in an array of elements, or a drag coefficient for the entire field of elements. If total drag of an array of elements is dominated by form drag, the total drag for the elements is additive; the total drag of the array is a product of the array density and the drag of a single isolated element.

Drag coefficients for isolated cylinders penetrating open channel flow have been determined; arrays of cylinders have also been modeled. Assuming wetland flow through emergent vegetation is dominated by form drag, using a drag coefficient for a single isolated cylinder has disadvantages [*Roig*, 1994]

- (1) Wetland plants cannot be adequately represented by isolated cylinders. In nature they occur in densely packed groups where the wakes of the plants overlap;
- (2) Actual vegetation cannot be adequately represented by a simple cylinder;
- (3) Actual vegetation has a surface texture and these textures vary across species. The roughness length attempts to characterize this parameter but the measurement of the parameter can be difficult if not impossible;
- (4) The drag coefficient measured under laboratory conditions is often adjusted for field conditions, creating an empirical coefficient, not an actual measured value.

For turbulent flows, the drag coefficient approaches a single value, often near one [*Tsihrintzis and Madiedo*, 2000]. However, for laminar and transitional flows, the drag coefficient may vary considerably with Reynolds number (Re). Additionally, vegetation may deviate substantially in shape and form from a rigid cylinder, especially relatively short herbaceous vegetation such as

the species typically found in wetlands and on floodplains. For natural vegetation, the reference area can vary greatly over a range of depths, further complicating drag coefficient estimation.

Determining the drag coefficient of a vegetated area is extremely complex, depending on many factors including the flow velocity and depth and the shape, structure, flexibility, and density of the plants. To date, drag coefficient estimation has been empirical, based on previous studies that measured the drag coefficient or bulk drag coefficient of real or simulated vegetation [Wu *et al.*, 1999; Lee *et al.*, 2004; Harvey *et al.*, 2009]. As noted earlier, the only difference in the flow models presented in Table 2.1 is the definition of the reference area, A_r . To model flow through wetland vegetation, the drag coefficient must also be determined. Several methods to estimate the drag coefficient were also considered: the drag coefficient for an infinite isolated cylinder, a constant value (1.05), and four empirical relations presented in Table 2.2.

Table 2.2 Summary of drag coefficient predictors.

Drag Model	Drag Coefficient Predictor ¹
<i>Lindner</i> [1982] (as presented by <i>Järvelä</i> [2004])	$C_d = \left(1 + 1.9 \frac{d}{a_y} C_{d\infty} \right) \left(0.2025 \left(\frac{a_x}{d} \right)^{0.46} C_{d\infty} \right) + \left(\frac{2a_y}{a_y - d} - 2 \right)$
<i>Taylor et al.</i> [1985]	$\log_{10} C_d = -0.125 \log_{10} \text{Re}_{stem} + 0.275 \text{ for } \text{Re}_{stem} < 60,000$
<i>Choi and Kwon</i> [1999]	$C_d = 0.07(ad + 0.151)^{-1.49} \text{ for } 0.001 \leq ad \leq 0.03$
<i>Harvey et al.</i> [2009] (for ridge conditions)	$C_d = \frac{2 \cdot \log_{10}(2.37) \text{Re}_{stem}^{-1.54}}{(ad)^{0.5}}$

¹where C_d is the drag coefficient, d is the stem diameter, a_y is the spanwise stem spacing, $C_{d\infty}$ is the isolated stem drag coefficient, a_x is the streamwise stem spacing, Re_{stem} is the stem Reynolds number, a is the projected streamwise plant area per unit volume

The bulk drag coefficient (C_d') (L^{-1}) is a lumped parameter that is a function of the drag coefficient and the reference area. Like C_d , C_d' is estimated empirically from regression relationships. Bulk drag coefficient estimations considered in this research are summarized in

Table 2.3. Using the additive property of the drag coefficient in systems dominated by form drag, a vegetal drag coefficient for a stand of vegetation based on the drag coefficient of a single stem can be calculated using the vegetal area coefficient [*Wu et al.*, 1999; *Jarvela*, 2002b].

$$C_d' = \lambda \cdot C_d \quad [2.9]$$

where λ is the vegetal area coefficient (L^{-1}). However, if other types of friction losses are significant, simply multiplying the array density by the drag from a single element leads to an underestimation of the total drag due to vegetation since the drag for a single isolated element is smaller than the drag per element within the stand [*Lawrence*, 2000].

Table 2.3 Summary of bulk drag coefficient predictors.

Bulk Drag Model	Bulk Drag Coefficient Predictor ¹
<i>Wu et al.</i> , [1999]	$C_d' = \frac{3.44 \times 10^6 S^{0.5}}{Re_{depth}}$
<i>Lee et al.</i> , [2004] (lab conditions)	$C_d' = \left(\frac{2 \cdot 10^{1.46}}{\Delta s} \right) Re_{depth}^{-0.70}$
<i>Lee et al.</i> , [2004] (field conditions)	$C_d' = \left(\frac{2 \cdot 10^{4.56}}{\Delta s} \right) Re_{depth}^{-1.35}$

¹where C_d' is the bulk drag coefficient, S is the slope (unspecified), Re_{depth} is the depth Reynolds number, Δs is the stem spacing

2.8.1-1 Measuring drag coefficient

Measuring the drag coefficient of natural vegetation, whether it is for an individual element or for a stand of vegetation, is not simple. The complex geometry of natural vegetation complicates the measurement of the drag coefficient due to the difficulties associated with isolating the physical characteristics of vegetation affecting the drag [*Thompson et al.*, 2003]. Natural

vegetation is also highly variable so even numerous measurements of the drag coefficient will only yield an average and range of values.

The bulk drag coefficient within a stand of simulated vegetation was measured using a 3-D acoustic Doppler velocimeter (ADV) [Garcia *et al.*, 2004]. The vegetation bulk drag coefficient at each point within the flow can be calculated:

$$C_d = 2 \frac{gS_b - \frac{\partial \overline{|u'v'|}}{\partial z}}{a_g |u|^2} \quad [2.10]$$

where S_b is the bed slope, u' is the instantaneous velocity in the streamwise direction (L/T), v' is the instantaneous velocity in the spanwise direction (L/T), a_g is the vegetation density given by ratio between the plant diameter and the horizontal area of influence of each plant (L^{-1}), and $|u|$ is the average velocity in the streamwise direction (L/T). In [2.10], brackets represent spatial averages, overbars represent the Reynolds averages, and prime marks represent temporal fluctuations. While the bulk drag coefficient does not require the definition of a reference area, the bulk drag coefficient depends on direct velocity measurements. Multiple measurements would be required to determine how the bulk drag changes over a range of flow conditions.

2.8.1-2 Drag coefficient and friction factor

The value of the drag coefficient depends on the definition of the drag reference area. Drag coefficients cannot be compared unless the definition of the drag reference area is the same [Jarvela, 2004]. Friction factor is independent of the defined characteristic area of the plants. The friction factor (f) is a function of the drag coefficient, the drag characteristic area, and the bed area over which the drag characteristic area is measured.

$$f = 4C_d \left(\frac{A_r}{A_*} \right) \quad [2.11]$$

Unlike the bulk drag coefficient, friction factor is dimensionless. The Darcy-Weisbach equation is frequently used to describe flow in open channels. Theoretically, there is no advantage to using Manning's n , friction factor, or drag coefficient [Yen, 2002]. However, because friction

factor does not rely of the definition of a characteristic drag area and the Darcy-Weisbach equation does not make any assumptions about the flow regime, hydraulic resistance expressed in terms of friction factor may be more desirable when comparing results from multiple studies [Jarvela, 2004].

2.8.2 Vegetative parameters that affect hydraulic resistance

Results from previous studies have found several parameters are related to hydraulic resistance due to vegetation. A summary of pertinent vegetation parameters is presented in Table 2.4. These parameters are either directly used in models describing hydraulic resistance due to vegetation or have been found to affect various empirical parameters used to describe hydraulic resistance due to vegetation. Independent vegetation parameters can be combined with independent flow parameters to completely describe hydraulic resistance. Simplifying the vegetation parameters from Table 2.4, vegetation friction factor can be expressed in terms of dimensionless vegetation and flow properties [Yen, 2002]:

$$f = f(\text{Re}, Fr, S_w, S_b, \frac{k}{h}, L_v, J, \frac{h}{z_v}, N) \quad [2.12]$$

where Fr is the Froude number, S_w is the water surface slope, k is the bed roughness height (L^{-1}), L_v is a vegetation geometry parameter, J is a dimensionless vegetation flexibility parameter, z_v is the vegetation height (L), and N is the stem density. The list of vegetation and flow parameters in Table 2.4 and [2.12] that affect hydraulic resistance is long, many of the parameters are dependent and/or not well-defined. For example, stem spacing (Table 2.4) is a function of d and N , so only two of the three parameters can be included in the final relationship. S_w and S_b [2.12] may not be independent; depending on the resistance of vegetation, S_w may be a function of or equal to S_b . Additionally, it is unclear how L_v should be defined. For flows through dense vegetation, bed roughness is negligible in comparison to vegetation roughness so k can be eliminated.

Table 2.4 Vegetation parameters relevant to predict hydraulic resistance from vegetation

Study	Stem Spacing	Stem Diameter	Stem Density	Vegetation Height	Flow Area	Vegetation Frontal Area	Canopy volume	Momentum-Absorbing Area (MAA)	Vegetation Porosity	Wetted Length of Vegetation	Flexural Rigidity	Vegetation Dry Biomass
<i>Hsieh [1964]</i>	X	X										
<i>Petryk et al. [1975]</i>					X	X						
<i>Kouwen et al. [1981]</i>			X			X						
<i>Pasche et al. [1985]</i>		X										
<i>Temple [1986]</i>				X	X							
<i>Kadlec [1990]</i>						X						
<i>Hall et al. [1994]</i>												X
<i>Roig [1994]</i>	X	X						X				
<i>Jadhav et al. [1995]</i>		X	X					X				
<i>Kutija et al. [1996]</i>		X								X	X	
<i>Naot et al. [1996]</i>	X	X	X									
<i>Darby et al. [1996]</i>				X								
<i>Fathi-Moghadam and Kouwen [1997]</i>				X		X	X	X			X	
<i>Wu et al. [1999]</i>				X								
<i>Righetti et al. [2002]</i>	X		X	X								
<i>Stone and Shen [2002]</i>		X	X							X		
<i>Hoffman [2004]</i>									X			

Equation [2.12] was used as a general model for the selection of variables to include in the Buckingham Π analysis. Specific vegetation parameters were selected from Table 2.4 and bed roughness and slope from [2.12] were excluded assuming the vegetated system would be dominated by vegetated roughness. The choice of independent vegetation parameters should theoretically not change the final form the hydraulic resistance relationship as long as the problem is completely defined. N was excluded from the Buckingham Π analysis since the stem count and density may not be a meaningful parameter for all vegetation architectures (especially branching vegetation). Buckingham Π theorem was utilized to derive seven dimensionless Π terms from ten variables below:

$$f = f(d, h, z_v, \lambda, MEI, V, g, \rho, \mu, S) \quad [2.13]$$

where z_v is the vegetation height (L), MEI is the density-dependent flexural rigidity ($M \cdot L^3 / T^2$), and μ is the fluid viscosity ($M / L \cdot T$). λ is a plant area per volume and can be defined as the unit MAA or the MAA per unit volume (maa) (L^{-1}) or A_f and is a function of N , d , and h .

Consequently, the inclusion of λ necessitates the exclusion of N , d , or h . Using the method of repeating variables, seven dimensionless parameters were created [2.14].

$$f = f \left(Re_{stem} \text{ or } Re_{depth}, \lambda d \text{ or } \lambda h, \frac{d}{h}, \frac{d}{z_v}, Fr, \frac{MEI}{\rho v^2 d^4}, S \right) \quad [2.14]$$

The measurement and/or calculation of d , h , z_v , Re , Fr , and S are straightforward. However, the determination of λ and MEI of vegetation are not standard. As mentioned previously, λ can be expressed in terms of maa or A_f . A_f is the projected plant area with stem overlap and maa neglects overlap. When flow causes vegetation to deflect, A_f may not accurately represent the actual area of the vegetation perpendicular to the flow [Fathi-Moghadam and Kouwen, 1997]. However, it is unclear if wetland flows are sufficient to deflect the vegetation so λ should be expressed in terms of both maa and A_f . The key difference between MAA and maa is the volume over which the value is measured; MAA is a continuous vegetative canopy value determined by volume. maa is determined for a unit volume. Fathi-Moghadam and Kouwen [1997] measured MAA by harvesting the vegetation canopy, cutting it into equal intervals, and photographing it in

black and white. The photo was analyzed using pixel classification to determine the total area. The same technique can be used for measuring *maa* but on a unit volume basis. However, *MAA* and *maa* for cylindrical vegetation can be calculated directly by multiplying the stem diameter by the stem density over the volume of interest.

A_f can be measured using a similar photographic technique to the MAA measurement techniques used by *Fathi-Moghadam and Kouwen* [1997]. *Jarvela* [2002b] used a grayscale digital image of vegetation against a whiteboard to determine the projected stem and branch area of leafless willows. Image processing software was used to establish a threshold level to convert grey pixels to black and white. The projected stem and branch area was determined by counting the number of black pixels at 10-cm increments from the bottom of the vegetation. The threshold level was determined by converting images of geometrically well-defined dark plastic, steel bars, and willow stakes with a known projected area. The method had expected errors of ~5%, which was within the expected variation of a willow canopy.

Vegetation flexibility has frequently been ignored in hydraulic resistance studies because rigid vegetation elements such as dowels were used or flows were not considered strong enough to significantly deflect the vegetation [*Yen*, 2002]. Flexural rigidity is a product of two separate parameters: moment of inertia and the modulus of elasticity. The moment of inertia is strictly a geometric measure of the vegetation while the modulus of elasticity is a measure of the propensity of a material to bend under an applied force. The amount the plant bends and the streamlining of the plant under hydrodynamic forces is crucial in quantifying resistance [*Copeland*, 2000].

Kouwen [1988] combined the moment of inertia and the modulus of elasticity into one parameter known as the *MEI* where M is a measure of stem density, E is the modulus of elasticity ($M/L \cdot T^2$), and I is the second area moment of inertia (L^4). This property may not be measureable in stands of natural vegetation [*Wilson and Horritt*, 2002]. For individual plants, E is a function of the force required to deflect a plant to 45° from vertical, F_{45} , ($M \cdot L/T^2$), z_v , and I calculated for the plant shape [*Copeland*, 2000]:

$$E = \frac{F_{45} z_v^2}{3I} \quad [2.15]$$

E was calculated for thirteen riparian plant species (*Salix* L., *Sambucus* L., for example) by applying a known force until the deflection of the center of the plant leaf mass was 45° from the base of the stems. The following empirical relationship was developed relating E to the z_v and d [Copeland, 2000]:

$$E = 7.648 \times 10^6 \left(\frac{z_v}{d_4} \right) + 2.174 \times 10^4 \left(\frac{z_v}{d_4} \right)^2 + 1.809 \left(\frac{z_v}{d_4} \right)^3 \quad [2.16]$$

where d_4 is the stem diameter (m) measured at a height of $z_v/4$ (m). E depends on plant size. To remove this dependence, the value for E can be divided by $(z_v/d_4)^{1.5}$. While this is a convenient expression, field measurements of E are recommended [Copeland, 2000].

The flexural rigidity of vegetation can be estimated in the field using a simple board drop test developed by *Eastgate* [1966]; the method was first presented in a masters' of engineering thesis and outlined again by *Kouwen* [1988]. An 1829-mm by 305-mm board weighing 4.85 kg was placed on end within the vegetation. The board was allowed to freely fall pivoting about the end in contact with the surface. Upon contact with the vegetation, the weight of the board deflected the vegetation and slid along the surface similar to the deflection and friction exerted by fluid flow. The distance between the bottom of the board and the surface was recorded and the MEI , the product of the vegetation density, modulus of elasticity, and the moment of inertia, was determined using the following expression:

$$MEI = 3122 BH^{2.82} \quad [2.17]$$

where BH is the distance between the bottom of the dropped board and the surface (m). This procedure was developed for grasses and the MEI was related to grass length for both growing and dormant grasses.

2.9 Modeling wetland hydrology

Numerous models exist that simulate wetlands; models may simulate wetlands as only one component of the watershed while others focus only on modeling the immediate wetland area. As the focus of research was on hydraulic resistance within wetlands, only models that considered the wetland area in detail were examined. The models considered were DRAINMOD [Skaggs, 1978], MODFLOW – Wetland Simulation module developed by the South Florida Water Management District [Restrepo *et al.*, 1998], WETLAND [Lee *et al.*, 2002], and WETSAND [Kazezyilmaz-Alhan *et al.*, 2007].

DRAINMOD is a model used to simulate the hydrology and nutrient transport in poorly drained soils with high water tables. Originally developed in 1980 at North Carolina State University, DRAINMOD has been used to simulate hydrology in certain wetland types such as Carolina Bays and pocosins [Skaggs *et al.*, 1991]. DRAINMOD is simply structured with no surface flow component through the wetland area and simple one-dimensional flow through the soil. Runoff is the only surface flow component of DRAINMOD and is defined simply as the difference between the precipitation, the change in the surface storage, and the infiltration. DRAINMOD was designed to be used in systems with surface slopes that are essentially zero.

DRAINMOD has been successfully applied to wetland systems with hydrologically isolated or perched groundwater systems with little to no surface flow. In such systems, the water budget is dominated by precipitation and upland surface runoff inputs and evapotranspiration outputs [Sharitz and Gibbons, 1982]. Pocosins and Carolina Bays are two unique wetland types characterized by little groundwater interaction; groundwater has the least influence on the annual water budget of pocosin systems [Sharitz and Gibbons, 1982]. Fluctuations in water levels in Carolina Bays are not linked to groundwater fluctuations; instead, water levels in Carolina Bays appear to be more closely linked with precipitation and evapotranspiration [Sharitz and Gibbons, 1982].

The MODFLOW – Wetland Simulation package was developed and is administered by the South Florida Water Management District [Restrepo *et al.*, 1998]. The Wetland Simulation package for MODFLOW was created to model the effects of anthropogenic alterations on

wetland hydrology specific to the Everglades. The Wetland Simulation Module uses MODFLOW simulation routines for modeling groundwater flow. It divides the wetland into two layers: the top layer consists of surface water flow and flow through the peat layer and the bottom layer is modeled as an independent confined or unconfined layer linked to the surface wetland layer or as part of the underlying aquifer, depending on the site characteristics. The MODFLOW Wetland Simulation module describes surface flow as a combination of sheet flow through dense vegetation and channel flow through a slough network. Sheet flow through dense vegetation is described using a semi-empirical power-law stage-discharge model similar in form to Manning's equation (Kadlec, 1990). The majority of surface flow is conveyed through the slough network, which is modeled as channel flow. If the water surface in the top layer drops below the extent of the top layer, the lower layer is simulated as an unconfined aquifer. Flow between the surface wetland layer and the subsurface aquifer layer is determined based on the hydraulic gradient between the layers so the wetland may contribute water to aquifer or receive water from the aquifer.

WETLAND [Lee *et al.*, 2002] is a model developed to simulate hydrology, nitrogen, carbon dissolved oxygen, bacteria, vegetation, phosphorus, and sediment dynamics in constructed free-water surface and subsurface wetlands. The hydrology model is based on the water budget Kadlec and Knight [1996] outlined for treatment wetlands. Since the water budget was created for treatment wetlands, infiltration is assumed to be minimal and is incorporated into the outflow term. Surface flow is not specifically modeled as outflow is assumed to be approximately equal to inflow by design. WETLAND [Lee *et al.*, 2002] modified the Kadlec and Knight [1996] outflow estimation by using six different outlet options [Lee, 1999]: rectangular weirs, V-notch weirs, fixed pipe, pumped discharge, the Kadlec [1990] power law stage-discharge relationship, and subsurface flow using Darcy's law for the wetland media. While WETLAND uses a daily timestep, outflow is calculated on an hourly timestep. Groundwater-surface water interactions are modeled using user-provided percolation-infiltration rates.

WETSAND [Kazezyilmaz-Alhan *et al.*, 2007] is the newest wetland simulation model developed. The wetland area includes the upland areas that contribute runoff to the wetland, the wetland itself, and the stream system that can contribute flow or convey flow from the wetland system. The primary hydrologic model within WETSAND is the diffusion wave equation derived from

the Saint-Venant equations for shallow water flows. Groundwater interactions are described by the addition of a flow rate term, which is the sum of the time rate terms rainfall intensity and lateral inflow minus the infiltration and evapotranspiration rates plus or minus the rate of groundwater discharge or recharge depending on the direction of the hydraulic gradient. Surface water is modeled using the *Kadlec* [1990] equation with parameter values recommended by *Kadlec and Knight* [1996]. WETSAND discretizes the wetland area (upland, wetland, and stream) into reach-like segments connected by nodes. WETSAND only models flow in the longitudinal direction defined as the direction of decreasing terrain slope.

Table 2.5 compares each model considered based on groundwater-surface water interaction, surface flow modeling, and evapotranspiration modeling. Most interaction between the free-water surface of the wetland and the subsurface/groundwater was modeled as a one-way, one-dimensional process, namely as infiltration [*Skaggs*, 1978; *Lee et al.*, 2002]. Few models [*Restrepo et al.*, 1998; *Kazezyilmaz-Alhan et al.*, 2007] represented the interaction between the surface and subsurface as a dynamic process that would allow water to flow from the subsurface to the surface layer. Three models used the *Kadlec* [1990] surface flow equation to model wetland outflow. Only the MODFLOW Wetland Simulation module considered both shallow flow through vegetation and concentrated flow through sloughs. Only WETSAND considered the wetland as part of a stream network, which for mitigation wetlands, may or may not be the case. Evapotranspiration was primarily modeled using the *Thornthwaite* [1948] method for estimating potential evapotranspiration.

Table 2.5 Comparison of wetland water budget model components

Model	General Model Information	Groundwater Interaction Modeling	Surface Water Modeling
DRAINMOD	Black-box model – unit surface area located midway between subsurface drains	Vertical: Infiltration modeling – Green-Ampt equation [<i>Green and Ampt</i> , 1911] Horizontal: lateral subsurface drainage – <i>Bouwer and van Schilfgaarde</i> [1963] method	Runoff occurs when surface storage depth exceeds the average depth of depression storage
MODFLOW – Wetland Simulation module	3-D gridded model, Wetland Simulation module assumes two layers, surface and subsurface	Subsurface layer either transmits water to or receives water from the surface later depending on hydraulic gradient, flow modeled using Darcy’s law	<i>Kadlec</i> [1990] model for dense vegetated flow + open channel slough flow
WETLAND/ <i>Kadlec and Knight</i> , [1996]	Gridded model assuming a treatment wetland, bathtub design	WETLAND: user provided percolation/infiltration rates <i>Kadlec and Knight</i> [1996]: Little to no infiltration assumed	WETLAND: outflow options range from <i>Kadlec</i> [1990] model to outlet structure controlled outflow to subsurface flow only
WETSAND	1-D flow model	Groundwater recharge/discharge rates (horizontal hydraulic conductivity assuming isotropic soils, measured depth to groundwater for each segment), infiltration [Green-Ampt [<i>Green and Ampt</i> , 1911] with <i>Mein and Larson</i> update [1973], lateral inflow rate	<i>Kadlec</i> [1990] model with parameters indicated by <i>Kadlec and Knight</i> [1996].

Chapter 3 Flume methods

To achieve the goals set out in Chapter 1, a 12.2-m x 1.2-m outdoor flume at the Prices Fork Research Center near Blacksburg, VA U.S. was built from marine plywood. A substrate of potting media and sand was placed in the flume bottom and was planted with woolgrass (*Scirpus cyperinus* (L.) Kunth), a native wetland species commonly used in mitigation wetlands. The *Scirpus cyperinus* (L.) Kunth was germinated in greenhouse in the spring of 2005, transplanted in late summer 2005, and allowed to establish before experiments began in the summer of 2006. Water was supplied to a head tank from a nearby pond and the flow rate through the flume was maintained at either 3.1 L/s or 4.1 L/s using a butterfly valve (Figure 3.1).

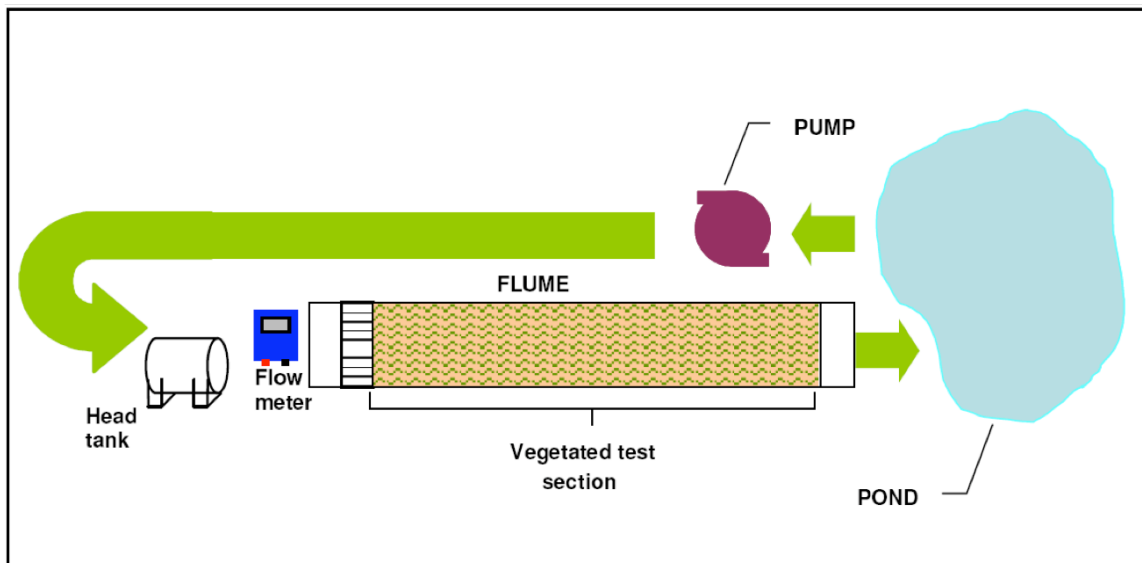


Figure 3.1 Flume experimental setup.

Flow rates were monitored continuously with an ultrasonic flow meter (Delta M-Flow Ultrasonic Flow Meter by Fuji Electric Corp. of America, Fremont, CA). A flow straightener calmed turbulence produced as the water entered the flume, before it flowed into the vegetated test section. Water depth was controlled by a sharp-crested outlet structure herein referred to as the tailgate; tailgate heights were 0, 0.1, 0.2, and 0.4 m above the soil surface. Three repeated measures of each combination of tailgate height and flow rate were conducted and the results

were averaged. Water surface elevation was measured at eight locations longitudinally and three locations laterally using a point gage (Figure 3.2).

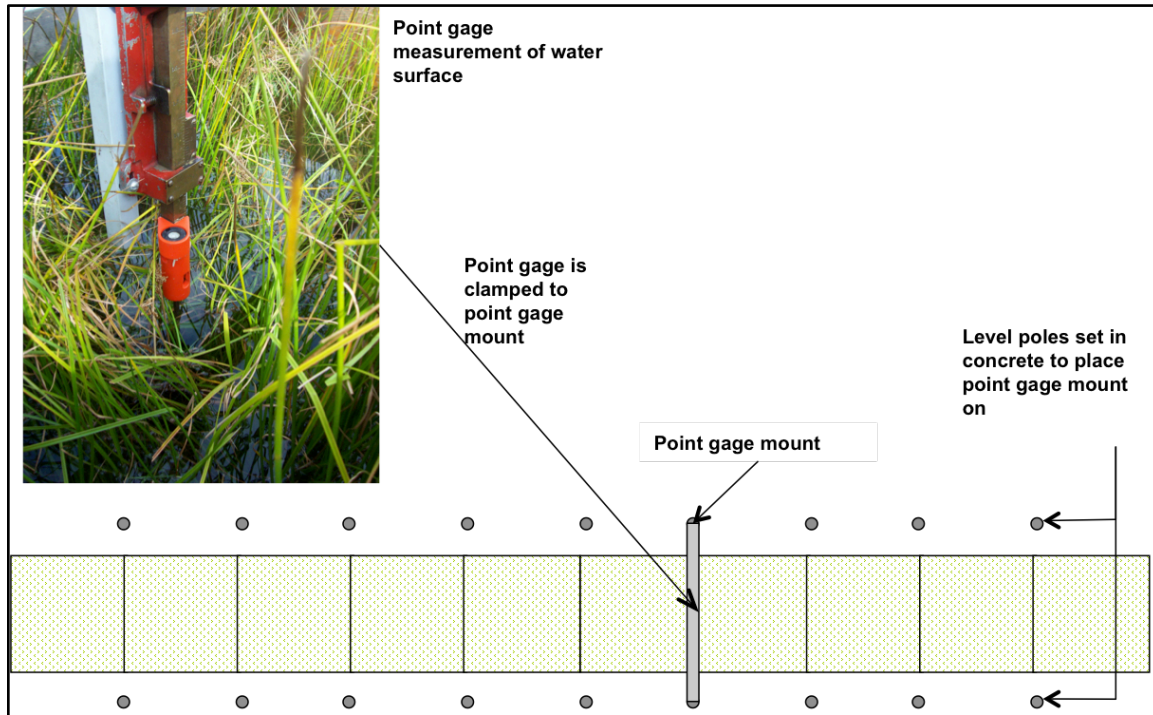


Figure 3.2 Point gage measurements of the flume water depth and water surface.

Flume measurements were repeated six times over the summer and fall of 2006 and 2007 at different planform stem densities, herein referred to as the vegetation state, for a total of 48 unique combinations of flow rate, stage, and vegetation state.

Pertinent vegetation characteristics were measured after each set of flume runs, corresponding to the six vegetation states. Stem density (N), stem diameter (d) (L) as a function of distance from the soil surface, vegetation height (z_b) (L), vegetation frontal area per unit volume (A_f) (L^{-1}), and vegetation flexural rigidity (MEI) ($M \cdot L^3 / T^2$) were measured using a stratified random sampling scheme. To assure a representative sample of vegetation was measured, the flume was divided into four 3-m long strata spanning the entire flume length.

Twelve stems were selected at random within the vegetated test section; the stem diameter was measured at 5-cm increments using calipers. N was measured by counting the number of stems

within 0.1-m² quadrats, randomly located within the vegetated test section. The stem count was repeated until the cumulative average did not change more than 1%.

A_f was measured using a photo-resolution technique. A 0.1-m² square sample plot was delineated perpendicular to the streamwise flow direction (Figure 3.3). An orange foamboard marked with a darker orange grid was placed vertically, immediately downstream of the sample plot. A digital photo was taken in the streamwise flow direction so the vegetation was in the foreground and the orange foamboard was in the background.

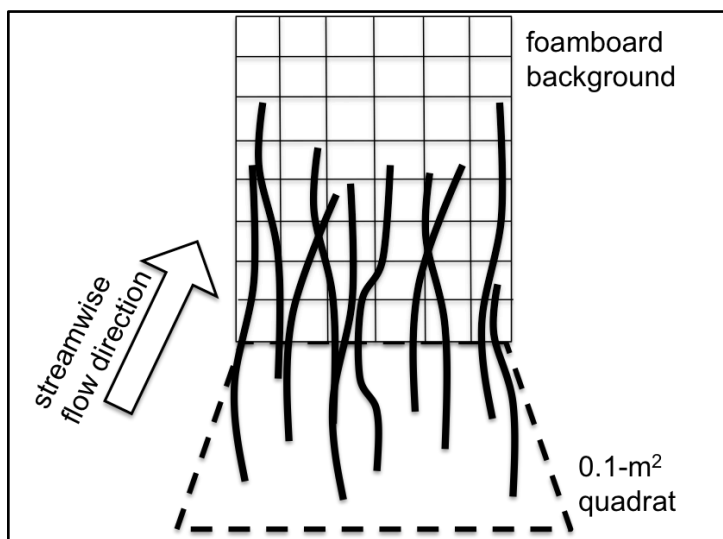


Figure 3.3 Diagram describing photo imaging technique for measuring streamwise frontal area of vegetation.

ArcGIS software was used to “georeference” the image to a grid corresponding to the size of the grid on the foamboard, creating an orthophoto from which measurements of length and area could be made. Remote sensing software [ERDAS *Imagine*, 2003] was used to classify each pixel of the orthophoto into either plant or background. The projected plant area for each water depth was calculated using the ArcGIS [2008] area function. The proportion of plant covering the area was calculated and reported as a blockage factor (BF). The blockage factor was used to determine A_f .

Vegetation flexibility was expressed as MEI and was measured using the method presented in *Kouwen* [1988]. An 1829 x 305-mm, 4.85-kg board was allowed to fall from a vertical

orientation in a streamwise direction onto the plants and the distance from the soil surface to the board was measured. The *MEI* parameter, which lumps flexural rigidity with overall vegetation density, was calculated using the expression reported by Kouwen [1988] and presented in Chapter 2 (Equation [2.17]).

Other required vegetation parameters were calculated using the measured vegetation parameters and included average stem spacing (Δs), the momentum absorbing area of the vegetation stand (*MAA*) (L^2), the momentum absorbing area per unit volume (*maa*) (L^{-1}), porosity (ϵ), and the area concentration of stems (bed area occupied by stems per unit bed area). Cross-sectionally averaged velocity was calculated in two ways: 1) the ideal velocity if the cross-section was free of vegetation ($A_x = h \cdot b$); and 2) the velocity based on the cross-sectional area available for flow (A_x minus the area occupied by plants). Point measurements of velocity were not made during the flume runs because velocity is strongly dependent on the measurement location, especially within dense vegetation [Liu *et al.*, 2008].

Chapter 4 Vegetation-induced roughness in low-Reynolds number flows

4.1 Introduction

Wetlands are environmentally and economically important, providing flood protection, habitat for wildlife and fisheries, improving water quality, and controlling coastal erosion [Townsend *et al.*, 2003]; however, over 53% of all wetlands in the U.S. have been lost since the mid 1780's [Dahl, 1990]. To counteract wetland losses, wetland land area is being replaced through wetland restoration and mitigation. Restoring and constructing wetlands is expensive: freshwater wetland restoration can cost from \$30,000 USD to \$104,000 USD per ha [Zentner *et al.*, 2003]. Despite the large price tag, replacing wetland area does not necessarily equate to the replacement of wetland function [Hilderbrand *et al.*, 2005]. Restored and constructed wetlands are often too wet to function effectively [Cole and Brooks, 2000], resulting in a loss of ecosystem services and a waste of financial resources.

Many factors lead to restored and constructed wetlands that are functionally too wet, including neglecting groundwater connectivity. For wetlands in which outflow is a component of the water budget, such as riparian wetlands, surface water stage is controlled all or in part by the hydraulic resistance within the wetland [Kadlec, 1990]. Several models quantify the hydraulic resistance from dense vegetation [Kadlec, 1990; Fathi-Moghadam and Kouwen, 1997; Nepf, 1999; Wu *et al.*, 1999; Stone and Shen, 2002; Hoffmann, 2004]. Our goal was to identify and assess the usefulness of models applicable to low-Reynolds number flows typical of low-gradient, densely-vegetated wetlands.

4.2 Methods

4.2.1 Flume Methods

Flowrate, water surface slope, and depth were measured in an experimental outdoor flume planted with dense emergent vegetation. The flowrate was maintained at 3.1 and 4.1 L/s for each of four tailgate heights (0, 0.1, 0.2, and 0.4 m). Experiments were repeated for six different

vegetation states for a total of 48 unique combinations of flowrate, depth, and vegetation density. Vegetation properties were quantified for each of the six vegetation states. Flow and vegetation properties were measured using methods detailed in Chapter 3.

4.2.2 Data Analysis

To estimate flow velocity through vegetation, a reference area (A_r) (L^2), and a drag coefficient (C_d) were determined. Six vegetated hydraulic resistance models, described earlier (Table 2.1), were identified to test: *Lindner* [1982] (as presented by *Järvelä*, [2004]), *Kadlec* [1990], *Fathi-Moghadam and Kouwen* [1997], *Nepf* [1999], *Stone and Shen* [2002], and *Hoffman* [2004]. As noted earlier, the only difference in the six models is the definition of A_r . Two C_d estimates were used: the C_d for an infinite isolated cylinder and a constant value (1.05). Four C_d predictors were also identified: *Lindner* [1982] (as presented by *Järvelä*, [2004]), *Taylor* [1985], *Choi and Kwon* [1999], and *Harvey et al.* [2009] (for ridge conditions). Two bulk drag coefficient (C_d') predictors were considered as well: the *Wu et al.* [1999] C_d' predictor and the field and lab formulations of the *Lee et al.* [2004] C_d' . The estimate of C_d' was substituted for the vegetal area coefficient (λ) (L^{-1}) and C_d in [2.8].

Model parameters were estimated using vegetation and flow data collected from the flume. Since it was often difficult to determine which slope definition was used in each model definition, hydraulic grade slope (S_g) and the friction slope (S_f) were considered in addition to the bed slope (S_b). Water surface was measured at three locations at each cross-section of the flume. The water surface measurements at each cross-section were averaged and the water surface slope was estimated from linear regression. S_f was estimated using the linear division of the slope into the slope due to stem resistance and the stem due to bed resistance [*Meyer-Peter and Muller*, 1948]. (The slope due to the bed resistance was determined by measuring the water surface slope of flow over the bare bed after the vegetation was removed.) Each combination of flow model and C_d predictor was tested, in addition to the three C_d' predictors, with each of the three slope definitions, for a total of 117 unique model formulations.

Model fit was assessed using a combination of qualitative judgment of fit to a 1:1 line, relative error analysis (defined as the difference between the predicted and average velocity divided by the average velocity), and typical goodness-of-fit statistics. The goodness-of-fit statistics considered were root mean square error ($RMSE$), root square ratio (ratio of $RMSE$ to the standard deviation) (RSR), and the Nash-Sutcliffe efficiency (NSE). The NSE is theoretically the same as R^2 except NSE can be negative, indicating the mean of the measured values is a better estimator than the model [Nash and Sutcliffe, 1970]. The NSE is calculated in the same way as R^2 .

4.3 Results

4.3.1 General Results

Hydraulic grade slope (S_g), friction slope (S_f), flow depth (h) (L), and cross-sectionally averaged velocity (V) (L/T) for the total cross-sectional area and the cross-sectional area modified by vegetation were derived from the measured water surface elevation, bed elevation, and flow rate. Depth and stem Reynolds numbers (Re_{depth} and Re_{stem}) were calculated using the depth and stem diameter as the respective characteristic lengths for both the total and vegetation-modified cross sections. Figure 4.1 shows the range of slopes, cross-sectionally averaged velocities, and stem Reynolds number (Re_{stem}) for each outlet elevation across the range of vegetation densities. Note the number of total successful experiments was not equal to 48 because some field data was eliminated due to inconsistent water surface measurements and/or the lack of a free nappe at the outlet weir.

Since depth was controlled using an outlet structure, the flow velocity and Re_{stem} decreased with increasing tailgate height. Energy grade slope and friction slope both decreased with increasing tailgate height due in part to the change in gravitational force applied by the flowing water and in part to the decreasing vegetation density with increasing tailgate height. Flows were steady and best characterized as gradually varying due to the variations in the cross-sectional area caused by microtopography and vegetation. The overall bed slope measured using the same point gage setup used to measure the water surface. The bed slope was not significantly different from 0% ($\alpha=0.05$), although the soil surface was not smooth. Point gage measurements of the soil surface had a standard deviation of 3.1 cm. The average height of the microtopographic features (likely

caused by tunneling and burrowing by rodents and erosion caused by repeated water releases under the tailgate) was 3.0 cm, nearly equal to the standard deviation of the soil surface measurements.

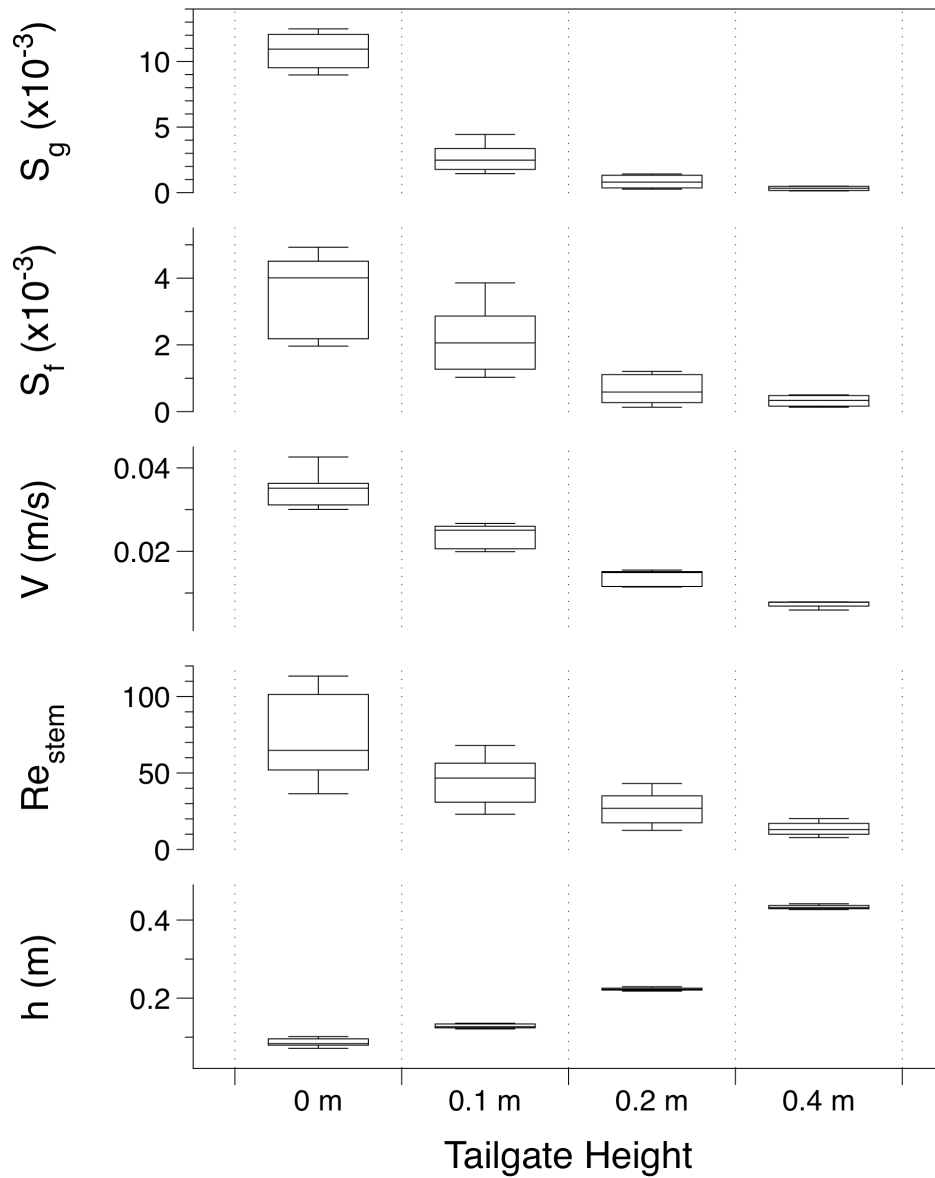


Figure 4.1 Boxplots of measured hydraulic grade slope (S_g), friction slope (S_f), cross-sectionally averaged velocity (V), stem Reynolds number (Re_{stem}), and depth (h) by tailgate height ($n=43$). Boxes represent the interquartile range, horizontal lines represent the median, and whiskers represent the maximum and minimum observed value.

S_g ranged from 1.4% for 0-m tailgate height, to 0.03% for 0.4-m tailgate height. S_f ranged from 0.5% for the 0-m tailgate height to 0.01% for 0.4-m outlet elevation relative to the soil surface. V

ranged from 0.036 m/s for 0-m tailgate height to 0.0058 m/s for 0.4-m tailgate height. Values of Re_{stem} were in the laminar range (7 – 134) across all tailgate heights although signs of instability, such as vortex shedding behind stems, were observed at higher Re_{stem} . The vortex patterns observed were consistent with the Von Karman vortex street phenomenon, as described in Kundu [1990].

N was high, ranging from 1,000 to nearly 10,000 stems per m^2 . However, the median stem diameter was small (0.2 cm) and did not vary much over the two-year study period (interquartile range = 0.1 cm). Since the stem densities were so high, the measured blockage factor (defined as the proportion of the flow area blocked by vegetation) was large. Vegetation occupied a median 67% of the available flow area for shallow flows (0-m tailgate height). The maximum blockage factor at the 0-m tailgate height was 92%. The blockage factor at larger depths (0.4-m tailgate height) was smaller, blocking a median value of 32% of the available flow area.

As discussed previously, slope can be defined as S_b , S_g , or S_f . The slope used for each model affected the agreement between the model and the measured data. Overall for all depths, all models, and all C_d and C_d' predictors, S_f gave the best agreement between the modeled and the measured velocities. For clarity, only the results for S_f are presented.

The cross-sectional area was calculated in two ways: the product of the flume width and the average depth and the product of the flume width and the average depth minus the area occupied by stems. However, the calculated velocity was not significantly different if the cross-sectional flow area included or excluded stem area, likely since stems only occupied 1% of the total fluid volume. Only results for the total cross-sectional area (neglecting the area occupied by stems) are presented.

4.3.2 Model Fit

Measures of fit such as NSE , $RMSE$, and RSR (ANOVA, $p < 0.0001$) were affected by the flow model and C_d predictor combination or C_d' predictor used, as well as experimental conditions including tailgate height and vegetation state. Comparisons between the final models were the same whether NSE , $RMSE$, or RSR was used. The partial sum of squares error was largest for the

C_d predictor and the flow model or C_d' predictor, indicating the choice of model definition had the largest effect on model fit.

The flow model that produced the best agreement between the measured and predicted average velocity for all C_d predictors, tailgate heights, and vegetation states was the *Fathi-Moghadam and Kouwen* (FMK) flow model with a mean NSE of -1.39 and a mean relative error of -0.68. A negative value of NSE indicates the mean of the measured data better describes the data than the model. Negative NSE values are not unexpected, as the study focused on a small range of velocities. While the FMK flow model resulted in the lowest mean NSE , NSE was not significantly different between flow models, except for the *Kadlec* definition, which had a significantly smaller NSE ($p < 0.0001$).

The C_d predictor that produced the best agreement between the measured and predicted average velocity for all C_d predictors, tailgates, and vegetation states was the *Harvey et al.* [2009] C_d predictor for ridge conditions (HR) with a mean NSE of -1.99 and a mean relative error of -0.10.

The variance among goodness-of-fit indices for each flow model and C_d predictor was large (coefficient of variation up to -0.63 for all flow models and up to -2.5 for all predictors), so no broad statements as to which C_d predictor or flow model should be used can be confidently made. To make conclusions about the performance of the flow models and the C_d predictors, each combination of flow model and C_d predictor was examined and compared individually.

C_d' is a lumped parameter combining the reference area (A_r) (L^2) definition and the C_d predictor into one parameter. Estimates of velocity obtained using C_d' predictors [*Wu et al.*, 1999; *Lee et al.*, 2004] were directly compared to each of the 36 combinations of flow model and C_d predictor. Of all 39 combinations of flow model and C_d predictor, as well as C_d' predictors, only six produced positive NSE s, indicating the model performed better than the mean of the measured values (Figure 4.2).

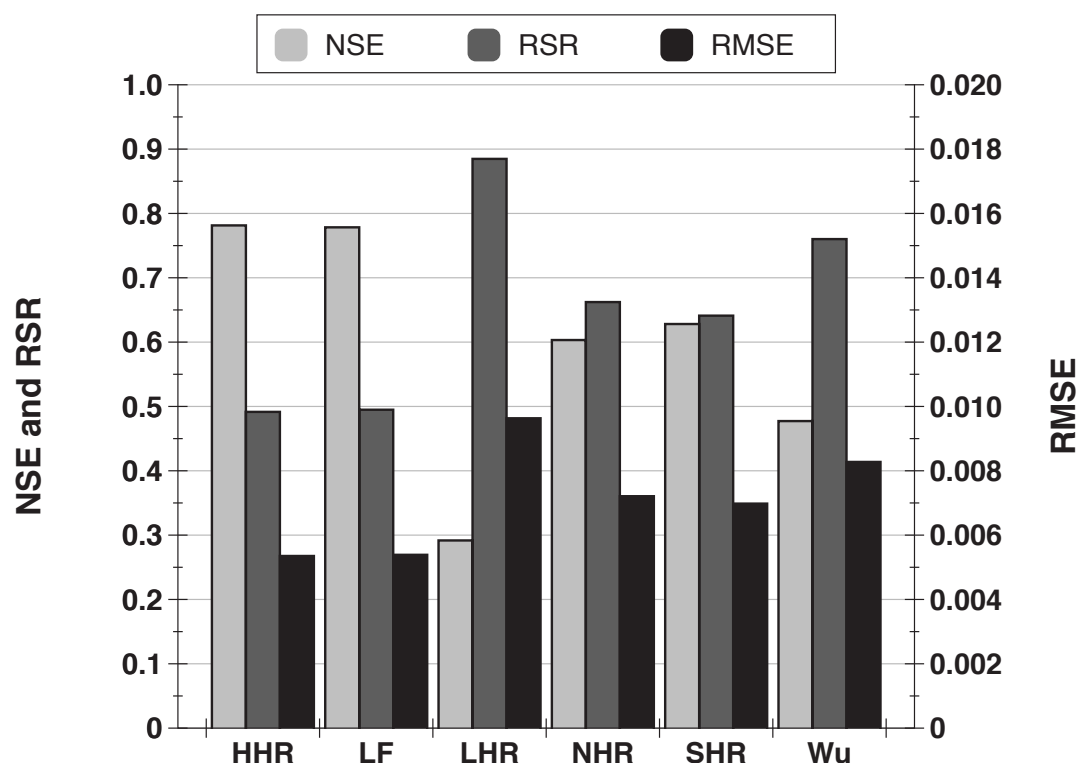


Figure 4.2 Goodness of fit statistics for the six best-performing models. Models include a drag coefficient predictor and a flow model. Fit statistics include the Nash-Sutcliffe Efficiency (*NSE*), root square ratio (*RSR*), and the root mean square error (*RMSE*). Models presented are the *Harvey et al.* [2009] model with the *Harvey et al.* [2009] drag coefficient predictor for ridge conditions, the *Lee et al.* [2004] bulk drag model for field conditions, the *Lindner* [1982] model with the *Harvey et al.* [2009] drag coefficient predictor for ridge conditions, *Nepf* [1999] model with the *Harvey et al.* [2009] drag coefficient predictor for ridge conditions, *Stone and Shen* [2002] model with the *Harvey et al.* [2009] drag coefficient predictor for ridge conditions, and the *Wu et al.* [1999] bulk drag model.

From hereon, only the six best-performing models (flow model + C_d predictor or C_d' predictor) will be discussed. Four of the six best flow model + C_d predictor combinations used the HR C_d predictor. The flow model combined with the HR C_d predictor that produced the best model fit were *Hoffman* [2004] ($NSE = 0.78$) (HHR), *Stone and Shen* [2002] ($NSE = 0.63$) (SHR), *Nepf* [1999] ($NSE = 0.60$) (NHR), and *Lindner* [1982] (presented by *Järvelä*, [2004]) ($NSE = 0.29$) (LHR). The other two positive NSE values were obtained using the *Wu et al.* [1999] C_d' predictor ($NSE=0.48$) (Wu) and the *Lee et al.* [2004] C_d' predictor for field conditions ($NSE=0.78$) (LF).

4.3.3 Relative Error Analysis

Relative errors were analyzed using ANOVA and Duncan-Waller multiple comparisons test (or a t-test for pairwise population comparisons) so the effects of tailgate height, flowrate, general vegetation state, measurement month, and specific vegetation parameters (e.g. stem diameter (d) (L), stem density (N), blockage factor (BF), and flexibility (MEI) ($M \cdot L^3/T^2$) on relative error magnitude and distribution could be examined for each “model”. Relative error analysis was conducted in place of residual analysis because the experimental velocities varied across an order of magnitude. A residual of the same size may indicate a relatively good model fit at the upper range of velocities but may be quite poor at the lower range. ANOVA of the relative error was conducted for each of the six best-performing models (C_d predictor or the combination of flow model and C_d predictor). Categorical variables such as tailgate height, flow rate, measurement month, measurement season, and general vegetation state were included in the ANOVA to determine if any interaction effects between relative error and the categorical variables were present.

Interaction effects between relative error and tailgate height and vegetation state were significant ($p < 0.0001$). The relative errors of the Wu and LF models were affected by the measurement month ($p < 0.010$). The relative error of the LF model was also affected by the measurement season ($p = 0.0018$), with larger relative errors during the summer than the fall. Vegetation parameters were correlated with the season, measurement month, and general vegetation state, which was to be expected, as plants multiply and grow during the growing season. The relative error for flow models and C_d predictors was affected by the measurement month and season but the effect is likely due to seasonal changes in vegetation properties rather than a true seasonal variation in model performance.

The relative error plots (similar to standard residual versus predicted value plots) of the models were heteroscedastic, indicating the variance of the relative error was not constant across the range of observations (Figure 4.3a). When the predicted velocity was large (> 0.02 - 0.035 m/s), LHR, NHR, SHR, and HHR overpredicted the velocity. However, when the predicted velocities were low (< 0.02 m/s), LHR, NHR, SHR, and HHR underpredicted the velocity. Linear and

nonlinear patterning was also evident, indicating the model error was not random and the model may require other variables to refine the fit.

The relative error plots of the Wu and LF C_d' predictors (Figure 4.3b and Figure 4.3c) did not show the same degree of linear and nonlinear patterning as the LHR, NHR, SHR, and HHR models. The Wu model showed some signs of heteroscedasticity, predicting more accurately at higher velocities than lower velocities. There was evidence of nonlinear patterning (note the parabolic shape of the error distribution) again indicating that the model may require the addition of other variables to refine the fit. The error distribution of the LF C_d' predictor (Figure 4.3c) was slightly heteroscedastic, but otherwise the error distribution appeared randomly distributed about the zero relative error line.

Since the relative error distributions for none of the best six models were ideal, the interaction of the relative error and other vegetation parameters was analyzed. Significant interactions are presented for all data and divided by tailgate height (Table 4.1).

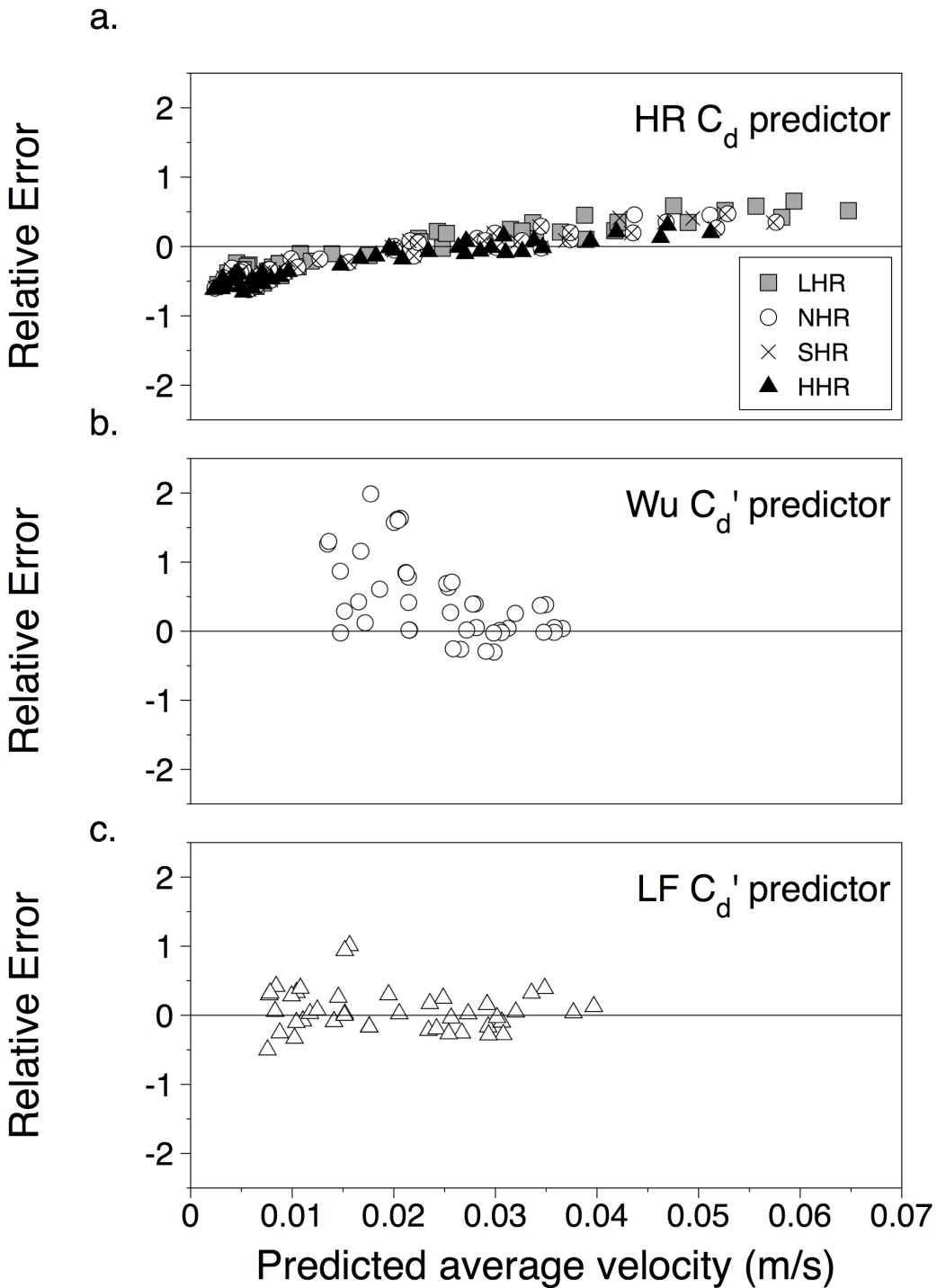


Figure 4.3 Relative error plots for the six best-performing models. a. *Lindner* [1982] (LHR), *Nepf* [1999] (NHR), *Stone and Shen* [2002] (SHR), and *Hoffman* [2004] (HHR) models with the *Harvey et al.* [2009] (HR) drag coefficient (C_d) predictor for ridge conditions; b. *Wu et al.* [1999] (Wu) bulk drag (C_d') predictor; and c. *Lee et al.* [2004] (LF) C_d' predictor for field conditions.

Table 4.1 Summary of significant relative error interactions for the six best-performing models by tailgate height. Significant interactions are described by the interaction trend direction, the effect of the interaction on model fit, and the p-value. Blank cells indicate the interaction was not significant.

Model Combination	Tailgate (m)		Stem diameter d	Blockage Factor BF	Flexural Rigidity MEI	Stem Density N
<i>Lindner</i> [1982] + <i>Harvey et al.</i> [2009] (LHR)	0	Trend Effect on fit p-value	+ Fit worsens w/ d <0.0001			
	0.1	Trend Effect on fit p-value	+ Fit worsens w/ d 0.0452			
	0.2	Trend Effect on fit p-value		+ Fit improves w/ BF 0.0230	+ Fit improves w/ MEI 0.0015	
	All data	Trend Effect on fit p-value	+ Optimal fit around $d \sim 0.2$ cm 0.0111	+ Optimal fit around $BF \sim 0.6$ 0.0380		
<i>Nepf</i> [1999] + <i>Harvey et al.</i> [2009] (NHR)	0	Trend Effect on fit p-value	+ Fit worsens w/ d <0.0001		+ Fit worsens w/ MEI 0.0484	
	0.1	Trend Effect on fit p-value	+ Fit worsens w/ d 0.0443			
	0.2	Trend Effect on fit p-value		+ Fit improves w/ BF 0.0182	+ Fit improves w/ MEI 0.0010	+ Fit improves w/ N 0.0060
	All data	Trend Effect on fit p-value	+ Optimal fit around $d \sim 0.26$ cm 0.0080	+ Optimal fit around $BF \sim 0.8$ 0.0295		
<i>Stone and Shen</i> [2002] + <i>Harvey et al.</i> [2009] (SHR)	0	Trend Effect on fit p-value	+ Fit worsens w/ d <0.0001			
	0.1	Trend Effect on fit p-value	+ Fit worsens w/ d <0.0454			

Table 4.1 (cont.) Summary of significant relative error interactions for the six best-performing models by tailgate height.

Model Combination	Tailgate (m)		Stem diameter d	Blockage Factor BF	Flexural Rigidity MEI	Stem Density N
<i>Stone and Shen [2002] + Harvey et al. [2009] (SHR)</i>	0.2	Trend Effect on fit p-value		+ Fit improves w/ BF 0.0230	+ Fit improves w/ MEI 0.0015	+ Fit improves w/ N 0.0091
	All data	Trend Effect on fit p-value	+ Optimal fit around $d\sim 0.27$ cm 0.0114	+ Optimal fit around $BF\sim 0.9$ 0.0396		
<i>Hoffman [2004] + Harvey et al. [2009] (HHR)</i>	0	Trend Effect on fit p-value		- Fit improves w/ BF 0.0260		
<i>Lee et al. [2004] for field conditions (LF)</i>	0	Trend Effect on fit p-value	- Optimal fit near $d\sim 0.15$ cm 0.0003			
	0.1	Trend Effect on fit p-value	- Optimal fit near $d\sim 0.22$ cm 0.0087			
	All data	Trend Effect on fit p-value	- Optimal fit near $d\sim 0.23$ 0.0002			
<i>Wu et al. [1999] (Wu)</i>	0	Trend Effect on fit p-value		+ Optimal fit near $BF\sim 0.83$ <0.0001		+ Optimal fit near 6500 stems/m ² 0.0101
	0.1	Trend Effect on fit p-value	- Fit improves w/ d 0.0420	+ Optimal fit near $BF \sim 0.22$ 0.0004		+ Fit worsens w/ N 0.0202
	0.2	Trend Effect on fit p-value		+ Optimal fit near $BF\sim 0.07$ 0.0030		+ Fit worsens w/ N 0.0319
	0.4	Trend Effect on fit p-value		+ Fit worsens w/ BF 0.0203		+ Fit worsens w/ N 0.0433

Relative error increased with increasing stem diameter for the LHR, NHR, and SHR models ($p=0.0111$, 0.0080 , and 0.0114 , respectively; Figure 4.4a) and decreased with increasing d for the LF C_d' predictor ($p=0.0002$; Figure 4.4b). The effect of d on relative error magnitude was amplified at the lower tailgate heights: no tailgate ($p<0.0001$) and the 0.1-m tailgate ($p<0.0454$).

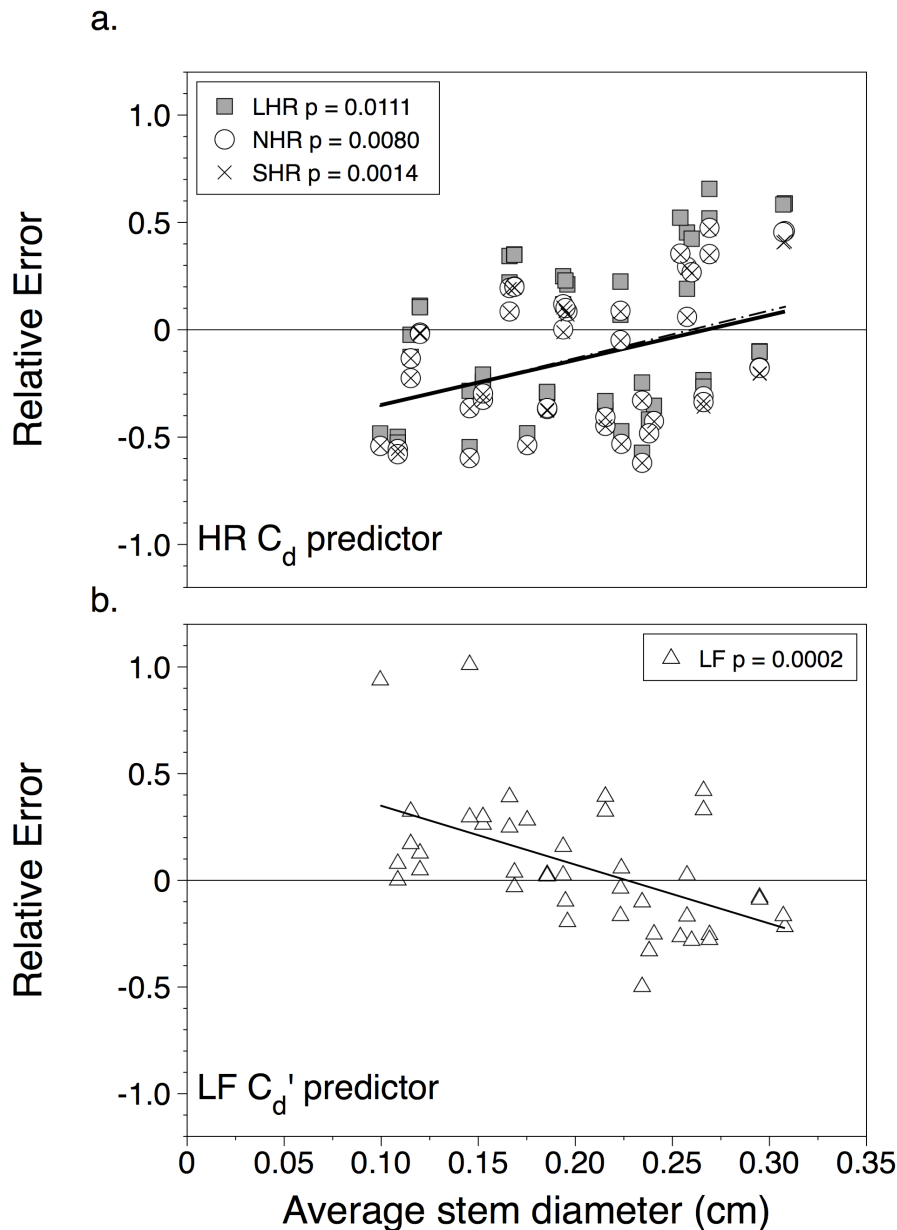


Figure 4.4 Interaction between relative error and average stem diameter. a. *Lindner* [1982] (LHR), *Nepf* [1999] (NHR), and *Stone and Shen* [2002] (SHR) models with the *Harvey et al.* [2009] (HR) drag coefficient (C_d) predictor for ridge conditions and b. *Lee et al.* [2004] bulk drag (C_d') predictor (LF).

While *BF* was not an input parameter into any of the best performing models, *BF* was a predictor of relative error magnitude. The magnitude of the relative error increased with increasing blockage factor for the LHR, NHR, and SHR models ($p < 0.0230$) at the 0.2-m tailgate height, with the best model fit occurring with large *BF* (Figure 4.5a). The same trend was significant when the data were not subdivided by tailgate height but the trend was not as evident ($p < 0.0396$). Relative error decreased with increasing blockage factor for the HHR model but only at the 0-m tailgate height ($p = 0.0260$). *BF* was a strong predictor of relative error at each tailgate height for the Wu model (Figure 4.5b) ($p < 0.0203$) indicating the addition of *BF* to the Wu model may improve the fit. For all but the 0-m tailgate height, the Wu model fit deteriorated with increasing *BF*; the model fit improved with increasing *BF* for the 0-m tailgate.

Flexural rigidity was another vegetation parameter not used as input to any of the best performing models. However, at the 0.2-m tailgate height, *MEI* was a significant predictor of relative error magnitude for the LHR, NHR, and SHR models ($p < 0.0015$; Figure 4.6). Model fit improved with increasing *MEI*, with the best model fit occurring when the vegetation was the stiffest (i.e. the most resistant to bending). The only significant interaction between *MEI* and relative error occurred at the 0.2-m tailgate height. At water depths approximately equal to 0.2 m, the vegetation was approximately 50% submerged.

The bending moment on the vegetation increased with depth and decreased with average velocity (the bending moment resultant force is located at $0.5 h$ assuming a uniform velocity distribution). The largest median bending moment was observed at the 0.4-m depth (0.40 N-m). The median bending moment at the 0.1-m and 0.2-m tailgate heights was approximately the same (0.23 and 0.22 N-m, respectively). The smallest median bending moment was observed at the 0-m tailgate height (0.18 N-m). The interaction between model fit and *MEI* would be expected to be the strongest when the bending moment is the largest. However, the only significant interaction between model fit and *MEI* occurred at the 0.2-m tailgate. The mean bending moment for the 0.1-m and 0.4-m tailgate heights was nearly equal to and was nearly twice as large as the bending moment at the 0.2-m tailgate, respectively. However, no significant interactions between *MEI* and relative error were observed at the 0.1-m and 0.4-m tailgates.

The only significant interactions between relative error and stem density were observed for the Wu C_d' predictor. The relative error increased with the stem density, with the best model fit occurring at the lowest stem density for all tailgate heights. While the strongest interaction was linear, the shape of the relative error plot appears slightly logarithmic or parabolic.

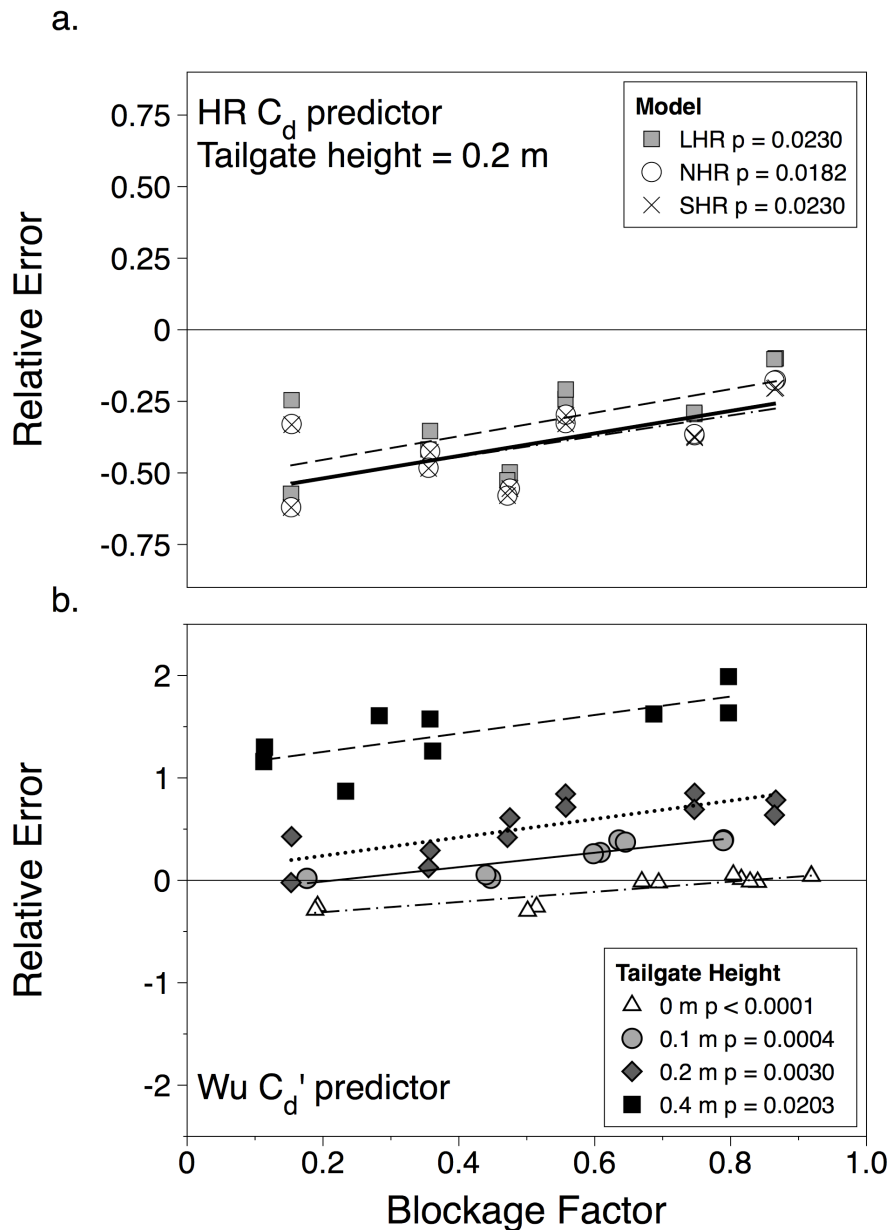


Figure 4.5 Interaction between relative error and blockage factor. a. *Lindner* [1982] (LHR), *Nepf* [1999] (NHR), and *Stone and Shen* [2002] (SHR) models with the *Harvey et al.* [2009] (HR) drag coefficient (C_d) predictor for ridge conditions at 0.2-m tailgate height and b. *Wu et al.* [1999] (Wu) bulk drag (C_d') predictor for each tailgate height.

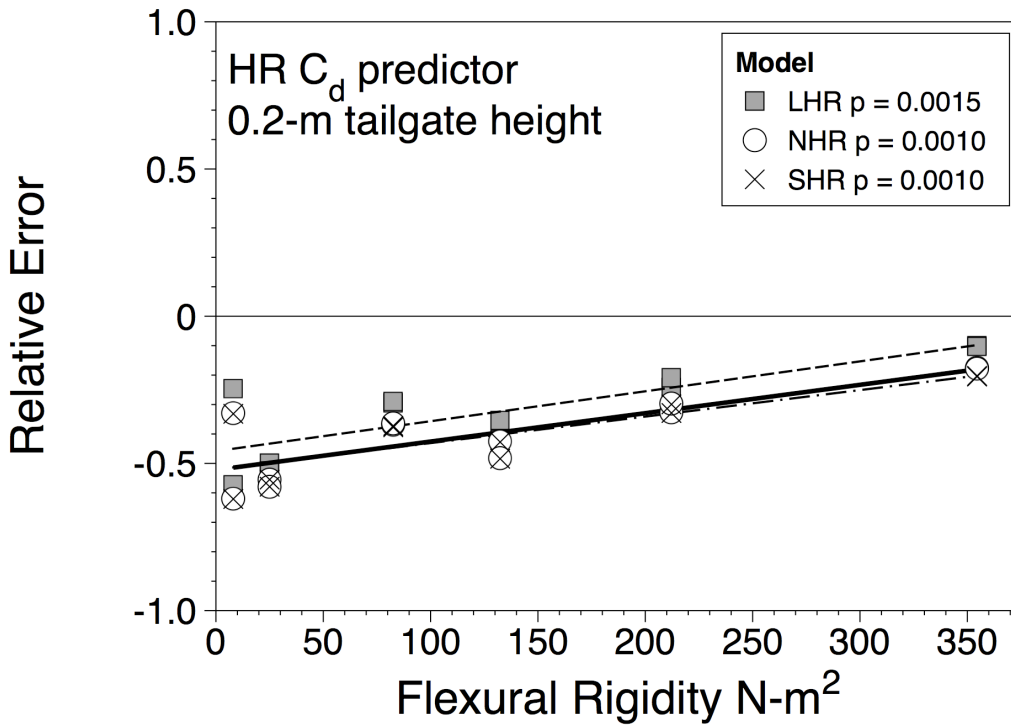


Figure 4.6 Interaction between relative error and *MEI*. Lindner [1982] (LHR), Nepf [1999] (NHR), and Stone and Shen [2002] (SHR) models with the Harvey et al. [2009] (HR) drag coefficient (C_d) predictor for ridge conditions at the 0.2-m tailgate height.

4.4 Discussion

4.4.1 Fit of individual models

The LF and the HHR models best described velocity through emergent *Scirpus cyperinus* (L.) Kunth and had the largest *NSE*, lowest *RMSE*, and the lowest *RSR* of all models tested. As compared with other models with positive *NSE* values, the relative error of the LF and HHR models had fewer interactions with vegetation parameters, such as stem diameter or density. Since interactions with model residuals or error are indicative of an underfit model, the lack of such interactions indicates the LF and HHR models describe flow through *Scirpus cyperinus* (L.) Kunth well.

The Wu C_d' predictor tended to overestimate velocity through *Scirpus cyperinus* (L.) Kunth, performing best for shallow flows (0-m tailgate height) (Figure 4.3c). The Wu model performed worse than any of the six best-performing models at large tailgate heights with relative error values approaching 2.0 at the 0.4-m tailgate. The Wu model fit was the only model that showed consistent relative error interactions with stem density; model fit deteriorated as more vegetation blocked the channel, especially as tailgate heights and depths increased Table 4.1. The interaction with stem density and BF is expected because the Wu model includes no metric for vegetation density; the prediction of the Wu C_d' depends only on S_f and Re_{stem} .

The HR C_d predictor overestimated drag at low Re_{stem} (i.e. high tailgates) and underestimated drag at high Re_{stem} (i.e. low tailgates). The slope of the relationship between Re_{stem} and C_d in the HR C_d predictor was larger than the observed relationship through *Scirpus cyperinus* (L.) Kunth (Figure 4.7). The HR C_d predictor worked fairly well for mid-ranges of Re_{stem} but not for the extreme values of Re_{stem} , likely because the experimental conditions of this study deviated from the conditions for which the relationships were developed. Re_{stem} in this study were similar to the reported Re_{stem} values in the *Harvey et al.* [2009] study but average velocities were nearly an order of magnitude higher and d was nearly seven times smaller. Consequently, the average $a \cdot d$, one of the input parameters into the HR C_d predictor, was an order of magnitude smaller in this study than the *Harvey et al.* [2009] study (0.0049 – 0.0024 vs. 0.012 - 0.028). The interaction of relative error with other parameters not included in the HR C_d predictor or λ (e.g. BF , MEI) indicates the HR fit may be improved by the inclusion of plant blockage or flexibility parameters.

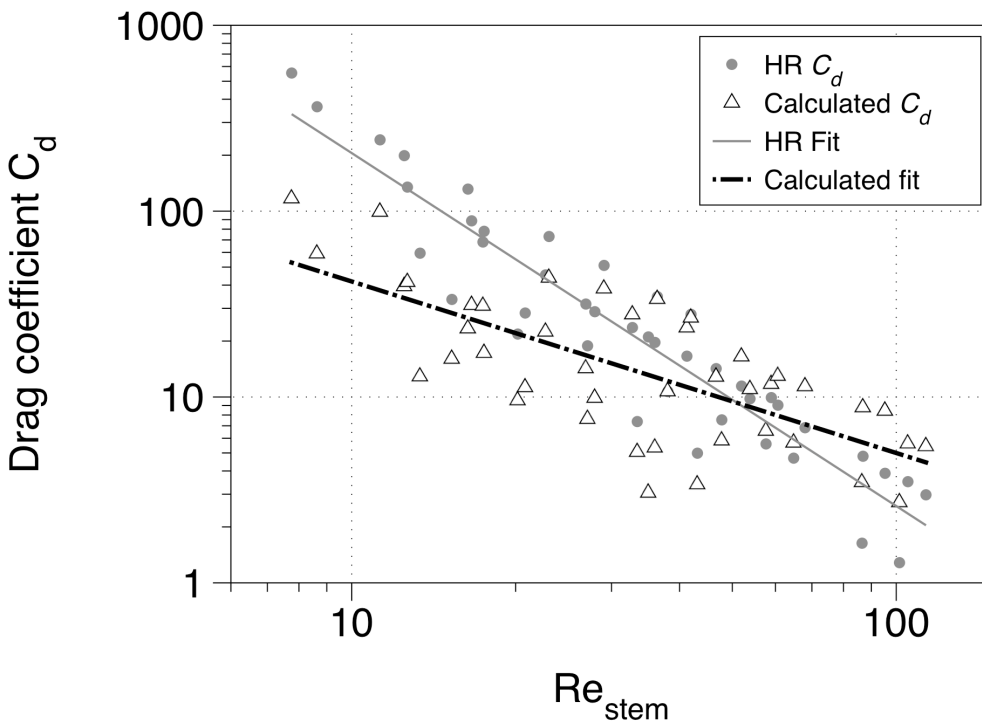


Figure 4.7 Drag coefficient versus Re_{stem} for the *Harvey et al.*[2009] drag coefficient prediction relationship (HR). Circles are the drag coefficient as predicted by the HR drag coefficient prediction. Triangles are the calculated drag coefficient for this study assuming the use of the *Nepf* [1999] flow model.

4.4.2 Overall trends in model fit

Tailgate height significantly affected model fit for all of the best-performing models. The HHR, LHR, NHR, SHR, and LF models all performed well (Figure 4.8) at the 0.1-m tailgate height when the flow depth was about 30% of the total plant height. The LF model also performed well at the 0.2-m tailgate when the flow depth was about 50% of the total plant height. Vegetation flexibility, *MEI*, and the proportion of the channel area blocked by vegetation influenced the model fit for the LHR, NHR, and SHR models at the 0.2-m tailgate. At water depths about 50% of the total plant height, the LHR, NHR, and SHR models may require the addition of *MEI* or *BF* parameters to completely describe the flow through *Scirpus cyperinus* (L.) Kunth.

For all models, the relative error was the greatest at the 0.4-m tailgate, likely due to the relatively low water surface slopes at higher water depths (Figure 4.8). However, the relative error did not show significant interactions with vegetation properties at the 0.4-m tailgate height except for interactions with *BF* and *N* for the Wu model. At higher tailgate heights, the variance of S_g

increased: the S_g coefficient of variation at the 0.2-m and 0.4-m tailgates was larger than the coefficient of variation for smaller tailgate heights (0.51 and 0.48 for the 0.2-m and 0.4-m tailgates, respectively, versus 0.11 and 0.35 for the 0-m and 0.1-m tailgates, respectively). At the 0.4-m tailgate, cross-sectionally averaged velocity was the smallest and friction slope was the lowest. At small friction slopes, the water surface was susceptible to effects from wind or other disturbances such as rain. The change in elevation head across the experimental section was small (0.003 m) and close to the margin of error of the measurement apparatus (0.001 m) so the uncertainty in the estimate of the friction slope at the 0.4-m tailgate was larger in relation to the true friction slope at lower tailgate heights.

The performance and error distribution of the LHR, NHR, and SHR models was similar. The similarity between the performances of several models is due to the fact that the reference area definitions of these models are identical or similar. The NHR and the SHR models produce similar results as shown in Figure 4.4, Figure 4.5, and Figure 4.6). The reference areas for the NHR and SHR models are identical ($N \cdot d \cdot h$). The bottom area definitions differ slightly; the NHR model uses the whole bottom area, while the SHR model excludes the bottom area occupied by stems.

All of the best-performing models employed an empirical regression relationship (HR, HF, and Wu) to estimate C_d or C_d' . While some of the model error may be due to the exclusion of important vegetation parameters such as MEI , another source of error may be the regression coefficients. To expand model use, the empirical regression coefficients should be examined over a range of vegetative and flow conditions. The regression coefficients are a function of flow and vegetation parameters [Tsihrintzis, 2001]; however, it is still uncertain how the coefficients change over a range of flow depths and Re_{stem} . While vegetation stem diameter and stem density are relatively simple to measure for simple vegetation structures such as cylindrical rush, branching or leafed vegetation is more difficult to analyze. Even determining Re_{stem} is difficult for plants in which a characteristic stem diameter is uncertain. MAA or BF may be easier to determine and may be a more appropriate way to quantify A_r than N or d .

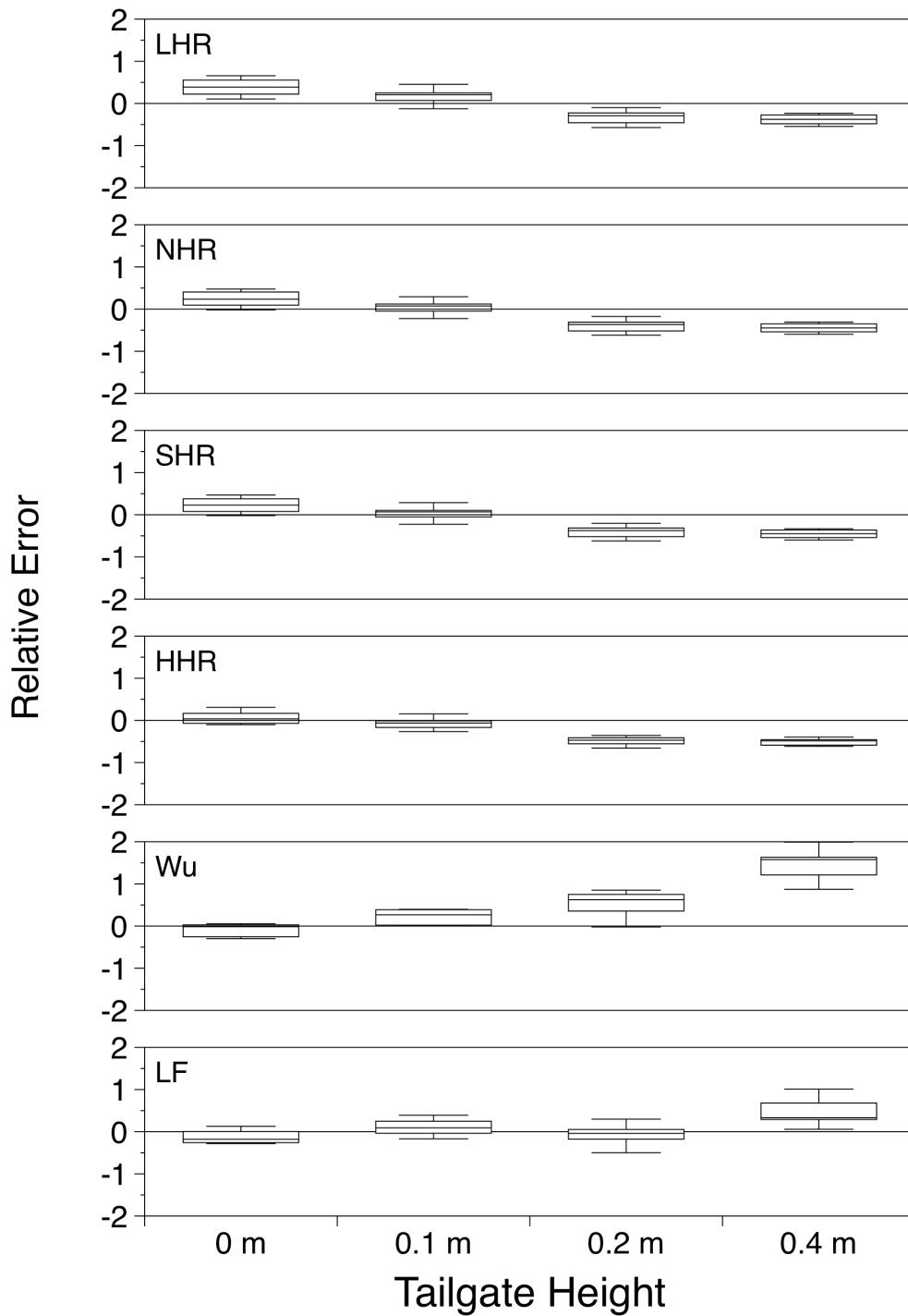


Figure 4.8 Model relative error by tailgate height. Models from top to bottom are: *Lindner* [1982] (LHR), *Nepf* [1999] (NHR), *Stone and Shen* [2002] (SHR), and *Hoffman* [2004] (HHR) models with the *Harvey et al.* [2009] drag coefficient predictor for ridge conditions; *Wu et al.* [1999] bulk drag predictor (Wu); and *Lee et al.* [2004] bulk drag predictor for field conditions (LF).

4.5 Conclusions

The goal of this study was to determine which models were most useful in describing flow through densely vegetated emergent flows typical of those found in wetlands. The models identified in the literature differed only in the definition of the drag reference area and the corresponding bottom area. Despite the drag reference area used, C_d must also be predicted using either an assumption that C_d is constant or that C_d is equal to the C_d for a single isolated cylinder, or using any number of predictive relationships derived from laboratory and field experimental data. C_d' predictors combine the C_d prediction and the flow model. The best performing combinations of flow model and C_d prediction and/or C_d' predictors were the LHR, NHR, SHR, HHR, LF, and Wu. All of the best performing models were based on empirical regression relationships developed from field experiments, and in the case of the Wu C_d' predictor, a collection of existing lab and field data.

The best models performed well at low to moderate water depths (30-50% of the vegetation submerged) and poorly at water depths that approached the vegetation depth. While the goal of the study was not to predict model error, results indicated model relative error was a function of vegetation properties such as d , BF , and MEI . For the two models with the highest $NSEs$, the LF and HHR models, the dependency of model error on vegetation properties was not as strong as for the LHR, NHR, SHR, and Wu models.

Of the six models examined in this study, the *Lee et al.* [2004] C_d' model and the *Harvey et al.* [2009] C_d predictor in conjunction with the *Hoffman* [2004] flow model perform the best. However, Δs can be difficult to measure in natural vegetation and must be calculated. For non-cylindrical vegetation, Δs can be difficult to define, especially if the vegetation is branching. The *Harvey et al.* [2009] drag coefficient predictor in conjunction with the *Nepf* [1999] or the *Stone and Shen* [2002] flow models also perform well and do not require an estimate of Δs , which may be optimal in situations in which Δs is difficult to measure or quantify.

The interaction between model fit and vegetation properties indicates the models are not completely defined across all water depths. The regression coefficients of the C_d and C_d'

prediction relationships are functions of flow and vegetation properties [Tsihrintzis, 2001]. The C_d and C_d' regression coefficients should be allowed to vary depending on the vegetation structure and density. However, without refitting the regression equations for each vegetation community, it is unclear how to change the regression coefficients to reflect changes in vegetation structure and density.

Chapter 5 The relationship between friction factor and vegetation properties in emergent vegetated flows

5.1 Introduction

Wetlands are environmentally and economically important providing flood protection, improving water quality, controlling coastal erosion, and providing habitat for wildlife and fisheries [Townsend *et al.*, 2003]. Over 53% of all wetlands in the U.S. have been lost since the mid 1780's [Dahl, 1990]. To counteract wetland losses, wetland land area is being replaced through wetland restoration and mitigation. Restoring and constructing wetlands is expensive. It can cost from \$30,000 USD to \$104,000 USD per ha to restore a freshwater wetland [Zentner *et al.*, 2003]. Despite the large price tag, replacing wetland area does not necessarily equate to the replacement of wetland function [Hilderbrand *et al.*, 2005]. Restored and constructed wetlands are often too wet to effectively function [Cole and Brooks, 2000].

Many factors lead to restored and constructed wetlands that are functionally too wet, including neglecting groundwater connectivity. Modeling surface flow in wetlands and shallow overbank flows on floodplains requires accurate simulation of hydraulic resistance from vegetation. For wetlands in which outflow is a component of the water budget, such as riparian wetlands, surface water stage is controlled all or in part by the hydraulic resistance within the wetland [Kadlec, 1990]. Hydraulic models that consider vegetation rely on an accurate determination of a resistance parameter such as a friction factor or drag coefficient. At low Reynolds numbers typical of shallow flows through emergent vegetation, hydraulic resistance is orders of magnitude higher than fully turbulent flows and resistance parameters are functions of the flow regime and water depth as well as the vegetation density and structure.

The exact relationship between hydraulic resistance, flow regime, and vegetation properties at low-Reynolds number flows is unclear. Previous studies have modeled hydraulic resistance using vegetation properties; however, many studies were based on rigid and/or simplified vegetation models such as wooden dowels over a uniform bed [Nepf, 1999]. Studies in natural settings such as the Everglades did not collect the full range of vegetation parameters thought to affect hydraulic resistance [Lee *et al.*, 2004; Harvey *et al.*, 2009]. Vegetation flexibility is

acknowledged to affect hydraulic resistance [Fathi-Moghadam, 2007]. However, it is frequently not measured in studies on natural vegetation. This study aims to determine the relationship between friction factor and measurable properties of natural vegetation including the vegetation area, stem density, stem diameter, vegetation spacing, and flexibility.

5.2 Methods

5.2.1 Flume methods.

Flowrate, water surface slope, and depth (h) (L) were measured in an experimental outdoor flume planted with dense emergent vegetation. The flowrate was maintained at 3.1 and 4.1 L/s for each of four tailgate heights (0, 0.1, 0.2, and 0.4 m). Experiments were repeated for six different vegetation states for a total of 48 unique combinations of tailgate height, flowrate and vegetation state. Vegetation properties were quantified for each of the six vegetation states. Flow and vegetation properties were measured using methods detailed in Chapter 3.

Friction factor (f) was calculated using the Darcy-Weisbach equation. Velocity was assumed to be the cross-sectionally average velocity (V) (L/T) of the flow through the plants, not accounting for the area occupied by the plants. The hydraulic gradient was assumed to be equal to the friction slope since pressure was atmospheric and velocity was small. The hydraulic radius was assumed to be equal to the water depth.

5.2.2 Regression techniques

Multiple linear regression was employed to determine the combinations of Buckingham Π terms that best described the variance in friction factor (Equation [2.14]). Scatter plots of the response versus predictive variables indicated that transformation would be necessary to produce a linear relationship. The transformation was selected based on the best linear correlation with the response variable using guidance from *Montgomery et al.* [2006]. A log-log transform was chosen to produce a linear relationship and to damp the variance observed in the x and y data.

Combinations of regression parameters were selected using stepwise multiple linear regression with alpha level of 0.05 and 0.10 required for entrance and elimination to the model,

respectively. All model coefficients were significant at $\alpha=0.05$. Model multicollinearity was assessed using the variance inflation factor (VIF) and the condition index as defined by *Montgomery et al.* [2006]. Models with VIFs greater than 10 were rejected and condition indices greater than 100 were rejected.

Once the combination of Π terms was selected, the final model form was determined using the MM-estimator robust regression algorithm [*Yohai*, 1987]. Robust regression techniques were used due to the existence of outliers in the predictive and response variables as well as the unequal variance across the entire range of predictive variables. In simple linear regression, the further an x or y value is from the distribution mean, the more influence that value has on the final shape of the regression relationship. MM-estimator robust regression damps outlier values with the Legendre Chi function so observations near the distribution mean have the most weight. For data sets with constant variance or without outliers, robust regression produces nearly identical results to least squares regression [*Montgomery et al.*, 2006]. The MM-estimator algorithm was selected since it performs well for most outliers in x and y space [*Simpson et al.*, 1998]. All model coefficients were significant at $\alpha = 0.05$. The robust deviance was used to determine the suitability of the model fit. If the ratio of the deviance to the model degrees of freedom ($n-p$, where n is the number of observations and p is the number of model parameters including the intercept) was much greater than 1, the model was discarded as unsuitable [*Montgomery et al.*, 2006].

The robust Aikake information criterion (AICR) and robust Bayesian information criterion (BICR), two model selection criteria, were used to rank the final models. The AICR and BICR are the difference between the number of model parameters and the log of the maximum likelihood function. The AICR and the BICR weigh the cost of adding an additional model term versus the improvement in model fit.

Regression performance was also assessed visually using residual and relative error plots. Using the coefficient of variation, variation in model error was assessed visually and quantitatively using the relative error versus predicted f plots. The coefficient of variation is a good way to

compare variance between groups of observations since it is dimensionless and scale-independent.

5.2.3 Regression Validation

Regression models were derived from data collected in a monoculture of emergent *Scirpus cyperinus* (L.) Kunth over a limited range of flow rates. Due to the limited nature of the data set, validation of the regression models with independent data was desirable. However, no existing data set included all the parameters measured in this study over a comparable range of Reynolds numbers. *Harvey et al.* [2009] data were collected over comparable range of Reynolds numbers and vegetation densities; however, the dataset lacked the *MEI* parameter included in the Buckingham Π and regression analyses; therefore, only the performance of regression relationships that did not contain the flexibility parameter could be assessed. Friction factors were estimated using the *Harvey et al.* [2009] flow and vegetation data and the results were compared to the friction factors back-calculated using the Darcy-Weisbach equation. Model performance was assessed using residual and relative error plots and goodness-of-fit indices, the Nash-Sutcliffe Efficiency (*NSE*) and the root-mean square error (*RMSE*). The *NSE* is theoretically the same as R^2 except *NSE* can be negative, indicating the mean of the measured values is a better estimator than the model [*Nash and Sutcliffe*, 1970]. The *NSE* is calculated in the same way as R^2 .

5.3 Results and discussion

Regression analysis was conducted to develop predictive relationships that relate friction factor to flow and vegetation properties. The area coefficient was expressed both as the unit momentum absorbing area (*maa*) and the vegetation frontal area per unit volume (A_f). Four of the seven Π terms (Equation [2.14]) were combined to form five models. Four models were based on *maa* and one was based on A_f . Three of the five models were modified to include a tailgate height interaction term, which effectively changed the form of the regression relationship when the tailgate height was 0.2 m or when water depth was approximately 50% of the vegetation height. Independent validation of the simplest two-term *maa* regression model was conducted using flow and vegetation data collected in the Everglades, FL, U.S. [*Harvey et al.*, 2009].

5.3.1 Robust regression

5.3.1-1 *maa* Regressions

Four regression models satisfied the criteria described in the methods section for bias, multicollinearity, and significance: one two-term model, two three-term models, and one four-term model. The best models are summarized in Table 5.1. The simplest model (2M) included $maa \cdot d$ and Re_{stem} , and was similar to the model presented in *Harvey et al.* [2009] with slightly different regression coefficients.

Table 5.1 Summary of regression models for emergent vegetated flows using the area coefficient based on the unit momentum absorbing area (*maa*).

ABV.	Equation ¹	Robust R ²	AICR	BICR	Deviance
2M	$f = 10^{4.98} (maa \cdot d)^{0.47} Re_{stem}^{-1.52}$	0.71	34.1	42.2	0.72
3Ma	$f = 10^{-1.11} (maa \cdot d)^{0.43} \left(\frac{MEI}{\rho V^2 d^4} \right)^{0.09} \left(\frac{d}{h} \right)^{-1.27}$	0.72	34.5	45.8	0.64
3Mb	$f = 10^{3.50} (maa \cdot d)^{0.44} \left(\frac{MEI}{\rho V^2 d^4} \right)^{0.08} Re_{stem}^{-1.31}$	0.71	35.2	46.2	0.62
4M	$f = 10^{1.39} (maa \cdot d)^{0.44} \left(\frac{MEI}{\rho V^2 d^4} \right)^{0.08} \left(\frac{d}{h} \right)^{-0.64} Re_{stem}^{-0.69}$	0.73	33.7	48.2	0.57

¹ where Re_{stem} is the Reynolds number based on stem diameter, maa is the unit momentum absorbing area (maa), d is the stem diameter, h is the flow depth, MEI is the vegetation flexural rigidity, ρ is the fluid density, V is the flow velocity, AICR is the Akaike Information Criterion, BICR is the robust Bayesian Information Criterion

Figure 5.1 shows the relative model error versus the predicted friction factor for each of the four models. In general, as the number of regression terms increased, the relative error was reduced and the distribution was tighter around the line of zero relative error. There were two outlier points with relative errors near -0.6 that were excluded from Figure 5.1 so the distribution closer to zero relative error could be observed.

The 2M regression had the most scatter around the zero relative error line (coefficient of variation = -5.02). With the addition of a third term, the amount of scatter around the zero relative error was reduced slightly (coefficient of variation 3Ma = -3.86, 3Mb = -4.23). The four-term regression model had the largest robust R^2 (Table 5.1). The fit of the 4M regression improved near the center of the friction factor distribution. All models had near and far outliers and no model appeared to handle the outlier values better than any others. However, despite the presence of the outliers, the use of robust regression ensures that the outlier points do not have a disproportionate influence on the final form of the regression.

The robust R^2 increased and the deviance decreased with the addition of each term, although the increases were small (Table 5.1). The AICR increased with the addition of a third regression term (2M \rightarrow 3Ma or 2M \rightarrow 3Mb), indicating that the addition of a third term did not increase the overall model fit enough to be worth the cost of the additional complexity a third term added. However, the 4M model had a slightly lower AICR than the 3Ma and 3Mb models and the 2M model, which indicates the improvement in model fit is worth the additional complexity. Predictably, the BICR increased with the addition of each term since the “cost” of adding an additional term increases the BICR more than the AICR.

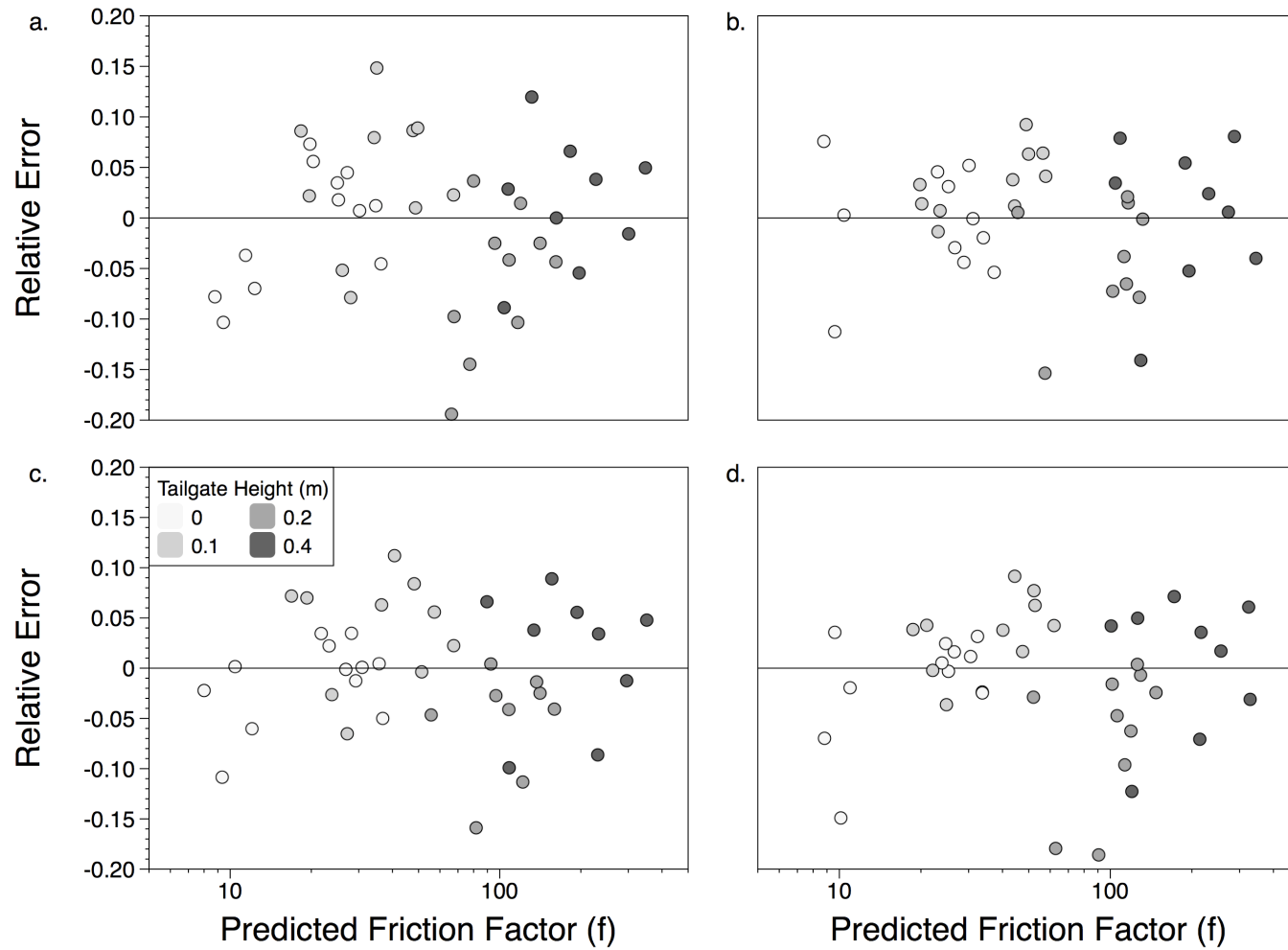


Figure 5.1 Relative error distribution for regressions a. 2M, b. 3Ma, c. 3Mb, and d. 4M shaded by tailgate height. Regressions predict friction factor (f) as a function of vegetation and flow properties.

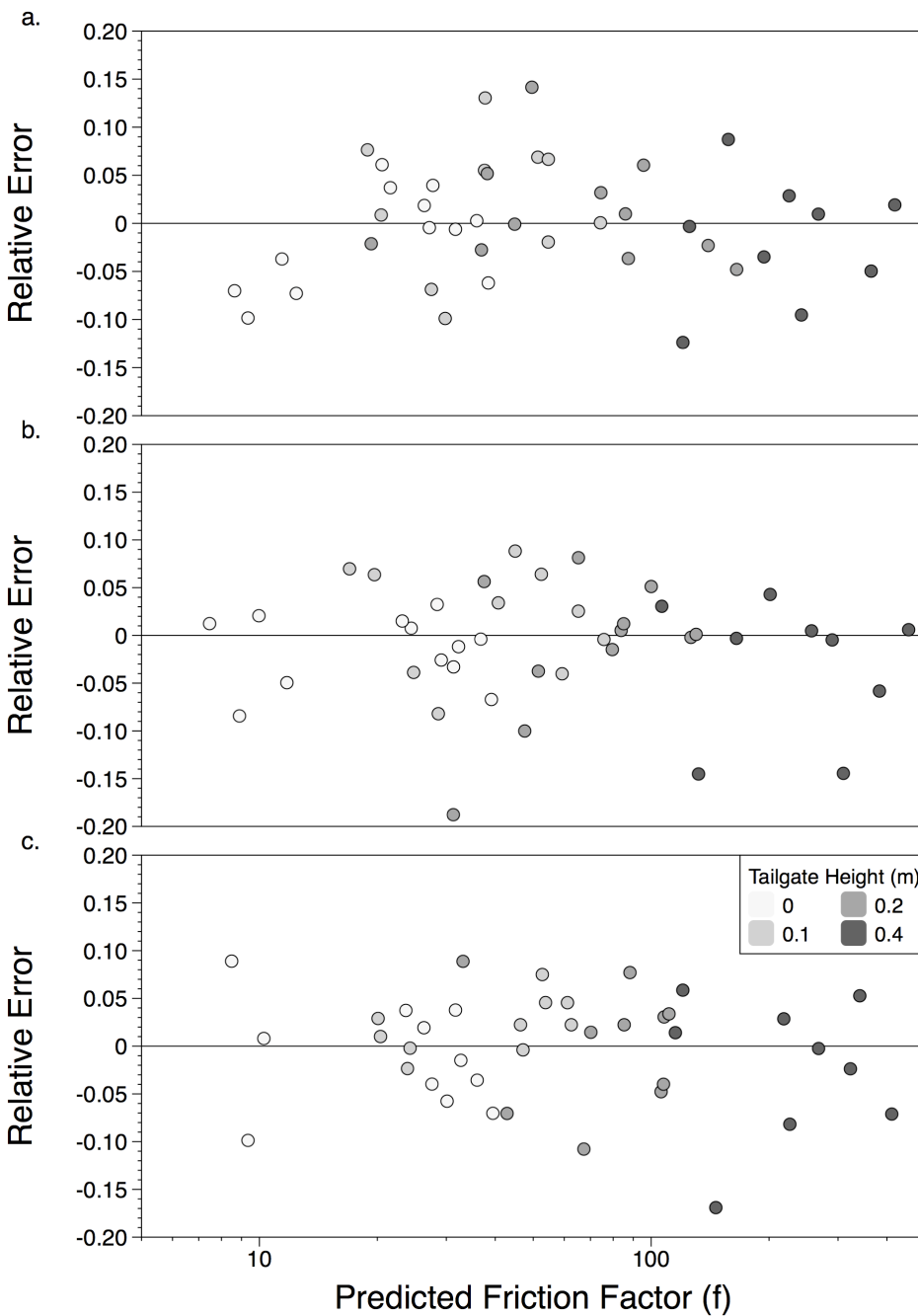


Figure 5.2 Relative error distribution for regressions a. 2MI, b. 3MIa, and c. 3MIb shaded by tailgate height. Regressions predict friction factor (f) as a function of vegetation and flow properties.

5.3.1-2 maa regressions with tailgate indicator variables

The relative error of the friction factor estimates was subdivided by tailgate height to determine if the relative error was affected by tailgate height. Figure 5.1 indicated the models did not

perform equally well at all tailgate heights. The relative error of the 0.2-m tailgate increased in a negative direction with increasing predicted friction factor. The degree of variation of the relative error for the 0.4-m tailgate was large (coefficients of variation for each model range from 3.98 to 14.31) in comparison to the relative error variation within other tailgate heights. The absolute value of the coefficient of variation was the largest for the 0.4-m tailgate height for all models but the 2M model. However, the distribution of relative error was fairly random (Figure 5.1). The 0-m tailgate and the 0.1-m tailgate produced relatively small relative errors that were mostly randomly distributed.

The robust regression procedure was repeated with the inclusion of a binary variable for each tailgate height. The binary variables are commonly referred to as indicator or “dummy” variables. Tailgate height indicator variables are essentially proxy variables for water depth. However, since depth was controlled by the tailgate, it is not a continuous random variable. Three indicator variables were necessary to compare the pairwise differences in regression coefficients for each of the four tailgate heights. However, for each of the four *maa* regressions, only the regression coefficients for the 0.2-m tailgate height were significantly different from the other tailgate heights. The 0-m and 0.1-m tailgate heights were not significantly different from each other. The estimated values of regression coefficients for the 0.4-m tailgate were not significantly different from zero since the variation in the friction factor estimates were so large.

The addition of a 0.2-m tailgate height indicator variable improved the overall model fit compared with the original *maa* regressions presented in Table 5.1, increasing the robust R^2 and decreasing the deviance (Table 5.2, Figure 5.2). The AICR increased with the addition of the 0.2-m tailgate height indicator variable for the two-term regression; however, the addition of the 0.2-m tailgate height term decreased the AICR for both three-term regressions. The addition of the indicator variable increased the BICR, which is expected since the BICR has a large “penalty” for adding additional model terms. Of all regressions (with and without indicator variables), the model with the largest robust R^2 , the lowest deviance, and the smallest AICR was the three-term regression including *maa·d*, *MEI*, *Re_{stem}*, and a 0.2-m tailgate height indicator variable on *maa·d*.

Table 5.2 Summary of regression models for emergent vegetated flows using the area coefficient based on the unit momentum absorbing area (*maa*) with the addition of a tailgate height indicator variable for the 0.2-m tailgate height.

ABV.	Equation ¹	Robust R ²	AICR	BICR	Deviance
2MI	If tailgate height is 0.2-m: $f = 10^{6.82} (maa \cdot d)^{0.82} Re_{stem}^{-2.48}$	0.75	34.8	51.1	0.43
	Otherwise: $f = 10^{5.19} (maa \cdot d)^{0.49} Re_{stem}^{-1.61}$				
3MIa	If tailgate height is 0.2-m: $f = 10^{-1.26} (maa \cdot d)^{0.53} \left(\frac{MEI}{\rho V^2 d^4} \right)^{0.10} \left(\frac{d}{h} \right)^{-1.33}$	0.75	33.0	47.2	0.51
	Otherwise: $f = 10^{-1.26} (maa \cdot d)^{0.45} \left(\frac{MEI}{\rho V^2 d^4} \right)^{0.10} \left(\frac{d}{h} \right)^{-1.33}$				
3MIb	If tailgate height is 0.2-m: $f = 10^{3.61} (maa \cdot d)^{0.56} \left(\frac{MEI}{\rho V^2 d^4} \right)^{0.09} Re_{stem}^{-1.43}$	0.76	32.5	47.1	0.38
	Otherwise: $f = 10^{3.61} (maa \cdot d)^{0.46} \left(\frac{MEI}{\rho V^2 d^4} \right)^{0.09} Re_{stem}^{-1.43}$				

¹ Re_{stem} is the Reynolds number based on stem diameter, *maa* is the unit momentum absorbing area (*maa*), *d* is the stem diameter, *h* is the flow depth, *MEI* is the vegetation flexural rigidity, ρ is the fluid density, *V* is the flow velocity, AICR is the Aikake Information Criterion, BICR is the robust Bayesian Information Criterion

The overall relative error distributions between the basic model and the model with the additional tailgate indicator variable were not significantly different. The addition of the 0.2-m tailgate term addition improved fit for 0.2-m tailgate heights ($p < 0.0012$) (Table 5.3). The two-

term regression was the most influenced by the addition of the 0.2-m tailgate height interaction term, improving the model fit for the 0.1- and 0.2-m tailgate heights and worsening the model fit for the 0-m tailgate height. The addition of the 0.2-m tailgate height indicator variable significantly changed the mean relative error of all regressions for 0.4-m tailgate from a slight overprediction (relative error $\sim 0.01 - 0.02$) to a slight underprediction (relative error $\sim -0.02 - -0.03$).

Table 5.3 Comparison of mean relative error between unit momentum absorbing area (*maa*) regression models with and without tailgate height indicator variables.

Regression ABV.	Tailgate Height	Indicator Variable?	Mean Relative Error	Mean change in relative error	p-value
2M	0	N	-0.01	0.01	0.0061
2MI		Y	-0.02		
2M	0.1	N	0.04	0.02	0.0010
2MI		Y	0.02		
2M	0.2	N	-0.13	-0.12	0.0007
2MI		Y	-0.01		
2M	0.4	N	0.02	0.03	0.0020
2MI		Y	-0.02		
3Mb	0.2	N	-0.13	-0.09	0.0007
3MIb		Y	-0.04		
3Mb	0.4	N	0.01	0.04	0.0020
3MIb		Y	-0.03		
3Ma	0.2	N	-0.13	-0.06	0.0012
3MIa		Y	-0.07		
3Ma	0.4	N	0.01	0.04	0.0273
3MIa		Y	-0.02		

5.3.1-3 A_f Regressions

The best performing A_f regression was a simple two-term regression based on $A_f \cdot d$ and Re_{stem} (Table 5.4). The robust R^2 for the A_f regression was lower than any *maa* regressions, even the two-term *maa* regression. The AICR, BICR, and deviance were also slightly larger than for the two-term *maa* regression (Table 5.1). Like the two-term *maa* regression, the friction factor was inversely related to Re_{stem} and directly related to the area-diameter term ($A_f \cdot d$ and *maa* · d for the A_f and *maa* regressions, respectively).

Table 5.4 Summary of regression models for emergent vegetated flows using the area coefficient based on the vegetation frontal area per unit volume (A_f) with and without the addition of a tailgate height indicator variable for the 0.2-m tailgate height.

ABV.	Equation ¹	Robust R^2	AICR	BICR	Deviance
2F	$f = 10^{5.60} (A_f \cdot d)^{0.62} \text{Re}_{stem}^{-0.99}$	0.69	34.3	42.6	0.83
	If tailgate height is 0.2 m: $f = 10^{9.27} (A_f \cdot d)^{1.35} \text{Re}_{stem}^{-1.81}$				
2FIa	Otherwise: $f = 10^{5.73} (A_f \cdot d)^{0.61} \text{Re}_{stem}^{-1.07}$	0.73	35.1	49.0	0.53
	If tailgate height is 0.2-m: $f = 10^{5.73} (A_f \cdot d)^{1.14} \left(\frac{MEI}{\rho V^2 d^4} \right)^{0.13} \text{Re}_{stem}^{-1.11}$				
2FIb	Otherwise: $f = 10^{5.73} (A_f \cdot d)^{0.59} \text{Re}_{stem}^{-1.11}$	0.75	32.5	49.6	0.56

¹ where Re_{stem} is the Reynolds number based on stem diameter, A_f is the vegetation frontal area per unit volume (A_f), d is the stem diameter, MEI is the vegetation flexural rigidity, ρ is the fluid density, V is the flow velocity, AICR is the Aikake Information Criterion, BICR is the robust Bayesian Information Criterion

The A_f regression fit was improved by the addition of tailgate interaction terms (Figure 5.3). Like the maa regressions, only the 0.2-m tailgate height interaction terms were significant. The addition of the 0.2-m tailgate interaction terms improved the robust R^2 and decreased the deviance. The AICR was the smallest for the regression with the highest robust R^2 but the BICR was the largest due to the increased “penalty” for adding addition regression terms (Table 5.4). The 0.2-m tailgate interaction took two forms: a change in all regression parameters for the 0.2-m tailgate height or the addition of the MEI Π term and a change in the $pa \cdot d$ term regression coefficient. The regression that included the MEI Π term had a slightly larger robust R^2 and

smaller deviance. The inclusion of the $MEI \Pi$ term for the 0.2-m tailgate height indicated vegetation flexibility was more important when the water depth was approximately 50% of the total vegetation height.

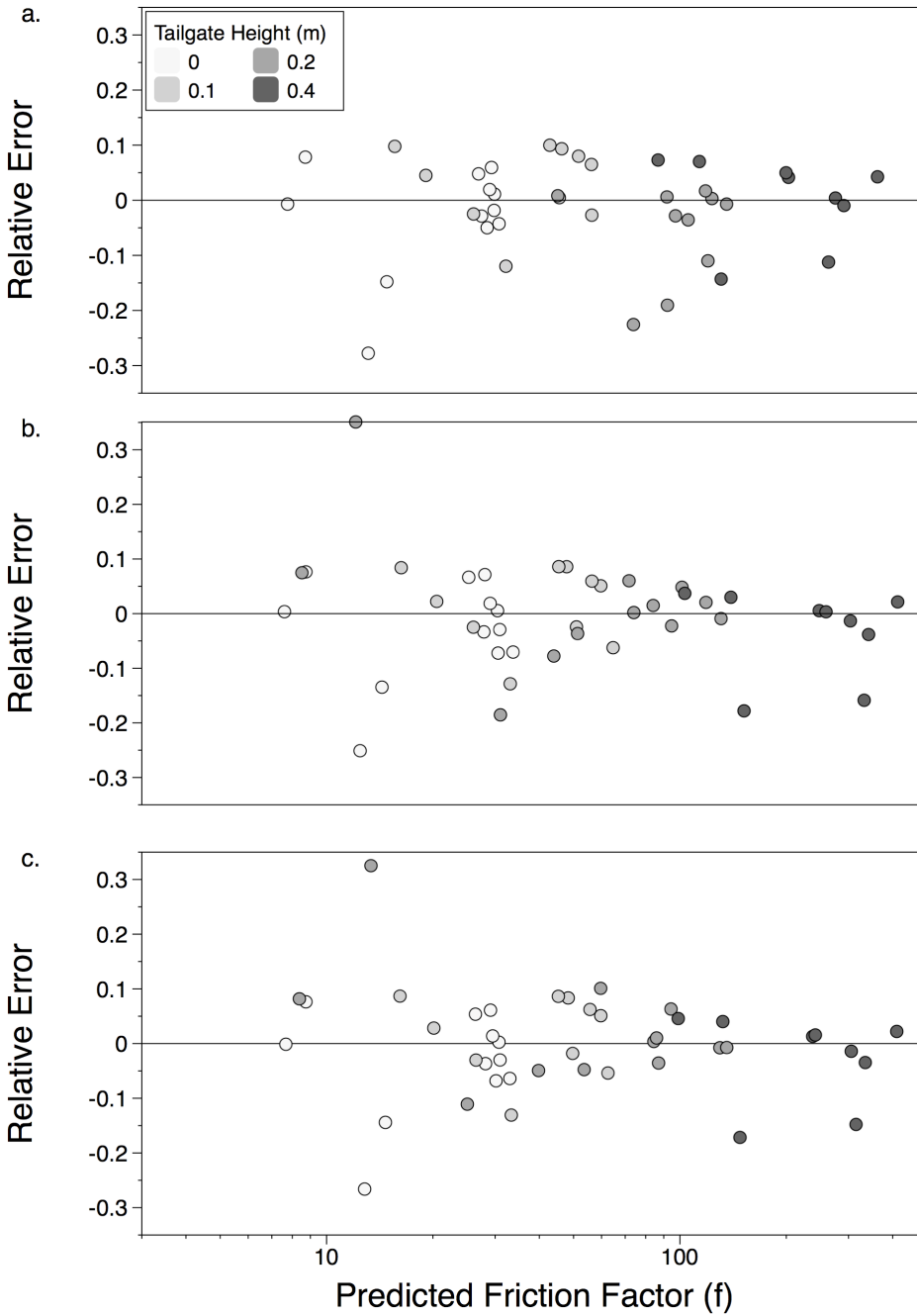


Figure 5.3 Relative error distribution for regressions a. 2F, b. 2FIa, and c. 2FIb shaded by tailgate height. Regression predict friction factor (f) as a function of vegetation and flow properties.

5.3.1-4 Regression coefficient sensitivity

The predicted friction factor for the 2M regression was very sensitive to changes in the regression coefficients even within the 95% confidence intervals of the model exponents (Figure 5.4 and Figure 5.5). Using the Everglades flow and vegetation data [Harvey *et al.*, 2009], 7% reduction of the premultiplier coefficient (premultiplier lower 95% confidence interval), resulted in a 57% reduction of the predicted friction factor. A 7% increase of the premultiplier coefficient (premultiplier upper 95% confidence interval) resulted in a 140% increase of the predicted friction factor. The other regression parameters did not affect the predicted friction factor to the same extent. An 11% reduction in the Re_{stem} exponent (Re_{stem} exponent lower 95% confidence interval) resulted in a 21% to 45% reduction in the predicted friction factor. An 11% increase in the Re_{stem} exponent (Re_{stem} exponent upper 95% confidence interval) resulted in a 26% to 83% increase in the predicted friction factor. A 22% decrease in the $maa \cdot d$ exponent ($maa \cdot d$ exponent lower 95% confidence interval) resulted in a 43% to 50% increase in the predicted friction factor while a 22% increase in the $maa \cdot d$ exponent ($maa \cdot d$ exponent upper 95% confidence interval) resulted in a 33% to 36% decrease in the predicted friction factor. Altering the model coefficients had a hysteretic effect on the predicted friction factor. For example, increasing the value of the premultiplier and the Re_{stem} exponent increased the predicted friction factor by a greater degree than decreasing the premultiplier and Re_{stem} exponent decreased the predicted friction factor.

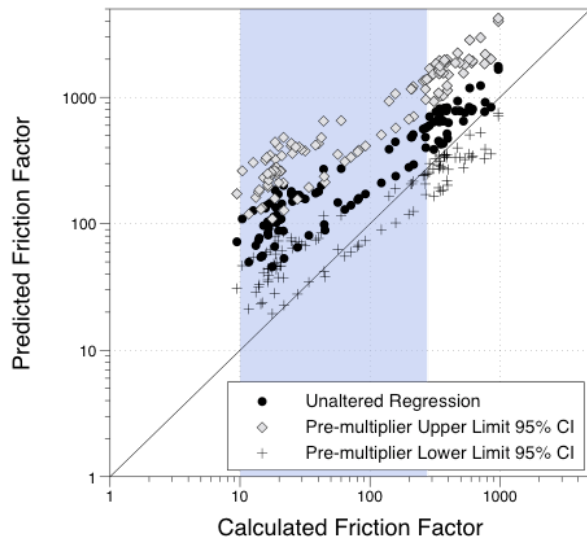


Figure 5.4 Regression 2M model fit using data collected by *Harvey et al.* [2009] for ridge conditions. Results using the upper and lower limits of the pre-multiplier regression coefficient 95% confidence interval are also shown. The shaded region represents the range of friction factors from which the regression relationships were derived.

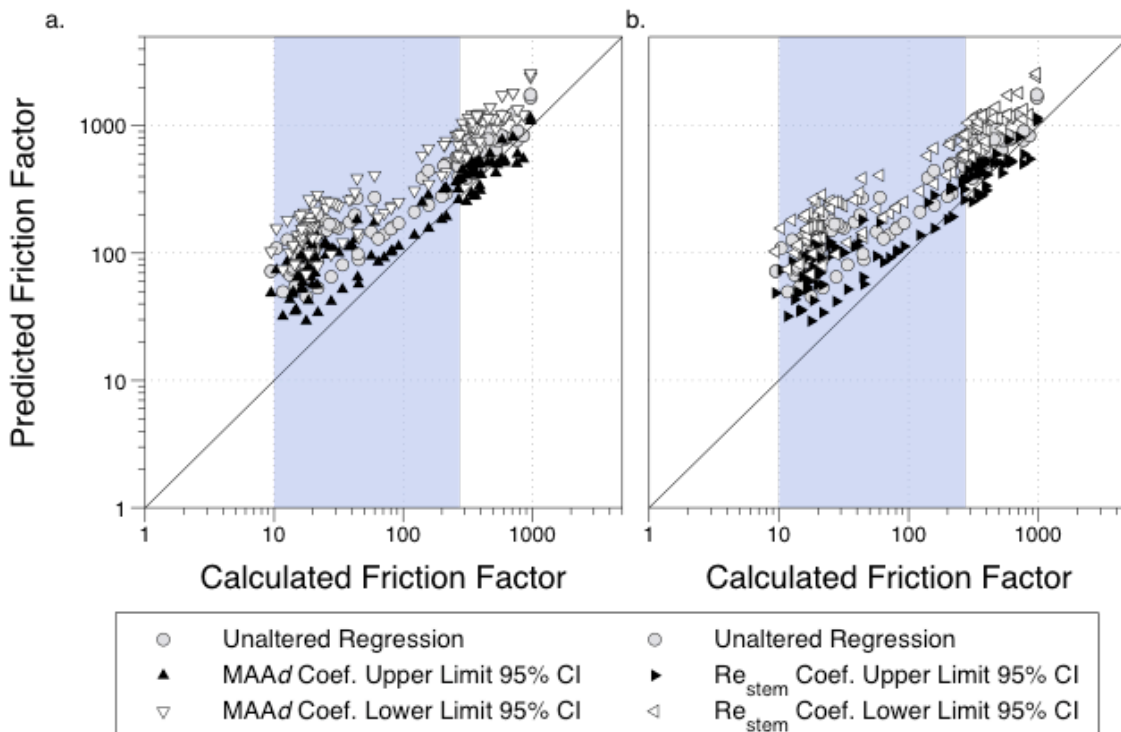


Figure 5.5 Regression 2M model fit using data collected by *Harvey et al.* [2009] for ridge conditions. Results using the upper and lower limits of the a. unit momentum absorbing area and stem diameter parameter ($maa \cdot d$) and b. stem Reynolds number (Re_{stem}) regression coefficient 95% confidence interval are also shown. The shaded regions represent the range of friction factors from which the regression relationships were derived.

5.3.1-5 Comparing regression coefficients

While the assumptions of regression do not allow for direct comparison of regression terms, some general observations can be made about the value of the regression coefficients. The value of maa - d term was fairly constant for all basic regressions, at or near 0.44. The maa - d term was the only term altered by the addition of the 0.2-m tailgate height indicator variable. For all tailgates but the 0.2-m tailgate, the maa - d term was between 0.45 and 0.49. For the 0.2-m tailgate height, the maa - d term was larger, ranging from 0.53 up to 0.82. The MEI term was nearly constant (0.08 - 0.13) for all regressions in which it was included (3Ma 3Mb, 4M, 3MIa, 3MIb, and 2FIb).

The value of the Re_{stem} regression coefficient was more variable, ranging from -2.48 for the 0.2-m tailgate height for the two-term regression to -0.69 for the four-term maa regression. The value of Re_{stem} regression coefficient appeared to be dependent on the other terms in the regression, varying as terms were added to the regression. However, the Re_{stem} regression coefficient was nearly always the largest coefficient in each regression, controlling the shape of the model.

The 2M regression with and without interaction can be easily compared to the 2F regression with and without interaction. The only difference between the 2M and 2F regressions is the definition of the reference area (maa neglecting stem overlap and A_f considering overlap). The A_f regression coefficient is larger in relation to the Re_{stem} regression coefficient than the maa regression coefficient so, A_f explains greater proportion of the variation in friction factor than maa .

The ratio between the maa and Re_{stem} regression coefficients is approximately equal for the 2MI equations (-0.33 for the 0.2-m tailgate, -0.30 otherwise); however, the ratio between the A_f and Re_{stem} regression coefficients in the 2FIa regression is different between the 0.2-m tailgate and the other tailgate heights (-0.75 for the 0.2-m tailgate, -0.57 otherwise). The ratio between the regression coefficients indicates the relative importance of each parameter in the model fit. Since the ratio between the regression coefficients for 2MI regression is similar between the 0.2-m tailgate and the other tailgate heights, the fundamental shape of the regression does not change between tailgate heights, although the value of the regression does change. However, the change

in the ratio of A_f and Re_{stem} regression coefficients in the 2FIa regressions between the 0.2-m tailgate and other tailgate heights indicates that at the 0.2-m tailgate height, A_f is more important in relation to Re_{stem} than it is at other tailgate heights.

For the two-term regressions 2M and 2F, the 95% confidence intervals of the maa and A_f regressions premultiplier term overlapped, indicating the premultiplier terms are similar. For the two term regressions with interaction, 2MI and 2FIa, only the 95% confidence intervals of the maa and A_f regression premultiplier terms for all tailgate heights but 0.2 m overlapped.

5.3.2 Validation

5.3.2-1 Validation results

The two-term regression model (2M) was tested using data collected in the Everglades water management area WCA-3A presented in *Harvey et al.* [2009]. The performance of the other three models developed using maa could not be assessed because vegetation flexibility was not measured in the *Harvey et al.* [2009] study. The reported vegetation and flow data were used to predict the friction factor using regression 2M. The friction factors predicted with regression 2M and calculated with the Darcy-Weisbach equation were calculated from the entire data set using the depth-averaged unit velocity covering the fall/winter wet seasons of 2006 and 2007, when the ridge was inundated. The overall fit was poor, with a NSE of -0.03, indicating the average calculated friction factor was a better predictor than the model. The regression overestimated the friction factor by two to three orders of magnitude. The overall trend of the regression was slightly skewed from the 1:1 perfect fit line in slope and value (Figure 5.4).

Examining the model residuals and relative errors indicated the model error was not random; the total model residual increased logarithmically, proportional to the value of the calculated friction factor (Figure 5.6a). However, since the calculated friction factor ranged over two orders of magnitude, the total value of the residual does not indicate how large the model error is in proportion to the value of the friction factor. The model relative error followed a trend opposite of the total residual value (Figure 5.6b). The relative error was largest at the lower range of friction factors and decreased logarithmically to an average value below 1 at the upper range of

friction factors. The regression model was developed for friction factors between 10 and 275, indicated by the shaded region on the plots. However, the model performed best (relative error the lowest) at friction factors greater than 275. The model fit, residuals, and relative error were not consistent between the 2006 and 2007 wet seasons. The *NSE* and *RMSE* for 2006 were -0.27 and 268, respectively. The *NSE* and *RMSE* for 2007 were -363 and 112, respectively. Part of the poor model fit for 2007 was due to consistently low water depths and a relatively small range of calculated friction factors (9-44 for 2007 versus 10-1000 for 2006).

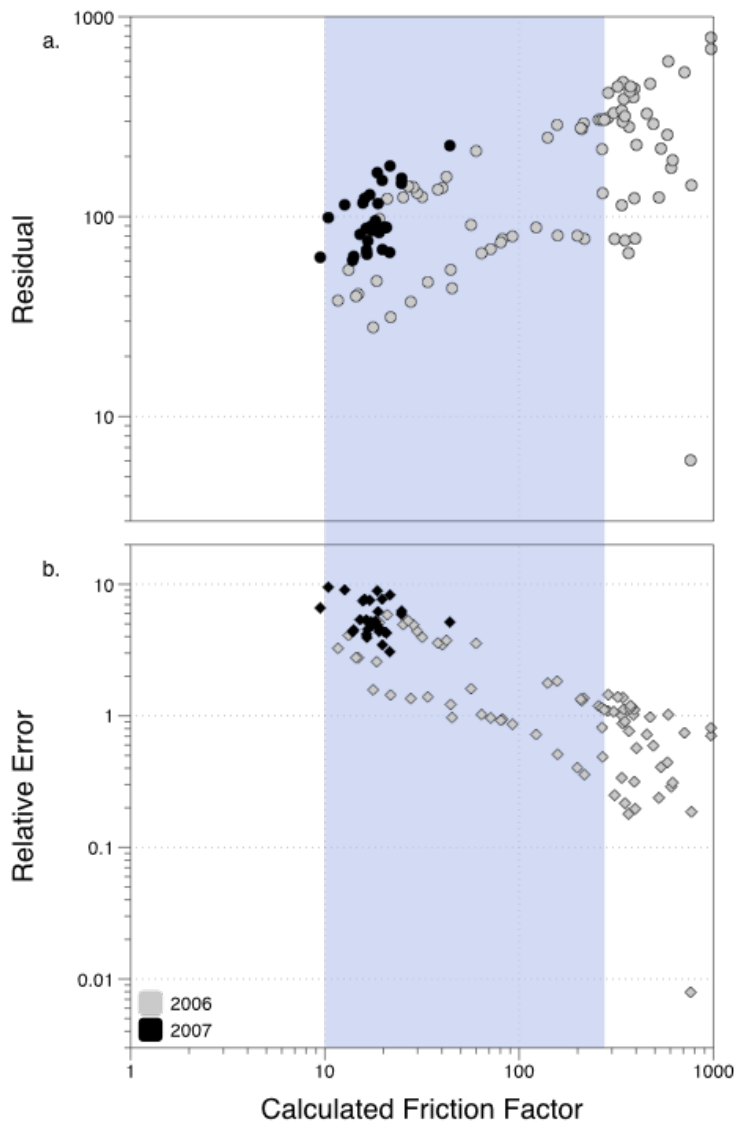


Figure 5.6 Regression 2M model residuals and relative error using data collected by *Harvey et al.* [2009] for ridge conditions. The shaded regions represent the range of friction factors for which the regression was developed.

Examining the effect of time on the model fit more closely revealed that water depth also varied seasonally. The model fit was the best (relative error was the lowest) at depths greater than 30 cm (Figure 5.7). The difference in relative error between 2006 and 2007 was likely due to a difference in water levels between the two years. However, the same inverse correlation between water depth and relative error was not observed during 2007. Other unknown variables appear to be influencing model performance for 2007.

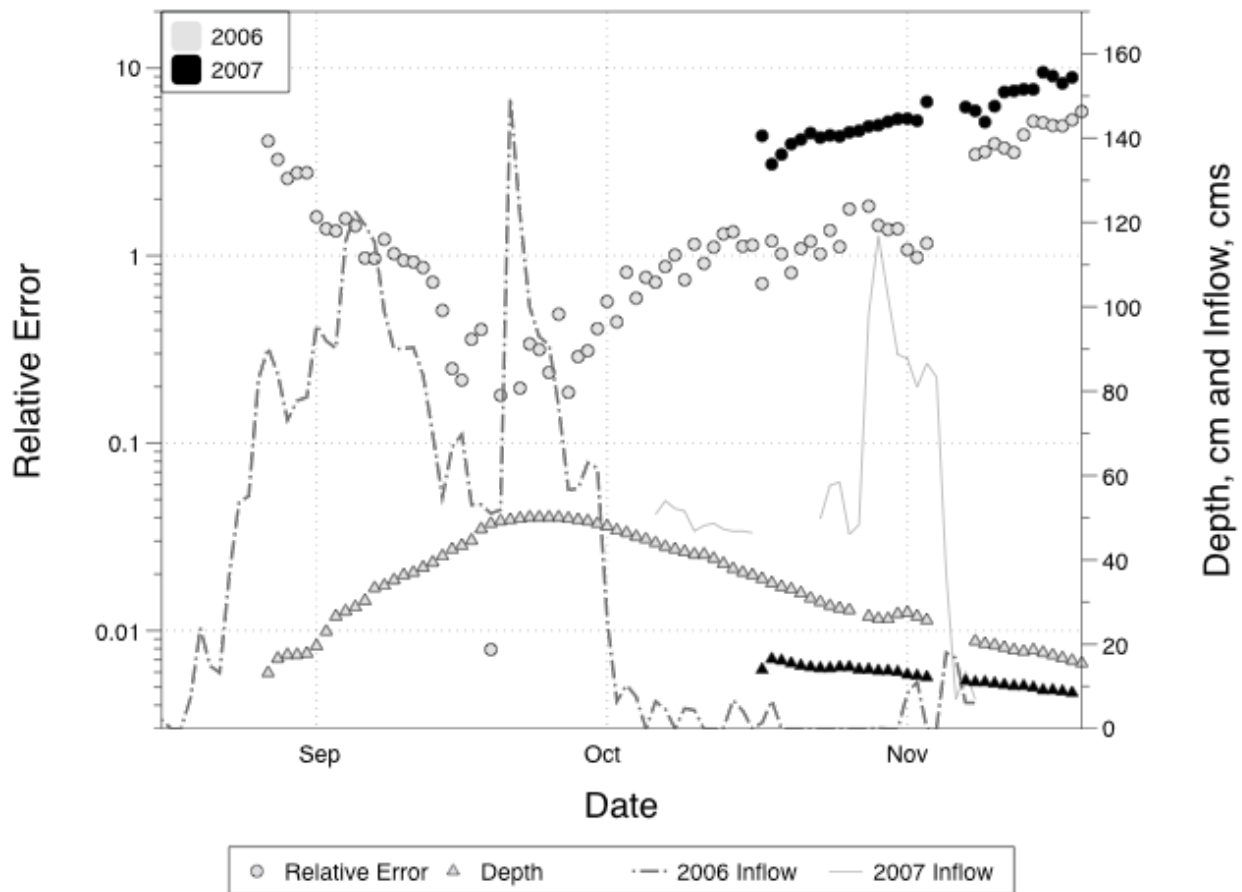


Figure 5.7 Regression 2M model relative error over time using data collected by *Harvey et al.* [2009] for ridge conditions. Also shown is the water depth and inflow rate into WCA-3A over time.

The outlet water depths in the flume study from which the regression relationships were developed ranged from 0 to 40 cm; 50% of all data collected were at depths less than or equal to 20 cm. If the Everglades system and the flume system were comparable, it would be expected that the regression model developed from the flume data would perform best at water depths near

the median flume water depth of 14 cm. However, the best model performance occurred at larger depths, especially at depths greater than 35 cm. While it is unclear as to the exact reason for the lack of model fit at depths less than 20 cm, there may be several possible reasons. The Everglades and flume vegetation architecture are different. The flume vegetation is the densest near the soil surface with the density decreasing with the distance from the soil surface. The region of minimum vegetation density in the Everglades system was close to the soil surface [Harvey *et al.*, 2009]. Additionally, the mean stem diameter in the flume system was smaller than the mean stem diameter in the Everglades. The flexural rigidity was not measured in the Harvey *et al.* [2009] study; however, the second area moment of inertia for larger-diameter vegetation is larger, which would increase the flexural rigidity of the plants, assuming similar values for the modulus of elasticity. If the flexural rigidity for the Everglades vegetation was larger, larger flows would be required to flex the Everglades vegetation similarly to the flume vegetation and illicit the same increase in hydraulic resistance that was observed in the flume study.

For 2006, on a same-day basis, relative error was most correlated with the daily water depth (correlation coefficient = -0.60). However, the relative error was more strongly correlated (correlation coefficient = -0.74) with the inflow rate into WCA-3A 15 days prior to the observation, indicating a dependence of model fit on inflow rate. For 2007, the relative error was not obviously correlated with inflow or depth. Large inflows were observed during the period for which the ridge was inundated but no associated increase in water depth or decrease in relative error was observed.

Given the same-day dependency of model fit on water depth and the serial dependency of water depth, the *NSE* and *RMSE* were recalculated for 2006 using a subset of data for a uniform distribution of water depths. For a uniform distribution of water depths, the *NSE* was -0.66 and the *RMSE* was 236. The slight decrease in *NSE* and increase in *RMSE* with the uniform distribution of water depths is due to the extended period of high flows observed during the 2006 wet season which inflated the *NSE* and deflated the *RMSE*.

The 2M regression model was modified with the upper and lower confidence interval limits of the premultiplier regression coefficient and the results were plotted (Figure 5.4). The lower

confidence interval limit of the premultiplier improved the regression fit drastically, increasing the *NSE* to 0.76. While the overall fit of the modified regression was good, with a larger *NSE* than the original robust R^2 , it did not perform equally across the entire range of friction factors. The model overpredicted friction factor at low values of friction factor and underpredicted at large friction factors.

5.3.2-2 Model lack of fit

The contrasting vegetation architectures may be the reason for the pronounced lack of fit observed at water depths below 30 cm in the Everglades. Reported velocity profiles on the ridges of the Everglades did not conform to the uniform profile often reported for flow through vegetation. Instead, maximum velocities were measured low in the velocity profile, close to the bed. While velocity was not directly measured in the flume study, dye studies indicated the flume system was well mixed through the profile (although lateral preferential flow paths were observed). Velocity is inversely proportional to the projected plant area so the depth at which the projected plant area is at a minimum is the area of maximum velocity [*Lightbody and Nepf, 2006*]. The zone of maximum streamwise projected plant area in the flume was slightly above the bed. Projected plant area decreases with height, reaching a minimum at the top of the water column.

The vegetation in the Everglades is not a monoculture. Species composition changes from the ridge to the slough communities. Each community is also made up of multiple species of varying heights, from floating macrophytes (*Utricularia* L.) to sedge species that can reach over 3.5 m at maturity. The structure of the vegetation community affects the *maa-d* exponent so the relative contribution of the *maa-d* parameter to the friction factor may be different for the same value of *maa-d* in the Everglades versus the flume system. While the *maa-d* parameter was comparable between the WCA-3A and the flume system, the mean stem diameter in the Everglades was larger and the MAA smaller.

Vegetation community changes may also account for the differences between the model performance between 2006 and 2007. Vegetation data were collected in August 2005 before Hurricane Wilma eliminated floating *Utricularia* L. mats and periphyton from the system. While

the exact vegetation condition in 2007 was not known, the *Utricularia* L. mat had begun to reestablish itself [Harvey *et al.*, 2009]. Since the flume experiments were conducted for a monoculture of *Scirpus cyperinus* (L.) Kunth, the effects of floating macrophytic vegetation were not accounted for.

5.4 Conclusions

This study focused on predicting friction factor in low-Reynolds number emergent vegetated flows based on properties of the vegetation and the flow conditions. Previous studies focused on predicting the drag coefficient instead of the friction factor. However, drag coefficient is a property of the characteristic drag area. Unless the characteristic drag areas are the same, drag coefficients are not comparable. Friction factor is a composite value and avoids any potential confusion over the characteristic drag area.

While seven models satisfied the criteria described in the methods section for bias, multicollinearity, and significance, the models based on *maa* have consistently higher robust R^2 values, had consistent interactions, and one was independently validated. The best overall model included a vegetation density term, *maa-d*, a vegetation flexibility term, *MEI*, a flow term, Re_{stem} , and a tailgate height interaction term for the 0.2-m tailgate height, at which approximately 50% of the vegetation is submerged. Previous studies found hydraulic resistance was a function of Re_{stem} and a measure of vegetation density. The results of this study suggest vegetation flexibility should be considered in future studies in addition to Re_{stem} and vegetation density.

The performance of the two-term *maa* model, which included *maa-d* and Re_{stem} , was assessed using data collected in the Florida Everglades. The two-term model generally overpredicted friction factor by a large margin (Relative errors ranged from 0.1 to 100), especially at depths below 0.3 m. However, it appears the lack of fit at shallow depths is due to a significant difference in vegetation architecture in the Everglades versus this study. When water levels are higher, the two-term regression still overpredicts friction factor but the relative error is considerably smaller than at shallower depths.

The two-term regression used in the validation was sensitive to changes in the premultiplier; changing the premultiplier to the lower limit of the 95% confidence interval increased the *NSE* from -0.03 to 0.76. The fit to measured data was still not perfect with the lower premultiplier, overpredicting friction factors below 50 and underpredicting friction factors above 300. Since the validation data set did not include estimates of flexibility, the three- and four-term models could not be tested to see if model fit could be improved if *MEI* were included.

Models based on the A_f had consistently lower robust R^2 values and the addition of other parameters did not improve the fit. Due to the presence of overlap and the heterogeneity of vegetated systems, the measurement of A_f included a greater degree of uncertainty, as compared to the measurement of *maa*. In the low Reynolds numbers flows examined in this paper, *maa* may indeed be a better analog for drag. In low Reynolds number flows, the degree of wake sheltering is less than that for more turbulent flows. While vortex shedding was observed in the flume study, the degree of flow separation was not large and the sheltering effect of clumped vegetation was not as great as would be expected in more turbulent flows. A_f may be better correlated with friction factor in more turbulent flows in which sheltering and streamlining of plants may reduce the drag considerably.

Chapter 6 Modeling surface water flow through emergent vegetation in a small floodplain wetland

6.1 Introduction

Wetlands are important features in the landscape and provide numerous services, including habitat, water quality improvement, and flood control [Townsend *et al.*, 2003]. Extensive loss of wetlands has prompted the construction and restoration of wetland area, but replacement of wetland area has not necessarily equated to restoration of wetland function [Dahl, 2000]. Frequently wetlands are wetter than they were designed to be. While neglect of groundwater influences on the annual wetland water budget is part of the reason constructed wetlands are frequently too wet, wetlands that receive surface flow may be wetter than designed due to inaccurate representation or neglect of surface flow hydraulics.

Flow through wetlands has not been extensively modeled although numerous models exist that have the ability or are designed to simulate wetlands [Hammer and Kadlec, 1986; Skaggs *et al.*, 1991; Kadlec and Knight, 1996; Feng and Molz, 1997; Lee, 1999; Kazezyilmaz-Alhan *et al.*, 2007]. Models may simulate wetlands as only one component of the watershed while others focus only on modeling the immediate wetland area. Few models [Restrepo *et al.*, 1998; Kazezyilmaz-Alhan *et al.*, 2007] represent the interaction between the surface and subsurface as a dynamic process that allows water to move from the subsurface to the surface.

MODFLOW [McDonald and Harbaugh, 1996] is a quasi-3D finite difference model that simulates groundwater flow. Riparian springs, hyporeic exchange in streams, vertical flow through peat, and hydraulics of water treatment wetlands have been simulated using various configurations of MODFLOW [Restrepo *et al.*, 1998; Reeve *et al.*, 2000; Grapes *et al.*, 2006; Lautz and Siegel, 2006; Ronkanen and Klove, 2008]. The MODFLOW Wetland Simulation package [Restrepo *et al.*, 1998] models the groundwater-surface water interaction as well as the hydraulic resistance from emergent vegetation and was designed for use in the Florida Everglades system. However, many components of the model (peat/muck layer, diversions, levees, etc.) are specific to the Everglades region and not applicable to a wide range of wetland types, especially recently constructed wetlands.

Ronkanen and Kløve [2008] used MODFLOW in conjunction with the Drain Package to successfully model surface flow through water treatment wetlands constructed on Northern Finnish peatlands. Mitigation wetland sites are similar in size to the simulated water treatment wetlands [Ronkanen and Kløve, 2008].

The goal of this study was to determine the feasibility and accuracy of using MODFLOW to model surface flow through a small constructed wetland. Wetland surface water flow was determined in part by the properties of the wetland emergent vegetation. The sensitivity of MODFLOW to changes in surface hydraulic conductivity (K) was also assessed.

6.2 Application of MODFLOW to surface-flow systems

MODFLOW [McDonald and Harbaugh, 1996] is based on the groundwater flow equation, which assumes Darcian flow. Darcy's law states that the flowrate of water through porous media is linearly proportional to the hydraulic head gradient. The proportionality constant is called the hydraulic conductivity (K) (L/T). The Darcian flow assumption is consistent for laminar flow conditions (Reynolds number < 1 to 60 , depending on properties of the media). At Reynolds numbers (Re) greater than 60 , flow is no longer linearly proportional to the hydraulic head gradient, which means K is no longer a constant. At $Re > 60$, K varies with flow by some unknown relationship specific to each system. A relationship is needed that estimates the shape of the relationship between flow and the hydraulic head gradient beyond the linear relationship between Re and K .

Outflow in constructed wetlands is a function of the outlet structure and the vegetation hydraulic resistance. Wetland flow is often in the laminar to transitional flow regime so hydraulic resistance is a function of vegetation and flow properties. The following relationship estimates the friction factor (f):

$$f = 10^{4.98} (maa \cdot d)^{0.47} Re_{stem}^{-1.52} \quad [6.1]$$

where maa is the unit momentum absorbing area of the vegetation (estimated as the one-sided area of the vegetation per unit volume) (L^{-1}), d is the average stem diameter (L), and Re_{stem} is the

stem Reynolds number. The f -prediction relationship [6.1] was developed from data collected in a flume system planted with a dense monoculture of woolgrass (*Scirpus cyperinus* (L.) Kunth). The R^2 of relationship was 0.71 as reported in Chapter 5.

f is an appropriate measure of hydraulic resistance in vegetated flows; however, MODFLOW describes hydraulic resistance using K . Darcy's Law and the Darcy-Weisbach equation both describe pressure loss over a given distance. In Darcy's Law, the pressure loss occurs through porous media. In the classic example, the Darcy-Weisbach equation describes pressure loss through a pipe, though the equations can be adapted for the open channel case by expressing the pipe diameter as four times the channel hydraulic radius (R) (L). To successfully use MODFLOW to model surface flow through a densely vegetated wetland, the friction factor due to the vegetation must be expressed as a hydraulic conductivity. Darcy's Law in its simplest form is:

$$q = KA_d \frac{dh}{dl} \rightarrow \frac{dh}{dl} = \frac{v}{K} \quad [6.2]$$

where q is the flow rate (L^3), A_d is the unit cross-sectional area of the media (L^2), dh/dl is the hydraulic head gradient (L/L), and v is the average velocity per unit cross-sectional area (L/T).

The Darcy-Weisbach equation for open channel flow is

$$\frac{dh}{dl} = \frac{f v^2}{8gR} \quad [6.3]$$

where g is the acceleration due to gravity (L/T^2). Equating the hydraulic head gradient terms results in the following equality.

$$\frac{v}{K} = \frac{f v^2}{8gR} \quad [6.4]$$

Rearranging the terms leads to the following equation expressing K in terms of f , R , and v :

$$K = \frac{8gR}{fv} \quad [6.5]$$

For vegetated flows, R is assumed to be equal to the water depth (h) (L).

6.3 Methods

To test the feasibility and sensitivity of using MODFLOW to predict flow in small constructed wetlands, an experimental constructed wetland was instrumented to measure surface flow characteristics including inflow, outflow, water depth, and velocity during a flow-through flood event. MODFLOW input parameters were directly measured or estimated. Vegetation was mapped and vegetation properties were measured to estimate the surface K .

6.3.1 Site Description

The experimental wetland site is situated on Hedgebrook Farm, in the 148-km² Opequon Creek watershed near Stephens City, VA U.S. The Opequon Creek watershed is located in far northern VA in the Ridge and Valley physiographic province (Figure 6.1).

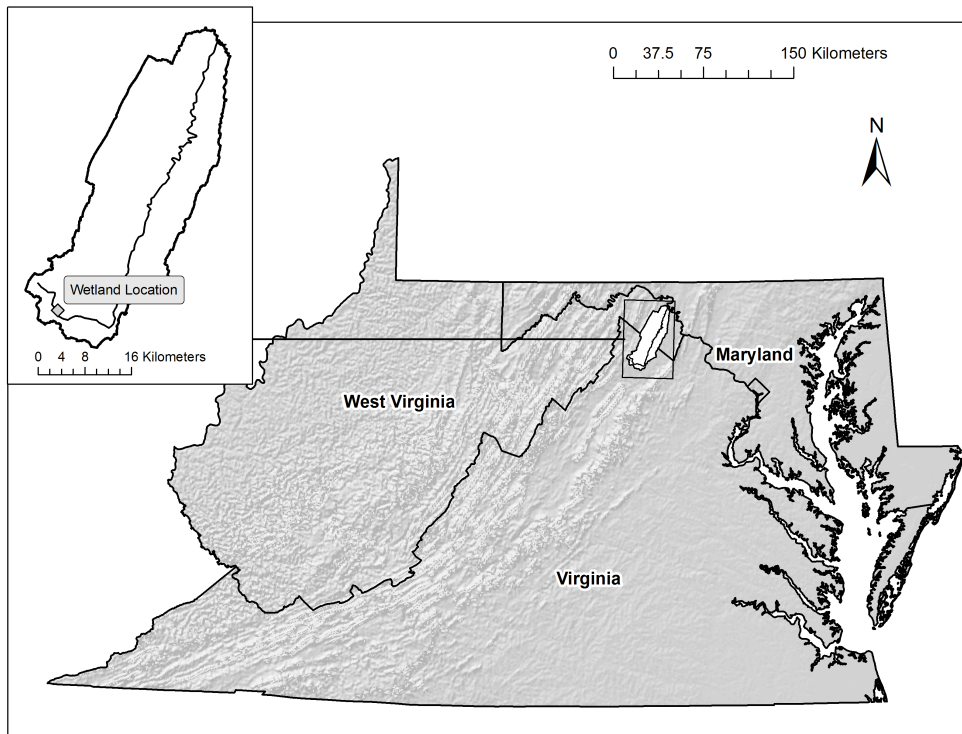


Figure 6.1 Regional location of the Opequon Creek watershed and the Hedgebrook Farm wetland site.

A 0.2-ha constructed wetland was built immediately adjacent to Opequon Creek (**Figure 6.2**). The wetland was designed to receive inflow when the stage in Opequon Creek rose above 2.0 m (2.8 cms). The captured flow is re-routed through the wetland before being discharged back to Opequon Creek through an outlet channel. The wetland was designed with three topographic zones: two deep pools immediately downstream and upstream of the wetland inlet and outlet, respectively; a low marsh area that is frequently inundated; and a high marsh area that is only periodically inundated. The wetland was constructed in May 2007 and was planted with a combination of wetland native seed mix and herbaceous vegetation plugs. Typical species included broad-leaved arrowhead (*Sagittaria latifolia* Willd.), bulrush (*Scirpus* L.), and pickerelweed (*Pontederia cordata* L.).

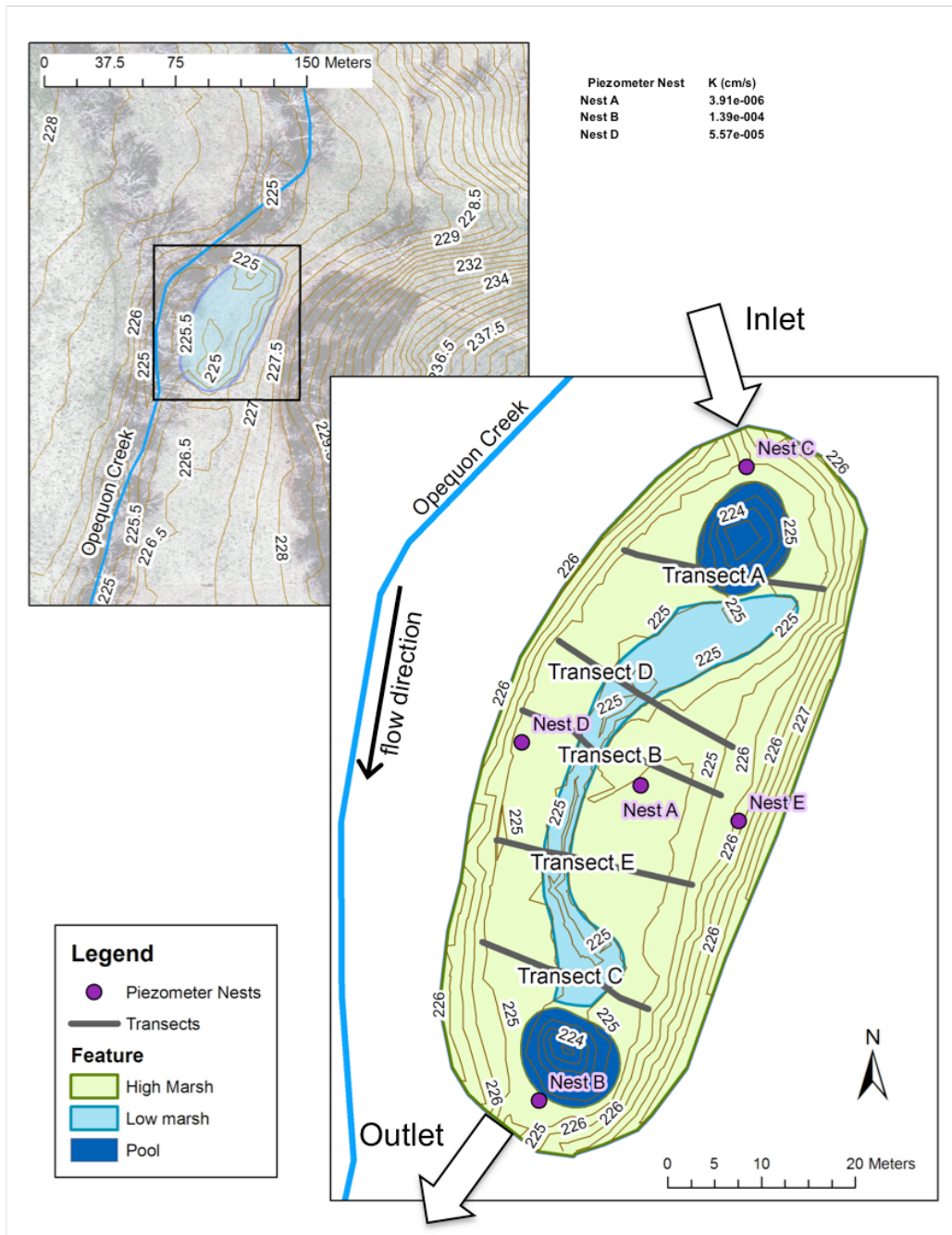


Figure 6.2 Map of Hedgebrook Farm wetland site topography piezometer nest locations, staff gage transects, and subsurface hydraulic conductivity. (elevation in m, vertical datum NAVD 88)

6.3.2 Field methods

Because the wetland site was designed to capture only large flows, an Artificial Overbank Event (AOE) was conducted to measure flow through the wetland. Water was pumped from Opequon

Creek with a 15.24-cm trash pump at a rate of 0.067 cms for eight hours November 18, 2008 and May 19, 2009 and for six hours May 20, 2009. Inflow through the inlet channel was calculated from velocity measurements made by an ISCO 750 Area Velocity Module (Teledyne ISCO, Lincoln, NE) located at the inlet channel. Outflow through the 0.3-m H-flume was monitored using a bubble-level reader and an ISCO 6712 portable sampler and data logger unit (Teledyne ISCO, Lincoln, NE). Water levels within the wetland were measured throughout the AOE using a grid of staff gages. Five staff gages were located along each of five transects; two staff gages were located in the high marsh on each side of the low marsh (for a total of four staff gages on the high marsh) and one staff gage was located in the low marsh (Figure 6.2). The cross sections were located between the inlet and outlet pools. Water depths at each staff gage were repeatedly measured throughout each AOE to within a tolerance of 0.3 cm. Groundwater levels were measured before, during and after each AOE using five nests of piezometers (Figure 6.2) using a combination of water level loggers (HOBO U20 Water Level Logger, Onset Computer Corporation, Bourne, MA) and direct water level measurements using a water level tape.

The wetland topography, instrument and piezometer locations, and other features of interest such as AOE high water levels were surveyed with a Topcon GTS-235W total station (Topcon Positioning Systems, Inc., Livermore, CA). The survey was georeferenced using a Topcon GR3 GPS+ receiver.

Velocity measurements were collected during the May 2009 AOE's at transect B using an acoustic Doppler velocimeter (16-MHz Side-looking MicroADV, SonTek/YSI, San Diego, CA). The ADV probe was mounted to a metric wading rod and measurements were taken approximately every 0.5 m across transect B. Measurements were collected at 0.2, 0.4, 0.6, and 0.8 of the water depth as long as the water depth was sufficient to accommodate the probe (depths greater than 20 cm). Otherwise, one velocity measurement was taken at 0.6 of the water depth.

The soil hydraulic conductivity was estimated using slug tests. One liter of water was added to the 1-m deep piezometers at each piezometer nest and the water level was measured until the water level returned to equilibrium (note the failure of the water level logger prevented measurement of the hydraulic conductivity at nest C and nest E was unsaturated) (Figure 6.2).

Hydraulic conductivity was estimated using the Hvorslev method [*Hvorslev*, 1951].

The wetland area was divided into 14 different vegetation structural communities. Communities were identified using a combination of ground reconnaissance and photographs. Vegetation communities were distinguished from each other based on vegetation height, density, and structure. The high marsh was divided into nine communities. The low marsh was relatively homogenous and was grouped as one community. Four transitional areas were identified near the outlet and inlet of the pools as well. Vegetation properties were measured within each community at the conclusion of the November 2008 and May 2009 AOE. A 1-m² quadrat was randomly located within each community. Percent cover within each quadrat was estimated and stems were harvested from ¼ of the quadrat. The stems were cut into 10-cm increments and the area and average stem diameter was measured using a leaf area meter (Model 3100 Area Meter, LI-Cor, Inc., Lincoln, NE).

6.3.3 Modeling

The MODFLOW model was set up using PMWIN 5.3 (Processing MODFLOW for Windows), [*Chiang and Kinzelbach*, 2001]. The wetland was simulated in MODFLOW as a two-layer model: the top layer was the wetland surface water and the bottom layer was the underlying soil layer, which for purposes of simulation was considered vertically homogeneous. MODFLOW was set up with a constant 0.5-m grid cell size for a steady state simulation with a one-minute time step. The MODFLOW unsaturated flow zone package was not used. Only the May 20, 2009 event was modeled because the soil was saturated from the previous day's event. Steady-state flow existed for a 4-hour period. Steady state flow was defined as the period when inflow was approximately equal to outflow and head within the wetland surface was not changing. Inflow from the pump was modeled as a well discharging to the surface layer. The MODFLOW drain package as written drains water from the system at a rate proportional to the head at the drain cell. The proportionality constant is called the drain conductance. For surface flow outlet structures, the proportionality constant or drain conductance changes with head at the structure. The drain package source code was changed so the outflow rate was calculated using the H-flume rating curve. Since the drain module was modified, the drain conductance in PMWIN was set to 1 so only the H-flume rating curve would be used to determine head at the outlet.

The hydraulic conductivity in the wetland surface and subsurface was heterogeneous and assumed isotropic. The soil hydraulic conductivity estimates obtained in the field were assigned to the subsurface. The surface hydraulic conductivity was estimated using [6.1]. No measured flow data were used to determine K . Instead, K was calculated based on the starting head assigned to the surface layer. For the initial model run, an evenly sloped water surface was interpolated between the measured water surface level at the inlet channel and the theoretical water surface level at the outlet flume if the flow rate at the outlet was equal to the inflow rate. An average water depth and an average velocity were calculated for each vegetation community. The average velocity was estimated by area-weighting the inflow rate at a cross-section located at the centroid of each vegetation community. Based on the average depth and velocity, a surface K was calculated for each vegetation community. The vertical leakance parameter that quantifies the connection between the surface and subsurface was assumed to be the average of the ratio between the hydraulic conductivity and the saturated thickness for each layer. MODFLOW was run and the output values for hydraulic head were assigned to the starting head values for the next run. Surface hydraulic conductivity and vertical leakance were recalculated for the new values of starting head and MODFLOW was rerun. The process was repeated until the difference between the starting head and the output head between model runs was within 0.3 cm (the precision of the field water surface measurement).

6.4 Results

6.4.1 Measured results

While 25 staff gages were mounted throughout the wetland, only 15 staff gages were readable during each of the three AOEs. Five staff gages were located in areas of the wetland that were dry and five staff gages were obscured by emergent vegetation. The results for the May 20, 2009 AOE are presented. The total inundated area was 1217 m², about 60% of the total wetland area. The water surface between direct measurement points was interpolated so spatial trends in the water surface elevation and slope could be ascertained. Figure 6.3a shows the water surface elevation throughout the wetland derived using a triangulated irregular network (TIN) from the depth measurement points and the surveyed edge of water. Four depth measurement points, A4, D1, E2, and C3 were much higher than the surrounding water surface, creating mounds of water

3 to 4 cm higher than the surrounding water surface. The water mounding effect was observed in the data during each of the three AOE; however, the effect was not observed by the experimenters nor was it observable in any photographs taken during the AOE. TIN surfaces are created by interpolating flat planes between points; the shape of TIN surfaces is strongly influenced by scatter in measurements and may not reflect regional trends well.



Figure 6.3 Measured water surface slope a. interpolated using triangulated irregular network (TIN) interpolation and b. trend surface analysis. (elevation in m, vertical datum NAVD 88)

To reduce the effects of differences between measurement points, trend surface analysis (TSA) was used to estimate an average water surface (Figure 6.3b). A 3rd-order trend surface (TS) was derived from the measured water surface elevations and the surveyed edge of water. The average slope of the water surface, TS, was 0.14%. The TS water surface slope is a cell-to-cell average and may not be representative of the water surface slope in the primary flow direction; the TS

slopes were large in the vicinity of the inlet and outlet and the northwestern side of the wetland. The large regional slopes near the inlet, outlet, and northwestern side of the wetland skew the mean, inflating the mean slope value. Instead the mean TS water surface slope was calculated in the direction of flow. The water surface slope along the thalweg of the low marsh was 0.05%, considerably lower than the mean slope.

Velocity measurements were made across transect B (Figure 6.2). The mean measured velocity in the low marsh was 5.7 cm/s. The mean measured velocity in the high marsh was 2.9 cm/s. The trend surface matched the depth measured directly at transect B well. The mean depth in the low marsh measured with the wading rod at transect B was 30.0 cm, compared to a predicted mean depth of 28.9 cm from the TS. For the high marsh, the measured and predicted mean depths at transect B were 13.1 cm and 13.7 cm, respectively.

6.4.2 Modeling results

After 13 iterations, the starting head for the surface layer was within ± 1 mm of the output head. The final predicted water depth was on average 0.21 m and ranged from 1.06 m in the pools to 0.01 m on the high marsh. The final distributions of estimated *maad* and surface *K* are shown in Figure 6.4.

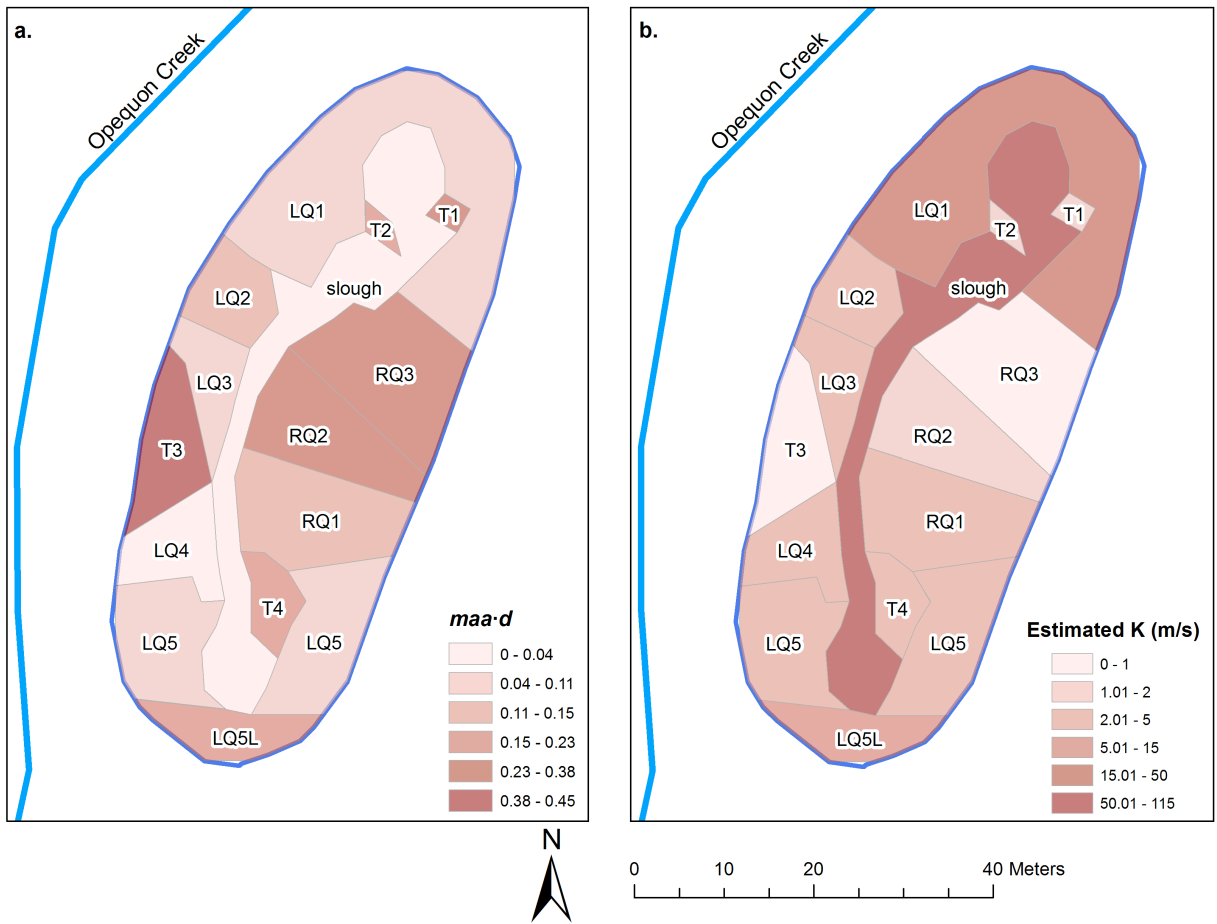


Figure 6.4 Hedgebrook Farm spatial distribution of vegetation. a. unit momentum absorbing area and stem diameter parameter (*maa-d*) and b. hydraulic conductivity (*K*).

Overall, MODFLOW underpredicted the water surface elevation (Figure 6.5). The mean water surface elevation error was -1.1 cm. The minimum absolute error was 0.0 cm at staff gage A2. The maximum error within the predicted saturated area was -4.3 cm at staff gage C3. The model predicted staff gage E1 would be dry; however, a 4.7 cm water depth was recorded at staff gage E1 so E1 was not dry as MODFLOW predicted. Nine of the 15 measurement points had errors within 1 cm of the actual water surface values. The mean low marsh error was -0.1 cm and the mean high marsh error was -1.4 cm. The predicted and observed water surface elevations were closer in the low marsh than the high marsh. The predicted inundated area was 1234 m²; the measured inundated area was 1273 m². The percent difference in inundated area was -3.1%, again indicating the model was slightly underpredicting the water surface elevation.

If the measurement points located at the water surface mounds were eliminated, the mean model error was reduced to within the detection limits of the water depth measurement (± 0.3 cm). The maximum error outside of the water surface mounds was 1.4 cm at staff gage A1. Since the trend surface predicted the water depth at transect B well, the model water surface was compared to the trend surface derived from the measured water surface elevation points and the water extent. The mean difference between the model water surface elevation and the trend surface water surface elevation was 0.08 cm. The trend surface water surface and the predicted water surface were within 1 cm of each other over 59% of the total inundated area.

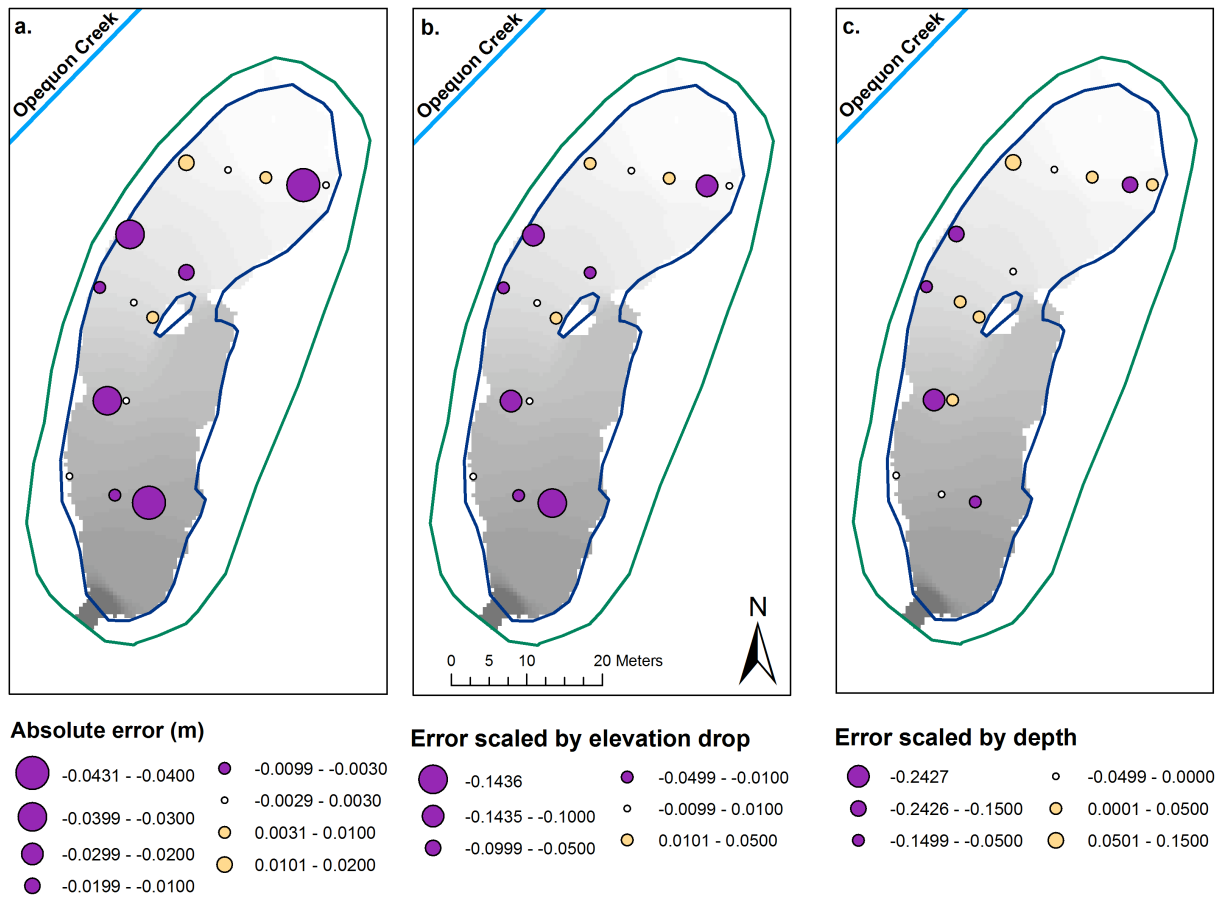


Figure 6.5 MODFLOW error a. absolute error, b. error scaled by elevation drop from the inlet to the outlet, and c. error scaled by water depth.

The predicted mean water surface slope was 0.04%. The TS water surface slope in the low marsh thalweg was 0.05% and reflects the TS water surface slope in the primary direction of flow. The estimated average velocities in the low marsh and high marsh at transect B for the 13th

MODFLOW iteration were 3.4 and 2.0 cm/s, respectively. The measured average velocities in the low marsh and high marsh at transect B were 5.7 and 2.9 cm/s, respectively. The percent difference between the estimated and measured velocity in the low marsh and the high marsh (LQ3 only) were -40% and -31%, respectively. The discrepancy between the estimated and measured average velocities at transect B is due to the difference in predicted and measured cross sectional areas at transect B. The estimated cross-sectional area at transect B was 2.4 m². The cross-sectional area at transect B included in the velocity measurements was 1.9 m². Community RQ2 (Figure 6.4) was partially inundated during the AOE; however, no measureable flow was occurring through RQ2, so the community was not included in the velocity measurements. If the flow velocity through RQ2 is assumed to be 0 cm/s, the area-weighted mean measured velocity in the high marsh is 1.7 cm/s, indicating the model is actually overpredicting velocity in the high marsh and underpredicting velocity in the low marsh.

The model error was scaled by the water depth and the elevation change from the wetland inlet to the wetland outlet. Scaling the model error contextualizes the value of the error in relation to the wetland conditions. Scaling the model error by the water depth determined the percent error in the water depth estimation. The mean water depth percent error was -4.7%. The percent error ranged from -24.3% for staff gage E2 to 10% for staff gage A1. Six of the 15 measurement points had percent errors within 1% of the water depth. Nine of the 15 points were within 10% of the measured water depth. The total elevation drop from the wetland inlet to the outlet was 0.3 m. Scaling the model error by the total elevation change across the wetland indicated how well the model performed in relation to topographic gradient. The mean error was -3.5% of the total elevation change. One third of the 15 direct measurement points had percent errors within 1% of the total elevation change. The largest negative error at staff gage C3 was -14.4% of the total elevation change. The largest positive error at staff gage A1 was 4.5% of the total elevation change.

Examining each cross section individually, it was clear MODFLOW predicted most poorly in areas in which water surface rose rapidly between adjacent measurement points (Figure 6.6). The worst model performance occurred at measurement points with water surface elevations higher than the surrounding points (the “mounds” of water mentioned previously). The magnitude of the model error was reduced if the predicted water surface was compared to the trend surface water

surface instead of the water surface linearly interpolated between direct measurement points. The measured and predicted edges of water generally were in agreement.

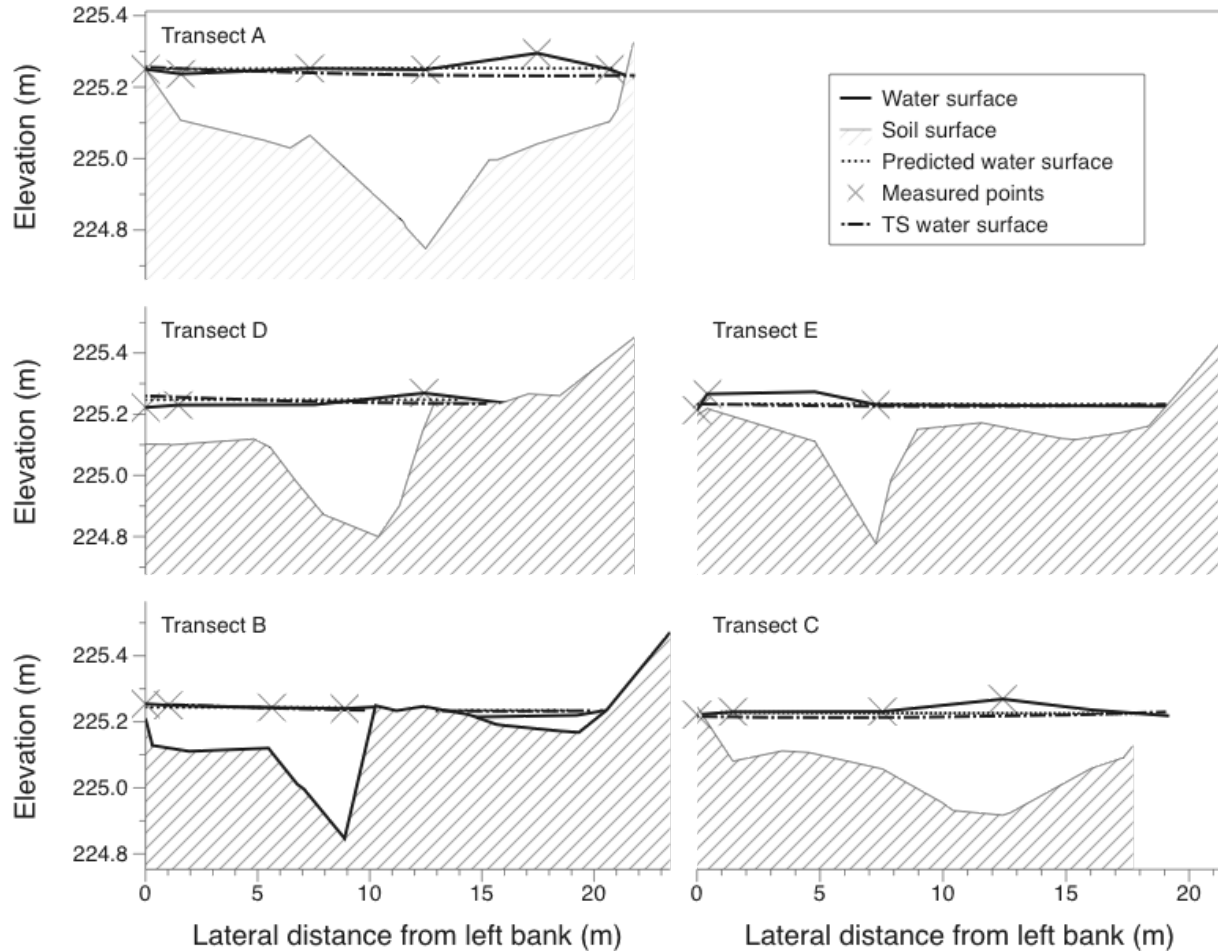


Figure 6.6 Predicted, measured, triangulated irregular network (TIN), and trend surface (TS) water surface at the five measurement transects. (vertical datum NAVD 88)

6.4.3 Model sensitivity analysis

6.4.3-1 MODFLOW sensitivity

To determine the feasibility of using MODFLOW to predict water surface head in wetlands, the sensitivity of MODFLOW to changes in surface K was determined. The surface K distribution was increased and decreased by 10, 25, 50 and 75% and the subsequent changes in water surface elevation and gradient were explored. Head and slope near the inlet and outlet changed considerably with each parameter change so only changes in the main body of the wetland were

considered. It is unclear exactly why the head and slope near the inlet and outlet was so sensitive to changes in model parameters but it may be because the inlet and outlet are modeled as points.

Table 6.1 summarizes the results of the sensitivity analysis. MODFLOW output responded more to the reduction in K than the increase in K . Reducing K by 75% resulted in an average water surface elevation increase of 22.5 cm. Increasing K by 75% only decreased the water surface elevation an average of 1.1 cm, indicating some threshold K exists beyond which wetland flow begins behave more like open channel flow than porous media flow. The inundated area of the wetland was more sensitive to increases in K than decreases in K . In the original model state, nearly all of the available wetland area was inundated. Once the entire wetland was inundated, the surface layer head was able to increase greatly. However, as K increased and the inundated area decreased, the remaining inundated areas (the low marsh and pools) were less sensitive to changes in head and depth.

Increasing or decreasing K did not change the water surface slope much. Increasing K by 75% resulted in an average water surface slope increase of 0.06%; decreasing K by 75% resulted in an average water surface slope decrease of 0.01%. However, the predicted water surface slope was small so even small absolute changes in the water surface slope were large relative changes in the water surface slope.

Table 6.1 MODFLOW sensitivity to changes in the surface hydraulic conductivity (K).

Change in K	Change in head (cm)		Change in slope (%)		Mean percent change in depth	Inundated area (m ²)
	Mean	Standard deviation	Mean	Standard deviation		
Overall average	-3.0	2.2	3.7E-02	428.1%	428.1%	614
High marsh - low marsh average	-1.7	0.1	2.5E-03	133.0%	133.0%	1115
-75%	22.5	1.3	6.1E-02	48.6%	48.6%	1186
-50%	7.0	0.6	2.7E-02	0.6%	0.6%	1186
-25%	2.9	0.2	1.1E-02	0.0%	0.0%	1185
-10%	0.0	0.0	1.3E-03	-7.9%	-7.9%	1185
+10%	0.0	0.0	-8.0E-04	-12.0%	-12.0%	1185
+25%	-0.9	0.1	-5.5E-03	-8.3%	-8.3%	1163
+50%	-1.5	0.2	-8.5E-03	428.1%	428.1%	1145
+75%	-1.1	0.9	-1.1E-02	133.0%	133.0%	1052

K was determined for 14 different vegetation “communities.” To determine if MODFLOW was sensitive to the level of vegetation survey detail, K was averaged using two averaging techniques: an overall average and a high-marsh low marsh average. For the overall average, the vegetation properties were averaged over the entire wetland using an area weight. For the high marsh-low marsh average, the wetland was divided into two zones of similar vegetation: the densely vegetated high marsh and the sparsely vegetated low marsh and pools. Both averaging techniques generally reduced the water surface elevation in the wetland: the overall area weighted average reduced head by an average of 3.0 cm and the high and low marsh averages reduced the water surface elevation by 1.7 cm on average. Averaging the K across vegetation communities increased the average water surface slope.

6.4.3-2 K -prediction sensitivity

MODFLOW is sensitive to changes in K . However, it is not intuitively clear how vegetation or flow properties would have to change to effect such changes in K . Equations [6.1] and [6.5] were combined and solved to determine how much d , maa , and v would have to change to produce 10, 25, 50, and 75% increases and decreases in K . The results of the K prediction sensitivity analysis are summarized in Table 6.2. K is most sensitive to changes in d . For example, a 25% decrease in K can be affected by a 24.0% reduction in d . In contrast, a 25% decrease in K would require an 84.4% increase in maa or a 42.5% decrease in v . Changes in K

caused by changes in d were nearly symmetrical; a 10% increase in K would require a 9.5% increase in d and a 10% decrease would require a 9.5% decrease in d . In contrast, a 25% increase in K would require a 38% decrease in maa while a 25% decrease in K would require an 84% increase in maa .

Table 6.2 Sensitivity of surface hydraulic conductivity (K) to changes in vegetation properties and the estimated velocity.

Change in K	Percent change in stem diameter (d)	Percent change in unit momentum absorbing area (maa)	Percent change in estimated velocity (v)
-75%	-73.3%	1809.8%	-93.0%
-50%	-48.3%	337.0%	-73.6%
-25%	-24.0%	84.4%	-42.5%
-10%	-9.5%	25.1%	-18.3%
+10%	9.5%	-18.4%	20.1%
+25%	23.7%	-37.8%	53.6%
+50%	47.1%	-57.8%	118.1%
+75%	70.4%	-69.6%	193.3%

6.5 Discussion

Overall, MODFLOW appeared to predict water surface elevation in the wetland well. Four inconsistent water depth measurements were the source of the most of the model error. MODFLOW slightly underpredicted the total inundated area within the wetland. MODFLOW predicted the water surface elevation most accurately in the low marsh area that was characterized by greater depths and higher velocities.

MODFLOW output is not very sensitive to small changes ($\sim \pm 10\%$) in K . In estimating K , the stem diameter is the most sensitive parameter so accurate determination of d is important. maa estimation is comparatively not as important, although measurement of d and maa is often coincident and dependent (d and maa were measured at the same time using a leaf-area meter). Accurate estimation of velocity is not crucial to the model function; a 20% under- or over-estimation of velocity in the model parameter estimation procedure will only result in a 10% under- or over-estimation of K . A 10% under- or over-estimation of K will not discernibly change the model results.

While piece-wise sensitivity analysis of K -prediction is useful, it is an oversimplification. As vegetation grows, stems increase in size and proliferate, resulting in an increase in d and maa . If the stems increase in size but the stem density remains the same, K will actually increase (insofar as d does not increase beyond 0.5 cm, which is the maximum stem diameter for which the f -prediction relationship was developed). The reason stem size is positively correlated with K is likely due to the nature of the vegetation for which it was developed. Equation [6.1] was developed for *Scirpus cyperinus* (L.) Kunth, which has a relatively small stem diameter (0.1 – 0.3 cm) but grows densely. Small stem diameters combined with high stem densities creates highly tortuous flow paths increasing hydraulic resistance. As stem diameters get larger, the flow paths become more streamlined and resistance is reduced. If the stem density (assuming cylindrical stems) increases while the stem size remains the same, K will decrease. If the stem diameter and density are both increasing (assuming cylindrical vegetation), the stem density must increase at a rate at least 1.3 times the rate at which the stem diameter is increasing to see no increase in K .

It is important to note, the f -prediction relationship [6.1] was developed from data collected in a flume system planted with a dense monoculture of *Scirpus cyperinus* (L.) Kunth, which is roughly cylindrical. Cylindrical vegetation can only increase in stem size and density. For other vegetation types, branching or the proliferation of leaves may occur, increasing the maa . It is unclear how or if the f -prediction relationship will change for other vegetation structures.

The inconsistent performance of the model may be caused by many factors. Surveying was conducted over many sessions, requiring repeated georeferencing to benchmarks. The model error was within the range of error in the surveyed elevation. The f -prediction relationship on predicts friction factor due to emergent stems. The R^2 of the f -prediction relationship was only 0.71. The application of the f -prediction relationship outside of a dense monoculture of *Scirpus cyperinus* (L.) Kunth may be an additional source of error. Additional roughness elements such as submerged vegetation and soil roughness were not considered. In systems with a combination of emergent and submerged vegetation and/or shallow flow over a soil surface with large microtopographic features, the friction factor prediction may have to be modified to consider the submerged roughness elements.

6.6 Conclusions

MODFLOW has the potential to predict water surface elevation in a wetland during a flow event. MODFLOW generally underpredicted water surface elevation, with an average model error of -1.1 cm or -3.5% of the total elevation change from the wetland inlet to outlet. However, changes in water surface elevation in the wetland system were small and it was unclear if the model error was due to error in the model prediction, error in the prediction of K , or error in the topographic survey, or a combination thereof. When the four water surface measurement points representing the odd water surface “mounds” are eliminated, the average error in the MODFLOW surface water elevation prediction drops to within the water surface measurement limits.

Changes in water surface elevation are sensitive to relatively large changes in surface K but no pronounced change in the predicted water surface elevation was evident if K was changed slightly ($\pm 10\%$). K was most sensitive to changes in stem diameter. The sensitivity analysis conducted will not be consistent for all wetland sites. Changes in the surface water head are dependent on the proportion of the wetland area inundated; once the total available wetland area is inundated, surface water head increases dramatically with decreases in the surface K .

Chapter 7 Summary and Conclusions

The goal of this research was to determine how emergent herbaceous vegetation affects hydraulic resistance in laminar to transitional flows typically observed in wetland systems. To achieve this goal, three main objectives were completed:

1. Identify and assess the usefulness of existing models applicable to low-Reynolds number flows typical of low-gradient, densely-vegetated wetlands. (Chapter 4);
2. Determine the relationship between friction factor and measureable properties of natural vegetation including streamwise projected area, stem density, stem diameter, vegetation spacing, and flexibility (Chapter 5); and,
3. Model wetland surface water flow through a small constructed wetland using properties of the wetland emergent vegetation to determine the hydraulic resistance (Chapter 6).

The results of this research will inform the development of a robust model describing vegetative hydraulic resistance. Ultimately, a robust vegetative resistance model can be used to predict flow events in existing wetlands or to predict flows in not-yet-constructed wetlands as part of the development of a comprehensive water budget. Knowledge of vegetative resistance can ultimately aid wetland designers in creating constructed wetlands that function in the way they were designed, replacing wetland function and services lost from widespread wetland destruction.

7.1 Objective 1: Identify, fit, and assess the usefulness of existing models applicable to low-Reynolds number flows

Six vegetative drag flow models [*Lindner*, 1982; *Kadlec*, 1990; *Fathi-Moghadam and Kouwen*, 1997; *Nepf*, 1999; *Stone and Shen*, 2002; *Hoffmann*, 2004] were selected for study and were combined with one of six drag coefficient (C_d) estimators (constant 1.05, C_d for a single isolated cylinder and four empirical C_d predictors [*Lindner*, 1982; *Taylor et al.*, 1985; *Choi and Kwon*, 1999; *Harvey et al.*, 2009]). The six flow models differed from each other only in the definition of the vegetal area coefficient (λ) (L^{-1}), which is defined as a plant area per volume. Additionally

three bulk drag coefficient (C_d') (L^{-1}) predictors were tested: two based on lab and field studies of sawgrass (*Cladium P. Br.*) [Lee *et al.*, 2004] and one based on a compilation of existing lab and field studies [Wu *et al.*, 1999]. Of the 36 combinations of flow models and C_d predictors as well as the three C_d' predictors, the six best-performing complete hydraulic resistance models were selected.

The best performing models were the Wu *et al.* [1999] C_d' predictor and the Lee *et al.* [2004] C_d' predictor for field conditions and the Harvey *et al.* [2009] C_d predictor relationship in combination with the Nepf [1999], Lindner [1982], Stone and Shen [2002], and Hoffman [2004] flow models. Each of the best-performing models included empirical relationships developed from real vegetation. The best C_d predictor was the Harvey *et al.* [2009] C_d predictor developed from Everglades field data for ridge conditions.

The best models performed well at low to moderate water depths (30-50% of the vegetation submerged) and poorly at water depths that approached the vegetation depth. While the goal of the study was not to predict model error, results indicated model relative error was a function of vegetation properties such as stem diameter (d) (L), blockage factor (BF), and vegetation flexural rigidity (MEI) ($M \cdot L^3 / T^2$). The interaction between model fit and vegetation properties indicated the models were not completely defined across all water depths and may require additional variables to improve the model fit. The C_d and C_d' regression coefficients should be allowed to vary depending on the vegetation structure and density. However, without refitting each C_d or C_d' predictor for each new vegetation type, it is unclear how to change the coefficients of the empirical C_d or C_d' predictor to reflect changes in vegetation structure and density.

7.2 Objective 2: Determine the relationship between friction factor and measureable properties of natural vegetation

Regression relationships were developed to predict friction factor (f) in low-Reynolds number emergent vegetated flows based on properties of the vegetation and the flow conditions. Previous studies focused on predicting the C_d instead of the f . However, C_d is a property of the characteristic drag area. Unless the characteristic drag areas are the same, C_d values are not comparable. f is a composite value and avoids any potential confusion over the characteristic drag area.

Seven regression models satisfied the criteria reducing bias and multicollinearity while maximizing the significance and goodness-of-fit. The models based on the unit momentum absorbing area (maa) (L^{-1}) had consistently higher robust R^2 values and consistent interactions; one model was independently validated. The best overall model included a vegetal area coefficient term, $maa \cdot d$; a vegetation flexibility term based on MEI); a flow term, Re_{stem} ; and a tailgate height indicator variable for the 0.2-m tailgate height, at which approximately 50% of the vegetation was submerged. Previous studies found hydraulic resistance was a function of Re_{stem} and a measure of vegetation density. The results of this study suggest vegetation flexibility should be considered in future studies in addition to Re_{stem} and vegetation density.

The regression models were sensitive to changes in the premultiplier; changing the premultiplier to the lower limit of the 95% confidence interval increased the NSE from -0.03 to 0.76. The fit to measured data was still not perfect with the lower premultiplier, overpredicting friction factors below 50 and underpredicting friction factors above 300. Since the validation data set did not include estimates of flexibility, the three- and four-term models could not be tested to see if model fit could be improved if MEI were included.

Models based on the frontal area per unit volume (A_f) (L^{-1}) had consistently lower robust R^2 values and the addition of other parameters did not improve the fit. Due to the presence of overlap and the heterogeneity of vegetated systems, the measurement of A_f included a greater degree of uncertainty, as compared to the measurement of maa . In the low Reynolds numbers flows examined in this paper, maa may indeed be a better analog for drag. In low Reynolds number flows, the degree of wake sheltering is less than that for more turbulent flows. While vortex shedding was observed in the flume study, the degree of flow separation was not large and the sheltering effect of clumped vegetation was not as great as would be expected in more turbulent flows. A_f may be better correlated with f in more turbulent flows in which sheltering and streamlining of plants may reduce the drag considerably.

The performance of the two-term maa model, which included $maa \cdot d$ and Re_{stem} , was assessed using data collected in the Florida Everglades [Harvey *et al.*, 2009]. The two-term model generally overpredicted f by a large margin (Relative errors ranged from 0.1 to 100.), especially

at depths below 0.3 m. However, it appears the lack of fit at shallow depths is due to a significant difference in vegetation architecture in the Everglades. When water levels are higher, the two-term regression still overpredicts f but the relative error is considerably smaller than at shallower depths.

7.3 Objective 3: Model wetland surface water flow through a small constructed wetland

A simple two-term regression developed in Chapter 5 was used to predict f during a 6-hour artificial overbank event based on vegetation properties and estimated flow properties in a small constructed floodplain wetland near Stephens City, VA. f was converted to a value of hydraulic conductivity (K) (L/T), allowing the wetland system to be modeled using MODFLOW. The surface flow was modeled as a highly-conductive unconfined aquifer atop a less conductive soil layer. MODFLOW slightly underpredicted the hydraulic head in the wetland. The model error relative to the water depth was smallest in the deepest portions of the wetland. The slope of the predicted water surface was slightly less (0.04) than the water surface slope in the primary flow direction along the low marsh channel (0.05). Sensitivity analysis indicated MODFLOW was sensitive to changes in the surface K , especially if the surface K was reduced (increasing hydraulic resistance). The vegetation parameter that had the greatest effect on the estimated K and the predicted hydraulic head was d .

The regression model used to predict the f was developed for a dense stand of woolgrass (*Scirpus cyperinus* (L.) Kunth) and its application outside of the system for which it was developed is a potential source of model error. Additionally, the f -prediction model assumes the primary source of hydraulic resistance is vegetation; for flow through dense vegetation over a relatively smooth boundary, this is a good assumption. However, in the high marsh regions, the microtopographic features of the wetland surface were large in comparison to the relatively shallow flow depth. Hydraulic resistance from the boundary may be significant in comparison to the stem resistance and should be quantified for shallow flows.

7.4 Study implications

The goal of this research was to determine how vegetation properties affect hydraulic resistance in low Reynolds number emergent vegetated flows. Existing drag models are similar in form and describe hydraulic resistance as a function of C_d and the characteristic drag area (A_r). However, since hydraulic resistance in laminar to transitional flows is dependent on flow characteristics as well as vegetation characteristics, the hydraulic resistance parameter (f , n , C_d , etc.) must be allowed to vary. Currently, hydraulic resistance must be measured or derived for each combination of vegetation and flow regime.

Good wetland design requires the accurate representation of all water budget components including surface flow characteristics. However, the unique relationship between vegetation and flow cannot be determined without experimentation, which is impractical or impossible in most wetland designs. A model is needed that can predict hydraulic resistance based on an assumed vegetation regime given the surface flow inputs and characteristics of the outlet structure are known.

This research has identified existing empirical C_d relationships developed in the Everglades can predict flow velocity (V) through a monoculture of *Scirpus cyperinus* (L.) Kunth, a common species found in constructed wetlands. Empirical relationships developed for a natural wetland system populated by various vegetation species of various architectures can reasonably describe one-dimensional emergent flow through a planted monoculture. It may be possible to describe vegetative hydraulic resistance from a set of vegetation parameters that can be defined regardless of vegetation species, indicating vegetated hydraulic resistance is controlled by a universal measure of vegetation geometry.

This study confirms previous study results that show hydraulic resistance can be described using Re_{stem} , λ , and d . λ can be described using the one-sided area of all vegetation within a unit volume (maa) or as the projected area of the vegetation (neglecting vegetation that is sheltered by upstream plants) per unit volume (A_f).

The results of this research also indicate that vegetation flexibility described by MEI is an important consideration in describing hydraulic resistance. While previous studies [Roig, 1994;

Fathi-Moghadam and Kouwen, 1997; Freeman et al., 2000] have described how vegetation flexibility can lead to streamlining of plants at higher flows leading to an overall reduction in drag, this study found vegetation flexibility at low flows leads to a slight increase in drag. Vegetation flexibility should be considered in future studies on vegetative resistance.

MODFLOW can be used to describe hydraulic resistance in wetland systems as long as the K is allowed to vary with the flow conditions. The structure of MODFLOW in its current form is not ideal for application to wetland systems, however. The base code of the model must be modified to accurately describe outflow through the wetland outlet structure. Additionally, the hydraulic conductivity of the surface layer must be converged upon using a manual iteration procedure. The difference in time steps between surface and subsurface flow must also be resolved since a one-minute time step is not meaningful in more subsurface systems. For MODFLOW to be a feasible modeling solution for wetland designers, the iteration procedure should be automated.

7.5 Limitations and future work

The nature of the flume study did not allow for a full range of flow and vegetation conditions. The flume was planted with a monoculture of *Scirpus cyperinus* (L.) Kunth, and while the species is commonly planted in constructed wetlands, *Scirpus cyperinus* (L.) Kunth is a cylindrical species and does not represent the full range of possible vegetation architectures. Future studies should consider a range of vegetation architectures including floating macrophytes and branching species.

The flume also did not allow a range of bed slopes to be considered. *Wu et al.* [1999] found bed slope (S_b) to be predictive of the bulk drag coefficient (C_d'). Future studies should be designed such that S_b can be varied so the dependence of hydraulic resistance on S_b can be determined.

The limitation of the flume setup also prevented a wide range of flowrates from being considered. The head tank was limited to small range of inflow rates (3.1 and 4.1 L/s). Consequently, V within the flume was correlated with the flow depth (h). Future studies designed with a larger range of inflow rates will uncouple h and V , allowing more insight to be gained into the relationship between hydraulic resistance and h .

Due to the manual iteration procedure required in the determination of K in the wetland surface layer in MODFLOW and the omission of the use of the unsaturated flow package, only steady-state conditions were simulated in the Hedgebrook Farm wetland. The application of MODFLOW to wetland design will require the ability to simulate transient conditions as well. The iteration procedure should be automated and optimized for efficiency. The addition of the unsaturated flow package should also be included so the wetting of the soil surface from surface flow can be accurately simulated.

Chapter 8 References

- (2001), Compensating for Wetland Losses under the Clean Water Act, Board on Environmental Studies and Toxicology, p. 322, Division of Earth and Life Sciences, National Research Council.
- (2003), ERDAS Imagine 8.7, ERDAS, Inc., Norcross, GA.
- (2008), ArcGIS 9.3, ESRI, Redlands, CA.
- Abdelsalam, M. W., A. F. Khattab, A. A. Khalifa, and M. F. Bakry (1992), Flow Capacity through Wide and Submerged Vegetal Channels, *Journal of Irrigation and Drainage Engineering-ASCE*, 118(5), 724-732.
- Arega, F., and B. F. Sanders (2004), Dispersion model for tidal wetlands, *Journal of Hydraulic Engineering-ASCE*, 130(8), 739-754.
- Bedford, B. L. (1996), The need to define hydrologic equivalence at the landscape scale for freshwater wetland mitigation, *Ecological Applications*, 6(1), 57-68.
- Bennett, S. J. (2004), Effects of Emergent Riparian Vegetation on Spatially Averaged and Turbulent Flow Within an Experimental Channel, in *Riparian Vegetation and Fluvial Geomorphology* edited by S. J. Bennett and A. Simon, pp. 29-41, American Geophysical Union, Washington, D.C.
- Beuselinck, L., P. B. Hairsine, G. Govers, and J. Poesen (2002), Evaluating a single-class net deposition equation in overland flow conditions, *Water Resources Research*, 38(7).
- Bolster, C. H., and J. E. Saiers (2002), Development and evaluation of a mathematical model for surface-water flow within the Shark River Slough of the Florida Everglades, *Journal of Hydrology (Amsterdam)*, 259(1/4), 221-235.
- Bouwer, O. W., and J. V. Schilfgaard (1963), Simplified method of predicting fall of water table in drained land, *Transactions of the American Society of Agricultural Engineering*, 6(4), 288-291.
- Brookes, C. J., J. M. Hooke, and J. Mant (2000), Modelling vegetation interactions with channel flow in river valleys of the Mediterranean region, *Catena*, 40(1), 93-118.
- Buchberger, S. G., and G. B. Shaw (1995), An Approach toward Rational Design of Constructed Wetlands for Waste-Water Treatment, *Ecological Engineering*, 4(4), 249-275.
- Carollo, F. G., V. Ferro, and D. Termini (2002), Flow velocity measurements in vegetated channels, *Journal of Hydraulic Engineering-ASCE*, 128(7), 664-673.
- Chiang, W. H.-., and W. Kinzelbach (2001), Processing MODFLOW. A simulation system for modeling groundwater flow and pollution.

- Choi, S.-U., and K. Kwon (1999), Simulation of Vertical Structure of Vegetated Open-Channel Flows using k- ϵ Turbulence Model, in *Hydraulic Modeling*, edited by V. P. Singh, I. W. Seo and J. H. Sonu, Water Resources Publication.
- Christiansen, T., P. L. Wiberg, and T. G. Milligan (2000), Flow and sediment transport on a tidal salt marsh surface, *Estuarine Coastal and Shelf Science*, 50(3), 315-331.
- Cole, C. A., and R. P. Brooks (2000), A comparison of the hydrologic characteristics of natural and created mainstem floodplain wetlands in Pennsylvania, *Ecological Engineering*, 14(3), 221-231.
- Copeland, R. R. (2000), Determination of flow resistance coefficients due to shrubs and woody vegetation, edited by U.S. Army Corps of Engineers.
- Dahl, T. E. (1990), Wetlands Losses in the United States 1780's to 1980's., edited by U.S. Fish and Wildlife Service, U.S. Department of the Interior, Washington, D.C., Jamestown, ND: Northern Prairie Wildlife Research Center Online.
- Dahl, T. E., C. E. Johnson, and W. E. Frayer (1991), Status and trends in the conterminous United States mid-1970's to mid-1980's, edited by U.S. Fish and Wildlife Service, U.S. Department of the Interior, Washington, D.C., p. 28.
- Dahl, T. E. (2000), Status and trends of wetlands in the conterminous United States 1986 to 1997, edited by U.S. Fish and Wildlife Service, Department of the Interior, p. 82, Washington, D.C.
- Darby, S. E., and C. R. Thorne (1996), Predicting stage-discharge curves in channels with bank vegetation, *Journal of Hydraulic Engineering-ASCE*, 122(10), 583-586.
- Dudley, S. J., J. C. Fischenich, and S. R. Abt (1998), Effect of woody debris entrapment on flow resistance, *Journal of the American Water Resources Association*, 34(5), 1189-1197.
- Dugan, P. (Ed.) (1993), *Wetlands in danger: a world conservation atlas*, Oxford University Press, New York, NY.
- Eastgate, W. I. (1966), Vegetated stabilization of grasses, waterways, and dam bywashes, University of Queensland, St. Lucia, Queensland, Australia.
- Fathi-Moghadam, M., and N. Kouwen (1997), Nonrigid, nonsubmerged, vegetative roughness on floodplains, *Journal of Hydraulic Engineering*, 123(1), 51-57.
- Fathi-Moghadam, M. (2007), Characteristics and mechanics of tall vegetation for resistance to flow, *African Journal of Biotechnology*, 6(4), 475-480.
- Feng, K., and F. J. Molz (1997), A 2-D, diffusion-based, wetland flow model, *Journal of Hydrology (Amsterdam)*, 196(1/4), 230-250.

Frayner, W. E., T. J. Monahan, D. C. Bowden, and F. A. Graybill (1993), Status and trends of wetlands and deepwater habitats in the conterminous United States 1950's to 1970's, book, 59 pp, National Wetlands Inventory U.S. Fish and Wildlife Service, Department of Forest and Wood Sciences Colorado State University, Fort Collins Colorado.

Freeman, G. E., W. J. Raymeyer, and R. R. Copeland (2000), Determination of resistance due to shrubs and woody vegetation, edited by U.S. Army Corps of Engineers, p. 64, US Army Engineer Research and Development Center.

Galatowitsch, S. M., and A. G. vanderValk (1996), Characteristics of recently restored wetlands in the prairie pothole region, *Wetlands*, 16(1), 75-83.

Garbisch, E. W. (2002), *The Dos and Don'ts of Wetland Construction: Creation, Restoration, and Enhancement*, Environmental Concern, Inc., St. Michaels, MD.

Garcia, M. H., F. Lopez, C. Dunn, and C. V. Alonso (2004), Flow, Turbulence, and Resistance in a Flume with Simulated Vegetation, in *Riparian Vegetation and Fluvial Geomorphology*, edited by S. J. Bennett and A. Simon, pp. 11-19, American Geophysical Union, Washington, D.C.

Grapes, T. R., C. Bradley, and G. E. Petts (2006), Hydrodynamics of floodplain wetlands in a chalk catchment: The River Lambourn, UK, *Journal of Hydrology*, 320(3-4), 324-341.

Green, J. C. (2005a), Velocity and turbulence distribution around lotic macrophytes, *Aquatic Ecology*, 39(1), 1-10.

Green, J. C. (2005b), Modelling flow resistance in vegetated streams: review and development of new theory, *Hydrological Processes*, 19(6), 1245-1259.

Green, W. H., and G. A. Ampt (1911), Studies on soil physics: the flow of air and water through soils, *Journal of Agricultural Science*, 4(1), 24.

Hall, B. R., and G. E. Freeman (1994), Study of hydraulic roughness in wetland vegetation takes new look at Manning's n, in *The Wetlands Research Program Bulletin*, edited, pp. 1-4.

Hammer, D. E., and R. H. Kadlec (1986), A Model for Wetland Surface-Water Dynamics, *Water Resources Research*, 22(13), 1951-1958.

Harvey, J. W., R. W. Schaffranek, G. B. Noe, L. G. Larsen, D. J. Nowacki, and B. L. O'Connor (2009), Hydroecological factors governing surface water flow on a low-gradient floodplain, *Water Resources Research*, 45.

Haslam, S. M. (1978), *River Plants : The Macrophytic Vegetation of Watercourses*, 396 pp., Cambridge University Press, New York.

Hilderbrand, R. H., A. C. Watts, and A. M. Randle (2005), The myths of restoration ecology, *Ecology and Society*, 10(1).

- Hoffmann, M. R. (2004), Application of a simple space-time averaged porous media model to flow in densely vegetated channels, *Journal of Porous Media*, 7(3), 183-191.
- Holland, J. F., J. F. Martin, T. Granata, V. Bouchard, M. Quigley, and L. Brown (2004), Effects of wetland depth and flow rate on residence time distribution characteristics, *Ecological Engineering*, 23(3), 189-203.
- Hsieh, T. (1964), Resistance of cylindrical piers in open-channel flow, *Journal of the Hydraulics Division - ASCE*, 90(HY1), 161-173.
- Hvorslev, M. J. (1951), Time lag and soil permeability in ground-water observations, edited by U.S. Army Corps of Engineers. Waterways Experiment Station, p. 50, Vicksburg, MS.
- Jadhav, R. S., and S. G. Buchberger (1995), Effects of Vegetation on Flow through Free Water Surface Wetlands, *Ecological Engineering*, 5(4), 481-496.
- James, C. S., A. L. Birkhead, A. A. Jordanova, and J. J. O'Sullivan (2004), Flow resistance of emergent vegetation, *Journal of Hydraulic Research*, 42(4), 390-398.
- Jarvela, J. (2002a), Flow resistance of flexible and stiff vegetation: a flume study with natural plants, *Journal of Hydrology*, 269(1-2), 44-54.
- Jarvela, J. (2002b), Determination of Flow Resistance of Vegetated Channel Banks and Floodplains, in *River Flow*, edited by D. Bousmar and Y. Zech, pp. 311-318, Swets and Zeitlinger, Lisse.
- Jarvela, J. (2004), Determination of flow resistance caused by non-submerged woody vegetation, *International Journal of River Basin Management*, 2(1), 10.
- Jarvela, J. (2005), Effect of submerged flexible vegetation on flow structure and resistance, *Journal of Hydrology*, 307(1-4), 233-241.
- Jenkins, G. A., and M. Greenway (2005), The hydraulic efficiency of fringing versus banded vegetation in constructed wetlands, *Ecological Engineering*, 25(1), 61-72.
- Kadlec, R. H. (1990), Overland-Flow in Wetlands - Vegetation Resistance, *Journal of Hydraulic Engineering-ASCE*, 116(5), 691-706.
- Kadlec, R. H., and R. L. Knight (1996), *Treatment Wetlands*, CRC Press, Boca Raton, FL.
- Kazezyilmaz-Alhan, C. M., M. A. Medina, and C. J. Richardson (2007), A wetland hydrology and water quality model incorporating surface water/groundwater interactions, *Water Resources Research*, 43(4).
- Kouwen, N., and R. M. Li (1980), Biomechanics of Vegetative Channel Linings, *Journal of the Hydraulics Division-ASCE*, 106(6), 1085-1106.

- Kouwen, N., R. M. Li, and D. B. Simons (1981), Flow Resistance in Vegetated Waterways, *Transactions of the ASAE*, 24(3), 684.
- Kouwen, N. (1988), Field Estimation of the Biomechanical Properties of Grass, *Journal of Hydraulic Research*, 26(5), 559-568.
- Kouwen, N., and M. Fathi-Moghadam (2000), Friction factors for coniferous trees along rivers, *Journal of Hydraulic Engineering-ASCE*, 126(10), 732-740.
- Krause, A. F. (1999), Modeling the Flood Hydrology of Wetlands using HEC-HMS, PDF thesis, 153 pp, University of California-Davis, Davis.
- Kutija, V., and H. T. M. Hong (1996), A numerical model for assessing the additional resistance to flow introduced by flexible vegetation, *Journal of Hydraulic Research*, 34(1), 99-114.
- Lautz, L. K., and D. I. Siegel (2006), Modeling surface and ground water mixing in the hyporheic zone using MODFLOW and MT3D, *Advances in Water Resources*, 29(11), 1618-1633.
- Lawrence, D. S. L. (2000), Hydraulic resistance in overland flow during partial and marginal surface inundation: Experimental observations and modeling, *Water Resources Research*, 36(8), 2381-2393.
- Lawrence, D. S. L., J. R. L. Allen, and G. M. Havelock (2004), Salt marsh morphodynamics: An investigation of tidal flows and marsh channel equilibrium, *Journal of Coastal Research*, 20(1), 301-316.
- Lee, E. R. (1999), SET-WET: a wetland simulation model to optimize NPS pollution control, 257 pp, Virginia Polytechnic Institute and State University, Blacksburg, VA.
- Lee, E. R., S. Mostaghimi, and T. M. Wynn (2002), A model to enhance wetland design and optimize nonpoint source pollution control, *Journal of the American Water Resources Association*, 38(1), 16.
- Lee, J. K., L. C. Roig, H. L. Jenter, and H. M. Visser (2004), Drag coefficients for modeling flow through emergent vegetation in the Florida Everglades, *Ecological Engineering*, 22(4-5), 237-248.
- Lightbody, A. F., and H. M. Nepf (2006), Prediction of velocity profiles and longitudinal dispersion in emergent salt marsh vegetation, *Limnology and Oceanography*, 51(1), 218-228.
- Lindner, K. (1982), Der Strömungswiderstand von Pflanzenbeständen, Leichtweiss-Institut für Wasserbau, Technische Universität Braunschweig, Braunschweig, DE.
- Liu, D., P. Diplas, J. D. Fairbanks, and C. C. Hodges (2008), An experimental study of flow through rigid vegetation, *J. Geophys. Res.*, 113.

- Maheshwari, B. L. (1992), Suitability of Different Flow Equations and Hydraulic Resistance Parameters for Flows in Surface Irrigation - a Review, *Water Resources Research*, 28(8), 2059-2066.
- Martin, J. F., M. L. White, E. Reyes, G. P. Kemp, H. Mashriqui, and J. W. Day (2000), Evaluation of coastal management plans with a spatial model: Mississippi delta, Louisiana, USA, *Environmental Management*, 26(2), 117-129.
- McDonald, M. G., and A. W. Harbaugh (1996), A modular three-dimensional finite difference groundwater flow model.
- Mein, R. G., and C. L. Larson (1973), Modeling infiltration during a steady rain, *Water Resources Research*, 9(2), 11.
- Meyer-Peter, E., and R. Muller (1948), Formulas for bed-load transport, paper presented at 3rd Meeting of IAHR, Stockholm, Sweden.
- Mitsch, W. J., and R. F. Wilson (1996), Improving the Success of Wetland Creation and Restoration with Know-How, Time, and Self-Design, *Ecological Applications*, 6(1), 77-83.
- Mitsch, W. J., and J. G. Gosselink (2000), *Wetlands, 3rd Edition*, John Wiley & Sons, Inc., New York, NY.
- Montgomery, D. C., E. A. Peck, and G. G. Vining (2006), *Introduction to linear regression analysis*, 4th ed., Wiley-Interscience, Hoboken, N.J.
- Naot, D., I. Nezu, and H. Nakagawa (1996), Hydrodynamic behavior of partly vegetated open channels, *Journal of Hydraulic Engineering-Asce*, 122(11), 625-633.
- Nash, J. E., and J. V. Sutcliffe (1970), River flow forecasting through conceptual models - Part I - a discussion of principles, *Journal of Hydrology*, 10(3), 282-290.
- Nepf, H. M. (1999), Drag, turbulence, and diffusion in flow through emergent vegetation, *Water Resources Research*, 35(2), 479-489.
- Pasche, E., and G. Rouve (1985), Overbank flow with vegetatively roughed flood plains, *Journal of Hydraulic Engineering*, 111(9), 17.
- Petryk, A. M., and G. Bosmajian (1975), Analysis of flow through vegetation, *Journal of the Hydraulics Division - ASCE*, 101(7), 871-884.
- Powell, K. E. C. (1978), Weed Growth - A Factor of Channel Roughness, in *Hydrometry: Principles and Practices*, edited by R. W. Herschy, pp. 327-352, John Wiley and Sons, Inc., Chichester.
- Raisin, G. W., and D. S. Mitchell (1995), The use of wetlands for the control of non-point source pollution, in *Water Science and Technology*.

- Reeve, A. S., D. I. Siegel, and P. H. Glaser (2000), Simulating vertical flow in large peatlands, *Journal of Hydrology*, 227(1-4), 207-217.
- Restrepo, J. I., A. M. Montoya, and J. Obeysekera (1998), A wetland simulation module for the MODFLOW ground water model, *Ground Water*, 36(5), 764-770.
- Righetti, A., and A. Armanini (2002), Flow resistance in open channel flows with sparsely distributed bushes, *Journal of Hydrology*, 269(1-2), 55-64.
- Roig, L. C. (1994), Hydrodynamic Modeling of Flows in Tidal Wetlands, diss thesis, 177 pp, University of California, Davis, Davis, CA.
- Ronkanen, A. K., and B. Klove (2008), Hydraulics and flow modelling of water treatment wetlands constructed on peatlands in Northern Finland (vol 42, pg 14, 2008), *Water Research*, 42(19), 4894-4894.
- Rouse, H. (1965), Critical analysis of open-channel resistance, *Journal of the Hydraulics Division - ASCE*, 91(4), 25.
- Sand-Jensen, K. (2003), Drag and Reconfiguration of Freshwater Macrophytes, *Freshwater Biology*, 48, 271-283.
- Sharitz, R. R., and J. W. Gibbons (1982), The ecology of southeastern shrub bogs (pocosins) and Carolina bays: a community profile, Washington, D.C.
- Simpson, #160, J. R., Montgomery, and D. C. (1998), A performance-based assessment of robust regression methods, *Communications in Statistics: simulation and computation*, 27(4), 19.
- Skaggs, R. W. (1978), A water management model for shallow water table soils., UNC Water Resource Research Institute, Raleigh, NC, US.
- Skaggs, R. W., J. W. Gilliam, and R. O. Evans (1991), A computer simulation of pocosin hydrology, *Wetlands*, 11(Supplement 1), 17.
- Smith, R. J., N. H. Hancock, and J. L. Ruffini (1990), Flood Flow through Tall Vegetation, *Agricultural Water Management*, 18(4), 317-332.
- Stone, B. M., and H. T. Shen (2002), Hydraulic resistance of flow in channels with cylindrical roughness, *Journal of Hydraulic Engineering-ASCE*, 128(5), 500 - 506.
- Taylor, R. P., H. W. Coleman, and B. K. Hodge (1985), Prediction of turbulent rough-wall skin friction using a discrete element approach, *Journal of Fluids Engineering*, 107(2), 7.
- Temple, D. M. (1986), Velocity Distribution Coefficients for Grass-Lined Channels, *Journal of Hydraulic Engineering-ASCE*, 112(3), 193-205.
- Thompson, A. M., B. N. Wilson, and T. Hustrulid (2003), Instrumentation to measure drag on idealized vegetal elements in overland flow, *Transactions of the ASAE*, 46(2), 295-302.

Thornthwaite, C. W. (1948), An approach toward a rational classification of climate, *American Geography Review*, 38, 40.

Tiner Jr., R. W. (1984), Wetlands of the United States: current status and recent trends, edited by F. a. W. S. U.S. Department of the Interior, Washington, D.C., p. 59.

Townsend, C. R., M. Begon, and J. L. Harper (2003), *Essentials of Ecology 2nd Edition*, 2 ed., 530 pp., Blackwell Publishing, Malden, MA.

Tsihrintzis, V. A., and E. E. Madiedo (2000), Hydraulic resistance determination in marsh wetlands, *Water Resources Management*, 14(4), 285-309.

Tsihrintzis, V. A. (2001), Variation of roughness coefficients for unsubmerged and submerged vegetation - Discussion, *Journal of Hydraulic Engineering-ASCE*, 127(3), 241-244.

Turner, A. K., and N. Chanmeesri (1984), Shallow flow of water through non-submerged vegetation, *Agricultural Water Management*, 8, 375 - 385.

U.S. EPA (2001), Functions and Values of Wetlands, edited by U.S. Environmental Protection Agency, p. 2, U.S. EPA.

Votteler, T. H., and T. A. Muir (2002), National Water Summary on Wetland Resources, edited by U.S. Geological Survey, Reston, VA.

Walton, R., R. S. Chapman, and J. E. Davis (1996), Development and application of the wetlands dynamic water budget model, *Wetlands*, 16(3), 347-357.

Wilson, C., and M. S. Horritt (2002), Measuring the flow resistance of submerged grass, *Hydrological Processes*, 16(13), 2589-2598.

Wu, F. C., H. W. Shen, and Y. J. Chou (1999), Variation of roughness coefficients for unsubmerged and submerged vegetation, *Journal of Hydraulic Engineering-ASCE*, 125(9), 934-942.

Yen, B. C. (2002), Open channel flow resistance, *Journal of Hydraulic Engineering-ASCE*, 128(1), 20-39.

Yohai, V. J. (1987), High Breakdown-Point and High Efficiency Robust Estimates for Regression, *The Annals of Statistics*, 15(2), 642-656.

Zentner, J., J. Glaspy, and D. Schenk (2003), Wetlands and riparian woodland restoration costs, *Ecological Restoration*, 21(3), 166-173.

Appendix A1: Flume data

Table A1. 1 Summary of flume flow data. Each point is the average of three repeated measurements.

Tailgate Height (m)	Flowrate (L/s)	Vegetation State	Water Depth (m)	Cross-Sectional Area (m ²)	Cross-Sectionally Averaged Velocity (m/s)	Energy Grade Slope (m/m)	Friction Slope (m/m)
0	3.1	2	0.09	0.11	2.99E-02	1.14E-02	4.59E-03
0	3.1	3	0.09	0.11	3.01E-02	1.09E-02	4.12E-03
0	3.1	4	0.08	0.10	3.11E-02	1.10E-02	4.21E-03
0	3.1	5	0.08	0.10	3.05E-02	1.06E-02	3.80E-03
0	3.1	6	0.07	0.09	3.58E-02	9.22E-03	2.40E-03
0	3.1	7	0.07	0.09	3.46E-02	8.97E-03	2.15E-03
0	4.1	2	0.10	0.12	3.51E-02	1.25E-02	4.93E-03
0	4.1	3	0.10	0.12	3.39E-02	1.21E-02	4.51E-03
0	4.1	4	0.09	0.11	3.63E-02	1.21E-02	4.51E-03
0	4.1	5	0.10	0.12	3.52E-02	1.16E-02	4.01E-03
0	4.1	6	0.08	0.10	4.26E-02	9.74E-03	2.18E-03
0	4.1	7	0.08	0.10	4.08E-02	9.52E-03	1.96E-03
0.1	3.1	3	0.13	0.17	2.01E-02	3.38E-03	2.96E-03
0.1	3.1	4	0.13	0.17	1.99E-02	3.28E-03	2.86E-03
0.1	3.1	5	0.13	0.14	2.01E-02	2.48E-03	2.06E-03
0.1	3.1	6	0.12	0.15	2.11E-02	1.46E-03	1.04E-03
0.1	3.1	7	0.12	0.15	2.11E-02	1.45E-03	1.03E-03
0.1	4.1	3	0.14	0.17	2.52E-02	3.12E-03	2.54E-03
0.1	4.1	4	0.13	0.16	2.51E-02	4.44E-03	3.86E-03
0.1	4.1	5	0.13	0.16	2.54E-02	3.45E-03	2.87E-03
0.1	4.1	6	0.13	0.15	2.67E-02	2.30E-03	1.72E-03
0.1	4.1	7	0.13	0.15	2.66E-02	2.08E-03	1.50E-03
0.2	3.1	2	0.22	0.27	1.20E-02	1.03E-03	1.03E-03
0.2	3.1	3	0.23	0.28	1.14E-02	9.69E-04	9.69E-04
0.2	3.1	4	0.22	0.27	1.15E-02	9.79E-04	9.79E-04
0.2	3.1	5	0.22	0.27	1.16E-02	5.78E-04	5.78E-04
0.2	3.1	6	0.22	0.27	1.17E-02	2.70E-04	2.70E-04
0.2	3.1	7	0.22	0.27	1.16E-02	3.61E-04	3.61E-04
0.2	4.1	2	0.23	0.28	1.55E-02	1.37E-03	1.15E-03
0.2	4.1	3	0.23	0.28	1.49E-02	1.33E-03	1.11E-03
0.2	4.1	4	0.23	0.27	1.50E-02	1.42E-03	1.21E-03
0.2	4.1	5	0.22	0.27	1.51E-02	8.05E-04	5.86E-04
0.2	4.1	6	0.22	0.27	1.53E-02	4.63E-04	2.44E-04
0.2	4.1	7	0.22	0.27	1.51E-02	3.51E-04	1.32E-04
0.4	3.1	2	0.44	0.54	5.93E-03	4.80E-04	4.80E-04
0.4	3.1	4	0.43	0.52	5.96E-03	1.59E-04	1.59E-04
0.4	3.1	7	0.43	0.53	5.91E-03	1.68E-04	1.68E-04
0.4	4.1	2	0.44	0.54	7.84E-03	5.00E-04	5.00E-04
0.4	4.1	3	0.44	0.54	7.75E-03	4.80E-04	4.80E-04
0.4	4.1	4	0.43	0.53	7.78E-03	4.56E-04	4.56E-04
0.4	4.1	5	0.43	0.52	7.83E-03	4.80E-04	4.80E-04
0.4	4.1	6	0.43	0.52	7.88E-03	1.31E-04	1.31E-04
0.4	4.1	7	0.43	0.53	7.76E-03	2.18E-04	2.18E-04

Table A1. 2 Summary of flume vegetation data

Vegetation State	Tailgate Height (m)	Average Stem Diameter (cm)	Average Stem Diameter at the Soil Surface (cm)	Average Vegetation Height (m)	N (stems/m ²)	Blockage Factor	MEI (N·m ²)
2	0	0.31	0.30	0.53	9365	0.92	355
2	0.2	0.30			9365	0.87	
2	0.4	0.27			6243	0.80	
3	0	0.20	0.23	0.63	6920	0.82	83
3	0.1	0.19			6920	0.79	
3	0.2	0.19			6920	0.75	
4	0	0.17	0.19	0.34	3058	0.84	212
4	0.1	0.17			3058	0.64	
4	0.2	0.15			3058	0.56	
4	0.4	0.15			1019	0.36	
5	0	0.12	0.11	0.43	1975	0.69	25
5	0.1	0.12			1975	0.61	
5	0.2	0.11			1975	0.48	
6	0	0.27	0.29	0.52	1608	0.51	132
6	0.1	0.26			1608	0.45	
6	0.2	0.24			1608	0.36	
7	0	0.25	0.26	0.43	1575	0.19	8
7	0.1	0.22			1575	0.18	
7	0.2	0.23			1575	0.15	
7	0.4	0.22			1050	0.11	

Table A1. 3 Derived parameters from flume data

Tailgate Height (m)	Flowrate (L/s)	Vegetation State	Froude number	Stem Reynolds number	Depth Reynolds number	Average Stem Spacing (m)	Porosity (m ³ /m ³)	Vegetal Area Coef-ficient <i>pa·d</i>	Vegetal Area Coef-ficient <i>maa·d</i>	Stem diameter to depth ratio (m/m)	Sub-mergence (m/m)	Friction factor <i>f</i>	
0	3.1	2	1.01E-03	87	2533	0.011	0.93	8.3E-02	8.9E-02	0.03	0.17	36.3	
		3	1.07E-03	58	2533	0.013	0.98	7.0E-02	2.7E-02	0.02	0.14	31.0	
		4	1.20E-03	52	2533	0.020	0.99	6.9E-02	8.7E-03	0.02	0.24	28.1	
		5	1.14E-03	36	2533	0.025	1.00	5.8E-02	2.8E-03	0.01	0.19	26.8	
		6	1.83E-03	95	2533	0.028	0.99	3.7E-02	1.2E-02	0.04	0.14	10.5	
		7	1.64E-03	87	2533	0.028	0.99	1.4E-02	1.0E-02	0.03	0.17	10.5	
		4.1	2	1.24E-03	101	3349	0.011	0.93	9.3E-02	8.8E-02	0.03	0.19	31.8
	3	1.17E-03	65	3349	0.013	0.98	8.1E-02	2.6E-02	0.02	0.16	31.0		
	4	1.44E-03	61	3349	0.020	0.99	7.7E-02	8.7E-03	0.02	0.27	25.0		
	5	1.32E-03	42	3349	0.025	1.00	6.4E-02	2.8E-03	0.01	0.22	24.3		
	6	2.33E-03	113	3349	0.028	0.99	4.0E-02	1.2E-02	0.03	0.15	7.5		
	7	2.05E-03	105	3349	0.028	0.99	1.6E-02	1.1E-02	0.03	0.19	7.7		
	0.1	3.1	3	3.18E-04	38	2533	0.013	0.98	1.0E-01	2.6E-02	0.02	0.20	74.4
			4	3.15E-04	33	2533	0.020	0.99	8.2E-02	8.4E-03	0.01	0.38	72.8
5			3.25E-04	23	2533	0.025	1.00	7.7E-02	2.6E-03	0.01	0.29	50.7	
6			3.76E-04	54	2533	0.028	0.99	5.4E-02	1.1E-02	0.02	0.23	22.2	
7			3.75E-04	47	2533	0.028	0.99	2.1E-02	7.9E-03	0.02	0.28	22.0	
4.1		3	4.77E-04	48	3349	0.013	0.98	1.1E-01	2.6E-02	0.01	0.21	68.8	
		4	4.75E-04	41	3349	0.020	0.99	8.7E-02	8.4E-03	0.01	0.40	65.0	
		5	4.94E-04	29	3349	0.025	1.00	7.9E-02	2.6E-03	0.01	0.31	46.4	
		6	5.72E-04	68	3349	0.028	0.99	5.6E-02	1.1E-02	0.02	0.24	24.1	
		7	5.70E-04	59	3349	0.028	0.99	2.2E-02	7.9E-03	0.02	0.30	21.0	
		0.2	3.1	2	6.59E-05	33	2533	0.011	0.94	1.9E-01	8.1E-02	0.01	0.42
3	5.92E-05	21		2533	0.013	0.98	1.7E-01	2.4E-02	0.01	0.36	131.0		
4	6.10E-05	17		2533	0.020	0.99	1.2E-01	7.1E-03	0.01	0.65	128.3		
5	6.19E-05	12		2533	0.025	1.00	1.0E-01	2.3E-03	0.00	0.51	74.7		
6	6.44E-05	28		2533	0.028	0.99	7.8E-02	9.3E-03	0.01	0.42	33.5		
7	6.21E-05	27		2533	0.028	0.99	3.4E-02	8.7E-03	0.01	0.52	46.6		

Tailgate Height (m)	Flowrate (L/s)	Vegetation State	Froude number	Stem Reynolds number	Depth Reynolds number	Average Stem Spacing (m)	Porosity (m ³ /m ³)	Vegetal Area Coef-ficient <i>pa·d</i>	Vegetal Area Coef-ficient <i>maa·d</i>	Stem diameter to depth ratio (m/m)	Sub-mergence (m/m)	Friction factor <i>f</i>
0.2	4.1	2	1.07E-04	43	3349	0.011	0.94	2.0E-01	8.1E-02	0.01	0.43	85.8
		3	9.87E-05	27	3349	0.013	0.98	1.7E-01	2.4E-02	0.01	0.36	89.9
		4	1.02E-04	23	3349	0.020	0.99	1.3E-01	7.1E-03	0.01	0.66	94.5
		5	1.05E-04	16	3349	0.025	1.00	1.0E-01	2.3E-03	0.00	0.51	44.7
		6	1.08E-04	36	3349	0.028	0.99	7.9E-02	9.1E-03	0.01	0.43	18.1
		7	1.04E-04	35	3349	0.028	0.99	3.4E-02	8.7E-03	0.01	0.52	10.1
		2	8.13E-06	15	2533	0.014	0.97	3.5E-01	4.4E-02	0.01	0.84	471.7
0.4	3.1	4	8.49E-06	9	2533	0.035	1.00	1.5E-01	2.2E-03	0.00	1.26	150.2
		7	8.27E-06	13	2533	0.035	1.00	4.9E-02	4.9E-03	0.00	1.01	162.5
		2	1.42E-05	20	3349	0.014	0.97	3.5E-01	4.4E-02	0.01	0.84	282.3
	4.1	3	1.39E-05	13	3349	0.013	0.98	3.0E-01	2.1E-02	0.00	0.69	275.8
		4	1.43E-05	11	3349	0.035	1.00	1.5E-01	2.2E-03	0.00	1.27	255.6
		5	1.45E-05	8	3349	0.031	1.00	1.2E-01	1.3E-03	0.00	0.99	264.0
		6	1.48E-05	18	3349	0.034	1.00	1.0E-01	5.4E-03	0.01	0.82	71.1
		7	1.41E-05	17	3349	0.035	1.00	4.9E-02	4.9E-03	0.00	1.02	123.4

Appendix A2: AOE May Event Data

Table A2. 1 May 20, 2009 Artificial Overbank Event (AOE) steady-state water depths

Transect	Point	Depth (m)
A	1	0.130
	2	0.187
	3	0.502
	4	0.254
	5	0.146
B	1	0.108
	2	0.124
	3	0.394
	4	dry
	5	dry
C	1	0.149
	2	0.175
	3	0.352
	4	obstructed
	5	dry
D	1	0.184
	2	obstructed
	3	0.460
	4	obstructed
	5	dry
E	1	0.048
	2	0.162
	3	0.454
	4	obstructed
	5	dry

Table A2. 2 Hedgebrook Farm wetland vegetation data by community

Vegetation Community ID	Percent Cover	Depth Increment	<i>maa</i> (cm ⁻¹)				Average Diameter (cm)			
			0-10 cm	0-20 cm	0-30 cm	0-40+ cm	0-10 cm	0-20 cm	0-30 cm	0-40+ cm
LQ1	15%		0.24	0.19	0.13	0.10	0.79	0.45	0.30	0.30
RQ1	20%		1.02	0.97	0.73	0.54	0.25	0.15	0.11	0.11
LQ2	10%		0.36	0.71	0.72	0.58	0.35	0.21	0.15	0.12
RQ2	30%		1.61	1.56	1.39	1.19	0.24	0.15	0.11	0.10
LQ3	10%		0.66	0.75	0.67	0.50	0.19	0.14	0.11	0.11
RQ3	30%		2.34	2.32	1.94	1.66	0.16	0.12	0.09	0.07
LQ4	5%		0.28	0.26	0.18	0.14	0.22	0.14	0.10	0.10
LQ5	15%		0.73	0.49	0.32	0.24	0.26	0.19	0.19	0.19
transition	35%		2.25	2.25	2.03	1.92	0.20	0.14	0.11	0.10
slough			2.79E-03	2.50E-03	1.96E-03	1.62E-03	0.20	0.14	0.10	0.09

Table A2. 3 Hedgebrook Farm wetland vegetal area coefficient by community

Vegetation Community ID	Depth Increment	<i>maa-d</i>			
		0-10 cm	0-20 cm	0-30 cm	0-40+ cm
LQ1		0.19	0.09	0.04	0.03
RQ1		0.25	0.14	0.08	0.06
LQ2		0.13	0.15	0.11	0.07
RQ2		0.38	0.23	0.16	0.11
LQ3		0.13	0.11	0.08	0.06
RQ3		0.38	0.27	0.18	0.12
LQ4		0.06	0.04	0.02	0.01
LQ5		0.19	0.09	0.06	0.05
transition		0.45	0.32	0.23	0.18
slough		5.63E-04	3.49E-04	2.03E-04	1.44E-04

Appendix A3: MODFLOW Iteration ArcGIS Toolbox Script

File Creator Step 1

```
' -----  
' step 1.vbs  
' Created on: Fri Mar 12 2010 09:31:13 AM  
' (generated by ArcGIS/ModelBuilder)  
' Usage: step 1 <theo_ws> <comm_centroids_shp> <wet_veg_shp__2_> <wet_depth>  
' -----  
  
' Create the Geoprocessor object  
set gp = WScript.CreateObject("esriGeoprocessing.GPDispatch.1")  
  
' Set the necessary product code  
gp.SetProduct "ArcInfo"  
  
' Check out any necessary licenses  
gp.CheckOutExtension "spatial"  
  
' Load required toolboxes...  
gp.AddToolbox "C:/Program Files (x86)/ArcGIS/ArcToolbox/Toolboxes/Spatial  
Analyst Tools.tbx"  
gp.AddToolbox "C:/Program Files (x86)/ArcGIS/ArcToolbox/Toolboxes/Data  
Management Tools.tbx"  
gp.AddToolbox "C:/Program Files (x86)/ArcGIS/ArcToolbox/Toolboxes/Analysis  
Tools.tbx"  
gp.AddToolbox "C:/Program Files (x86)/ArcGIS/ArcToolbox/Toolboxes/Conversion  
Tools.tbx"  
  
' Set the Geoprocessing environment...  
gp.extent = "wetlnd_dem"  
gp.cellSize = "0.5"  
  
' Script arguments...  
theo_ws = wscript.arguments.item(0)  
if theo_ws = "#" then  
    theo_ws = "theo_ws" ' provide a default value if unspecified  
end if  
  
'Creates the point file of the centroids of the inundated vegetation  
communities.  
comm_centroids_shp = wscript.arguments.item(1)  
if comm_centroids_shp = "#" then  
    comm_centroids_shp = "C:\Users\Candice\Documents\AOE\Survey  
Files\GIS\comm_centroids.shp" ' provide a default value if unspecified  
end if  
  
'Creates the polygon file of the inundated vegetation communities  
wet_veg_shp__2_ = wscript.arguments.item(2)  
if wet_veg_shp__2_ = "#" then  
    wet_veg_shp__2_ = "C:\Users\Candice\Documents\AOE\Survey  
Files\GIS\wet_veg.shp" ' provide a default value if unspecified  
end if  
  
'Creates the raster file of the water depth  
wet_depth = wscript.arguments.item(3)
```

```

if wet_depth = "#" then
  wet_depth = "C:\Users\Candice\Documents\AOE\Survey Files\GIS\wet_depth" '
provide a default value if unspecified
end if

' Creates the temporary files used in the processes
theo_depth = "C:\Users\Candice\Documents\AOE\Survey Files\GIS\theo_depth"
wetlnd_dem = "wetlnd_dem"
wet = "C:\Users\Candice\Documents\AOE\Survey Files\GIS\wet"
Input_raster_or_constant_value_2 = "0"
zone_avg_depth_dbf = "C:\Users\Candice\Documents\AOE\Survey
Files\GIS\zone_avg_depth.dbf"
wet_veg_geo = "C:\Users\Candice\Documents\AOE\Survey Files\GIS\wet_veg_geo"
centroid_left = "C:\Users\Candice\Documents\AOE\centroid_left"
centroid_right = "C:\Users\Candice\Documents\AOE\centroid_right"
centroids = "C:\Users\Candice\Documents\AOE\centroids"
centroids__2_ = "C:\Users\Candice\Documents\AOE\centroids"
centroid_left__3_ = "C:\Users\Candice\Documents\AOE\centroid_left"
centroid_right__3_ = "C:\Users\Candice\Documents\AOE\centroid_right"
wet_poly_shp = "C:\Users\Candice\Documents\AOE\Survey Files\GIS\wet_poly.shp"
wet_only = "C:\Users\Candice\Documents\AOE\Survey Files\GIS\wet_only"
wet_veg_shp = "C:\Users\Candice\Documents\AOE\Survey Files\GIS\wet_veg.shp"
communities = "communities"
centroids__3_ = "C:\Users\Candice\Documents\AOE\centroids"
centroids_Layer = "centroids_Layer"
GIS = "C:\Users\Candice\Documents\AOE\Survey Files\GIS"

'Calculates the water depth by subtracting the soil surface dem raster from
the water surface elevation raster
' Process: Minus...
gp.Minus_sa theo_ws, wetlnd_dem, theo_depth

'Identifies the regions of positive water depth (water surface above the soil
surface)
' Process: Greater Than Equal...
gp.GreaterThanEqual_sa theo_depth, Input_raster_or_constant_value_2, wet

'Reclassifies the positive water depth raster so it can be converted to a
polygon shapefile
' Process: Reclassify...
gp.Reclassify_sa wet, "VALUE", "0 NODATA;0 1 1", wet_only, "NODATA"

'Converts the positive water depth raster to a polygon shapefil
' Process: Raster to Polygon (2)...
gp.RasterToPolygon_conversion wet_only, wet_poly_shp, "SIMPLIFY", "VALUE"

'Clips the vegetation communities polygon shapefile to the extent of the
inundation
' Process: Clip...
gp.Clip_analysis communities, wet_poly_shp, wet_veg_shp, ""

'Clips the water depth raster to the inundated extent
' Process: Times...
gp.Times_sa theo_depth, wet, wet_depth

'Calculates the mean water depth in each vegetation community

```

```

' Process: Zonal Statistics as Table...
gp.ZonalStatisticsAsTable_sa communities, "ID_num", wet_depth,
zone_avg_depth_dbf, "DATA"

'Joins the mean water depth table to the inundated vegetation community
shapefile
' Process: Join Field...
gp.JoinField_management wet_veg_shp, "ID_num", zone_avg_depth_dbf, "VALUE",
"MEAN"

'Calculates the centroids of the inundated vegetation community shapefiles
' Process: Zonal Geometry as Table...
gp.ZonalGeometryAsTable_sa wet_veg_shp__2_, "ID_num", wet_veg_geo, "0.5"

'Copies the inundated vegetation community centroid table so extra points can
be added
' Process: Copy Rows (3)...
gp.CopyRows_management wet_veg_geo, centroids, "defaults"

'Deletes extraneous data from the inundated vegetation community centroid
table
' Process: Delete Field...
gp.DeleteField_management centroids,
"AREA;PERIMETER;THICKNESS;MAJORAXIS;MINORAXIS;ORIENTATION"

'Copies the inundated vegetation community centroid table so the x coordinate
can be changed to the leftmost extent
' Process: Copy Rows...
gp.CopyRows_management centroids__2_, centroid_left, "defaults"

'Changes the x coordinate of the centroid to the leftmost extent
' Process: Calculate Field...
gp.CalculateField_management centroid_left, "XCENTROID", "3524437.24588+1",
"VB", ""

'Copies the inundated vegetation community centroid table so the x coordinate
can be changed to the rightmost extent
' Process: Copy Rows (2)...
gp.CopyRows_management centroids__2_, centroid_right, "defaults"

'Changes the x coordinate of the centroid to the rightmost extent
' Process: Calculate Field (2)...
gp.CalculateField_management centroid_right, "XCENTROID", "3524481.74588-1",
"VB", ""

'Adds the left and right centroid tables to the original
' Process: Append...
gp.Append_management
"C:\Users\Candice\Documents\AOE\centroid_left;C:\Users\Candice\Documents\AOE\
centroid_right", centroids__2_, "NO_TEST", "VALUE 'VALUE' true false false 4
Long 0 0 ,First,#,C:\Users\Candice\Documents\AOE\centroid_left,VALUE,-1,-
1,C:\Users\Candice\Documents\AOE\centroid_right,VALUE,-1,-1;XCENTROID
'XCENTROID' true false false 4 Float 0 0
,First,#,C:\Users\Candice\Documents\AOE\centroid_left,XCENTROID,-1,-
1,C:\Users\Candice\Documents\AOE\centroid_right,XCENTROID,-1,-1;YCENTROID
'YCENTROID' true false false 4 Float 0 0

```

```
,First,#,C:\Users\Candice\Documents\AOE\centroid_left,YCENTROID,-1,-
1,C:\Users\Candice\Documents\AOE\centroid_right,YCENTROID,-1,-1", ""

'Change the centroid tables to XY point event layer
' Process: Make XY Event Layer...
gp.MakeXYEventLayer_management centroids__3_, "XCENTROID", "YCENTROID",
centroids_Layer,
"PROJCS['NAD_1983_StatePlane_Virginia_North_FIPS_4501',GEOGCS['GCS_North_Amer
ican_1983',DATUM['D_North_American_1983',SPHEROID['GRS_1980',6378137.0,298.25
7222101]],PRIMEM['Greenwich',0.0],UNIT['Degree',0.0174532925199433]],PROJECTI
ON['Lambert_Conformal_Conic'],PARAMETER['False_Easting',3500000.0],PARAMETER[
'False_Northing',2000000.0],PARAMETER['Central_Meridian',-
78.5],PARAMETER['Standard_Parallel_1',38.03333333333333],PARAMETER['Standard
_Parallel_2',39.2],PARAMETER['Latitude_Of_Origin',37.66666666666666],UNIT['Met
er',1.0]];IsHighPrecision"

'Change the XY point event layer to a permanent point shapefile
' Process: Feature Class to Feature Class...
gp.FeatureClassToFeatureClass_conversion centroids_Layer, GIS,
"comm_centroids.shp", "", "VALUE 'VALUE' true true false 4 Long 0 0
,First,#,C:\Users\Candice\Documents\AOE\centroids,VALUE,-1,-1;XCENTROID
'XCENTROID' true true false 4 Float 0 0
,First,#,C:\Users\Candice\Documents\AOE\centroids,XCENTROID,-1,-1;YCENTROID
'YCENTROID' true true false 4 Float 0 0
,First,#,C:\Users\Candice\Documents\AOE\centroids,YCENTROID,-1,-1", ""
```

File Creator Step 2

```
' -----
' step 2.vbs
' Created on: Fri Mar 12 2010 09:31:31 AM
' (generated by ArcGIS/ModelBuilder)
' Usage: step 2 <wet_veg__2_>
' -----

' Create the Geoprocessor object
set gp = WScript.CreateObject("esriGeoprocessing.GPDispatch.1")

' Set the necessary product code
gp.SetProduct "ArcInfo"

' Check out any necessary licenses
gp.CheckOutExtension "spatial"

' Load required toolboxes...
gp.AddToolbox "C:/Program Files (x86)/ArcGIS/ArcToolbox/Toolboxes/Spatial
Analyst Tools.tbx"
gp.AddToolbox "C:/Program Files (x86)/ArcGIS/ArcToolbox/Toolboxes/Data
Management Tools.tbx"
gp.AddToolbox "C:/Program Files (x86)/ArcGIS/ArcToolbox/Toolboxes/Analysis
Tools.tbx"

'Creates a modified version of the inundated vegetation communities
' Script arguments...
wet_veg__2_ = wscript.arguments.item(0)
```

```

if wet_veg__2_ = "#" then
  wet_veg__2_ = "wet_veg" ' provide a default value if unspecified
end if

' Creates the temporary files used in the processes
' Local variables...
comm_centroids__1_ = "comm_centroids"
xsec_1 = "C:\Users\Candice\Documents\AOE\Survey Files\GIS\xsec_1"
Output_RMS_file = ""
xsec_area_1 = "C:\Users\Candice\Documents\AOE\Survey Files\GIS\xsec_area_1"
xsec_1_re = "C:\Users\Candice\Documents\AOE\Survey Files\GIS\xsec_1_re"
xsec_area_1__4_ = "C:\Users\Candice\Documents\AOE\Survey
Files\GIS\xsec_area_1"
xsec_area_1__5_ = "C:\Users\Candice\Documents\AOE\Survey
Files\GIS\xsec_area_1"
xsec_area_1__3_ = "C:\Users\Candice\Documents\AOE\Survey
Files\GIS\xsec_area_1"
comm_centroids__13_ = "comm_centroids"
xsec_2__2_ = "C:\Users\Candice\Documents\AOE\Survey Files\GIS\xsec_2"
Output_RMS_file__2_ = ""
xsec_area_2 = "C:\Users\Candice\Documents\AOE\Survey Files\GIS\xsec_area_2"
xsec_2_re = "C:\Users\Candice\Documents\AOE\Survey Files\GIS\xsec_2_re"
xsec_area_2__1_ = "C:\Users\Candice\Documents\AOE\Survey
Files\GIS\xsec_area_2"
xsec_area_2__3_ = "C:\Users\Candice\Documents\AOE\Survey
Files\GIS\xsec_area_2"
xsec_area_2__2_ = "C:\Users\Candice\Documents\AOE\Survey
Files\GIS\xsec_area_2"
comm_centroids__3_ = "comm_centroids"
xsec_3 = "C:\Users\Candice\Documents\AOE\Survey Files\GIS\xsec_3"
Output_RMS_file__3_ = ""
xsec_area_3 = "C:\Users\Candice\Documents\AOE\Survey Files\GIS\xsec_area_3"
xsec_3_re = "C:\Users\Candice\Documents\AOE\Survey Files\GIS\xsec_3_re"
xsec_area_3__2_ = "C:\Users\Candice\Documents\AOE\Survey
Files\GIS\xsec_area_3"
xsec_area_2__6_ = "C:\Users\Candice\Documents\AOE\Survey
Files\GIS\xsec_area_3"
xsec_area_3__3_ = "C:\Users\Candice\Documents\AOE\Survey
Files\GIS\xsec_area_3"
comm_centroids__12_ = "comm_centroids"
Output_RMS_file__4_ = ""
xsec_4 = "C:\Users\Candice\Documents\AOE\Survey Files\GIS\xsec_4"
xsec_4_re = "C:\Users\Candice\Documents\AOE\Survey Files\GIS\xsec_4_re"
xsec_area_4 = "C:\Users\Candice\Documents\AOE\Survey Files\GIS\xsec_area_4"
xsec_area_4__3_ = "C:\Users\Candice\Documents\AOE\Survey
Files\GIS\xsec_area_4"
xsec_area_4__4_ = "C:\Users\Candice\Documents\AOE\Survey
Files\GIS\xsec_area_4"
comm_centroids__4_ = "comm_centroids"
Output_RMS_file__5_ = ""
xsec_5 = "C:\Users\Candice\Documents\AOE\Survey Files\GIS\xsec_5"
xsec_5_re = "C:\Users\Candice\Documents\AOE\Survey Files\GIS\xsec_5_re"
xsec_area_5 = "C:\Users\Candice\Documents\AOE\Survey Files\GIS\xsec_area_5"
xsec_area_5__2_ = "C:\Users\Candice\Documents\AOE\Survey
Files\GIS\xsec_area_5"

```

```

xsec_area_5_3_ = "C:\Users\Candice\Documents\AOE\Survey
Files\GIS\xsec_area_5"
xsec_area_5_4_ = "C:\Users\Candice\Documents\AOE\Survey
Files\GIS\xsec_area_5"
comm_centroids_11_ = "comm_centroids"
Output_RMS_file_6_ = ""
xsec_6 = "C:\Users\Candice\Documents\AOE\Survey Files\GIS\xsec_6"
xsec_6_re = "C:\Users\Candice\Documents\AOE\Survey Files\GIS\xsec_6_re"
xsec_area_6 = "C:\Users\Candice\Documents\AOE\Survey Files\GIS\xsec_area_6"
xsec_area_6_2_ = "C:\Users\Candice\Documents\AOE\Survey
Files\GIS\xsec_area_6"
xsec_area_6_3_ = "C:\Users\Candice\Documents\AOE\Survey
Files\GIS\xsec_area_6"
xsec_area_6_4_ = "C:\Users\Candice\Documents\AOE\Survey
Files\GIS\xsec_area_6"
xsec_area_7_4_ = "C:\Users\Candice\Documents\AOE\Survey
Files\GIS\xsec_area_7"
xsec_area_7_3_ = "C:\Users\Candice\Documents\AOE\Survey
Files\GIS\xsec_area_7"
xsec_area_7_2_ = "C:\Users\Candice\Documents\AOE\Survey
Files\GIS\xsec_area_7"
xsec_area_7 = "C:\Users\Candice\Documents\AOE\Survey Files\GIS\xsec_area_7"
xsec_7_re = "C:\Users\Candice\Documents\AOE\Survey Files\GIS\xsec_7_re"
xsec_7 = "C:\Users\Candice\Documents\AOE\Survey Files\GIS\xsec_7"
Output_RMS_file_7_ = ""
comm_centroids_2_ = "comm_centroids"
xsec_area_8_4_ = "C:\Users\Candice\Documents\AOE\Survey
Files\GIS\xsec_area_8"
xsec_area_8_3_ = "C:\Users\Candice\Documents\AOE\Survey
Files\GIS\xsec_area_8"
xsec_area_8 = "C:\Users\Candice\Documents\AOE\Survey Files\GIS\xsec_area_8"
xsec_8_re = "C:\Users\Candice\Documents\AOE\Survey Files\GIS\xsec_8_re"
xsec_8 = "C:\Users\Candice\Documents\AOE\Survey Files\GIS\xsec_8"
comm_centroids_10_ = "comm_centroids"
Output_RMS_file_8_ = ""
xsec_area_9_4_ = "C:\Users\Candice\Documents\AOE\Survey
Files\GIS\xsec_area_9"
xsec_area_9_3_ = "C:\Users\Candice\Documents\AOE\Survey
Files\GIS\xsec_area_9"
xsec_area_9_2_ = "C:\Users\Candice\Documents\AOE\Survey
Files\GIS\xsec_area_9"
xsec_area_9 = "C:\Users\Candice\Documents\AOE\Survey Files\GIS\xsec_area_9"
xsec_9_re = "C:\Users\Candice\Documents\AOE\Survey Files\GIS\xsec_9_re"
xsec_9 = "C:\Users\Candice\Documents\AOE\Survey Files\GIS\xsec_9"
Output_RMS_file_9_ = ""
comm_centroids_5_ = "comm_centroids"
comm_centroids_9_ = "comm_centroids"
Output_RMS_file_10_ = ""
xsec_10 = "C:\Users\Candice\Documents\AOE\Survey Files\GIS\xsec_10"
xsec_10_re = "C:\Users\Candice\Documents\AOE\Survey Files\GIS\xsec_10_re"
xsec_area_10 = "C:\Users\Candice\Documents\AOE\Survey Files\GIS\xsec_area_10"
xsec_area_10_2_ = "C:\Users\Candice\Documents\AOE\Survey
Files\GIS\xsec_area_10"
xsec_area_10_3_ = "C:\Users\Candice\Documents\AOE\Survey
Files\GIS\xsec_area_10"

```

```

xsec_area_10_4_ = "C:\Users\Candice\Documents\AOE\Survey
Files\GIS\xsec_area_10"
comm_centroids_6_ = "comm_centroids"
Output_RMS_file_11_ = ""
xsec_11 = "C:\Users\Candice\Documents\AOE\Survey Files\GIS\xsec_11"
xsec_11_re = "C:\Users\Candice\Documents\AOE\Survey Files\GIS\xsec_11_re"
xsec_area_11 = "C:\Users\Candice\Documents\AOE\Survey Files\GIS\xsec_area_11"
xsec_area_11_2_ = "C:\Users\Candice\Documents\AOE\Survey
Files\GIS\xsec_area_11"
xsec_area_11_3_ = "C:\Users\Candice\Documents\AOE\Survey
Files\GIS\xsec_area_11"
xsec_area_11_4_ = "C:\Users\Candice\Documents\AOE\Survey
Files\GIS\xsec_area_11"
comm_centroids_8_ = "comm_centroids"
Output_RMS_file_12_ = ""
xsec_12 = "C:\Users\Candice\Documents\AOE\Survey Files\GIS\xsec_12"
xsec_12_re = "C:\Users\Candice\Documents\AOE\Survey Files\GIS\xsec_12_re"
xsec_area_12 = "C:\Users\Candice\Documents\AOE\Survey Files\GIS\xsec_area_12"
xsec_area_12_4_ = "C:\Users\Candice\Documents\AOE\Survey
Files\GIS\xsec_area_12"
xsec_area_12_3_ = "C:\Users\Candice\Documents\AOE\Survey
Files\GIS\xsec_area_12"
xsec_area_12_2_ = "C:\Users\Candice\Documents\AOE\Survey
Files\GIS\xsec_area_12"
comm_centroids_14_ = "comm_centroids"
Output_RMS_file_14_ = ""
xsec_13 = "C:\Users\Candice\Documents\AOE\Survey Files\GIS\xsec_13"
xsec_13_re = "C:\Users\Candice\Documents\AOE\Survey Files\GIS\xsec_13_re"
xsec_area_13 = "C:\Users\Candice\Documents\AOE\Survey Files\GIS\xsec_area_13"
xsec_area_13_2_ = "C:\Users\Candice\Documents\AOE\Survey
Files\GIS\xsec_area_13"
xsec_area_13_3_ = "C:\Users\Candice\Documents\AOE\Survey
Files\GIS\xsec_area_13"
xsec_area_13_4_ = "C:\Users\Candice\Documents\AOE\Survey
Files\GIS\xsec_area_13"
xsec_areas_dbf = "C:\Users\Candice\Documents\AOE\Survey
Files\GIS\xsec_areas.dbf"
xsec_areas_dbf_2_ = "C:\Users\Candice\Documents\AOE\Survey
Files\GIS\xsec_areas.dbf"
xsec_areas_dbf_8_ = "C:\Users\Candice\Documents\AOE\Survey
Files\GIS\xsec_areas.dbf"
xsec_areas_dbf_4_ = "C:\Users\Candice\Documents\AOE\Survey
Files\GIS\xsec_areas.dbf"
xsec_areas_dbf_6_ = "C:\Users\Candice\Documents\AOE\Survey
Files\GIS\xsec_areas.dbf"
xsec_areas_sum_dbf = "C:\Users\Candice\Documents\AOE\Survey
Files\GIS\xsec_areas_sum.dbf"
xsec_areas_dbf_5_ = "C:\Users\Candice\Documents\AOE\Survey
Files\GIS\xsec_areas.dbf"
xsec_areas_dbf_9_ = "C:\Users\Candice\Documents\AOE\Survey
Files\GIS\xsec_areas.dbf"
xsec_areas_dbf_7_ = "C:\Users\Candice\Documents\AOE\Survey
Files\GIS\xsec_areas.dbf"
xsec_areas_View = "xsec_areas_View"
comm_centroids = "comm_centroids"
wet_veg = "wet_veg"

```

```

xsec_area_4__2_ = "C:\Users\Candice\Documents\AOE\Survey
Files\GIS\xsec_area_4"
xsec_area_8__2_ = "C:\Users\Candice\Documents\AOE\Survey
Files\GIS\xsec_area_8"
comm_centroids__15_ = "comm_centroids"
Output_RMS_file__13_ = ""
xsec_14 = "C:\Users\Candice\Documents\AOE\Survey Files\GIS\xsec_14"
xsec_14_re = "C:\Users\Candice\Documents\AOE\Survey Files\GIS\xsec_14_re"
xsec_area_14 = "C:\Users\Candice\Documents\AOE\Survey Files\GIS\xsec_area_14"
xsec_area_14__2_ = "C:\Users\Candice\Documents\AOE\Survey
Files\GIS\xsec_area_14"
xsec_area_14__3_ = "C:\Users\Candice\Documents\AOE\Survey
Files\GIS\xsec_area_14"
xsec_area_14__4_ = "C:\Users\Candice\Documents\AOE\Survey
Files\GIS\xsec_area_14"

```

```

'Select the centroids for inundated vegetation community 1
' Process: Select Layer By Attribute...
gp.SelectLayerByAttribute_management comm_centroids, "NEW_SELECTION",
""VALUE"" =1"

```

```

'Creates a 0.17-m tall raster connecting the leftmost and rightmost points
through the vegetation community centroid
' Process: Trend...
gp.Trend_sa comm_centroids__1_, "VALUE", xsec_1, "0.17", "1", "LINEAR",
Output_RMS_file

```

```

'Select the centroids for inundated vegetation community 2
' Process: Select Layer By Attribute (2)...
gp.SelectLayerByAttribute_management comm_centroids, "NEW_SELECTION",
""VALUE"" =2"

```

```

'Creates a 0.17-m tall raster connecting the leftmost and rightmost points
through the vegetation community centroid
' Process: Trend (2)...
gp.Trend_sa comm_centroids__13_, "VALUE", xsec_2__2_, "0.17", "1", "LINEAR",
Output_RMS_file__2_

```

```

'Select the centroids for inundated vegetation community 3
' Process: Select Layer By Attribute (3)...
gp.SelectLayerByAttribute_management comm_centroids, "NEW_SELECTION",
""VALUE"" =3"

```

```

'Creates a 0.17-m tall raster connecting the leftmost and rightmost points
through the vegetation community centroid
' Process: Trend (3)...
gp.Trend_sa comm_centroids__3_, "VALUE", xsec_3, "0.17", "1", "LINEAR",
Output_RMS_file__3_

```

```

'Select the centroids for inundated vegetation community 4
' Process: Select Layer By Attribute (4)...
gp.SelectLayerByAttribute_management comm_centroids, "NEW_SELECTION",
""VALUE"" =4"

```

```

'Creates a 0.17-m tall raster connecting the leftmost and rightmost points
through the vegetation community centroid

```

```

' Process: Trend (4)...
gp.Trend_sa comm_centroids__12_, "VALUE", xsec_4, "0.17", "1", "LINEAR",
Output_RMS_file__4_

'Select the centroids for inundated vegetation community 5
' Process: Select Layer By Attribute (5)...
gp.SelectLayerByAttribute_management comm_centroids, "NEW_SELECTION",
""VALUE"" =5

'Creates a 0.17-m tall raster connecting the leftmost and rightmost points
through the vegetation community centroid
' Process: Trend (5)...
gp.Trend_sa comm_centroids__4_, "VALUE", xsec_5, "0.17", "1", "LINEAR",
Output_RMS_file__5_

'Select the centroids for inundated vegetation community 6
' Process: Select Layer By Attribute (6)...
gp.SelectLayerByAttribute_management comm_centroids, "NEW_SELECTION",
""VALUE"" =6

'Creates a 0.17-m tall raster connecting the leftmost and rightmost points
through the vegetation community centroid
' Process: Trend (6)...
gp.Trend_sa comm_centroids__11_, "VALUE", xsec_6, "0.17", "1", "LINEAR",
Output_RMS_file__6_

'Select the centroids for inundated vegetation community 7
' Process: Select Layer By Attribute (7)...
gp.SelectLayerByAttribute_management comm_centroids, "NEW_SELECTION",
""VALUE"" =7

'Creates a 0.17-m tall raster connecting the leftmost and rightmost points
through the vegetation community centroid
' Process: Trend (7)...
gp.Trend_sa comm_centroids__2_, "VALUE", xsec_7, "0.17", "1", "LINEAR",
Output_RMS_file__7_

'Select the centroids for inundated vegetation community 8
' Process: Select Layer By Attribute (8)...
gp.SelectLayerByAttribute_management comm_centroids, "NEW_SELECTION",
""VALUE"" =8

'Creates a 0.17-m tall raster connecting the leftmost and rightmost points
through the vegetation community centroid
' Process: Trend (8)...
gp.Trend_sa comm_centroids__10_, "VALUE", xsec_8, "0.17", "1", "LINEAR",
Output_RMS_file__8_

'Select the centroids for inundated vegetation community 9
' Process: Select Layer By Attribute (9)...
gp.SelectLayerByAttribute_management comm_centroids, "NEW_SELECTION",
""VALUE"" =9

'Creates a 0.17-m tall raster connecting the leftmost and rightmost points
through the vegetation community centroid
' Process: Trend (9)...

```

```

gp.Trend_sa comm_centroids__5_, "VALUE", xsec_9, "0.17", "1", "LINEAR",
Output_RMS_file__9_

'Select the centroids for inundated vegetation community 10
' Process: Select Layer By Attribute (10)...
gp.SelectLayerByAttribute_management comm_centroids, "NEW_SELECTION",
""VALUE"" =10

'Creates a 0.17-m tall raster connecting the leftmost and rightmost points
through the vegetation community centroid
' Process: Trend (10)...
gp.Trend_sa comm_centroids__9_, "VALUE", xsec_10, "0.17", "1", "LINEAR",
Output_RMS_file__10_

'Select the centroids for inundated vegetation community 11
' Process: Select Layer By Attribute (11)...
gp.SelectLayerByAttribute_management comm_centroids, "NEW_SELECTION",
""VALUE"" =11

'Creates a 0.17-m tall raster connecting the leftmost and rightmost points
through the vegetation community centroid
' Process: Trend (11)...
gp.Trend_sa comm_centroids__6_, "VALUE", xsec_11, "0.17", "1", "LINEAR",
Output_RMS_file__11_

'Select the centroids for inundated vegetation community 12
' Process: Select Layer By Attribute (12)...
gp.SelectLayerByAttribute_management comm_centroids, "NEW_SELECTION",
""VALUE"" =12

'Creates a 0.17-m tall raster connecting the leftmost and rightmost points
through the vegetation community centroid
' Process: Trend (12)...
gp.Trend_sa comm_centroids__8_, "VALUE", xsec_12, "0.17", "1", "LINEAR",
Output_RMS_file__12_

'Select the centroids for inundated vegetation community 13
' Process: Select Layer By Attribute (13)...
gp.SelectLayerByAttribute_management comm_centroids, "NEW_SELECTION",
""VALUE"" =14

'Creates a 0.17-m tall raster connecting the leftmost and rightmost points
through the vegetation community centroid
' Process: Trend (13)...
gp.Trend_sa comm_centroids__15_, "VALUE", xsec_14, "0.17", "1", "LINEAR",
Output_RMS_file__13_

'Select the centroids for inundated vegetation community 14
' Process: Select Layer By Attribute (14)...
gp.SelectLayerByAttribute_management comm_centroids, "NEW_SELECTION",
""VALUE"" =13

'Creates a 0.17-m tall raster connecting the leftmost and rightmost points
through the vegetation community centroid
' Process: Trend (14)...

```

```

gp.Trend_sa comm_centroids__14_, "VALUE", xsec_13, "0.17", "1", "LINEAR",
Output_RMS_file__14_

'Reclassifies the value of the 0.17-m tall raster to 1, calculates the area
of the 0.17-m tall raster within each inundated vegetation community, and
adds a field containing the vegetation community ID number
' Process: Reclassify (15)...
gp.Reclassify_sa xsec_13, "Value", "13 1", xsec_13_re, "DATA"

' Process: Tabulate Area (14)...
gp.TabulateArea_sa wet_veg, "ID_num", xsec_13_re, "VALUE", xsec_area_13,
"0.17"

' Process: Join Field (14)...
gp.JoinField_management xsec_area_13, "ID_NUM", wet_veg, "ID_num", "MEAN"

' Process: Add Field (15)...
gp.AddField_management xsec_area_13__2_, "xsec_code", "SHORT", "", "", "",
"", "NON_NULLABLE", "NON_REQUIRED", ""

' Process: Calculate Field (16)...
gp.CalculateField_management xsec_area_13__3_, "XSEC_CODE", "13", "VB", ""

' Process: Reclassify (13)...
gp.Reclassify_sa xsec_12, "Value", "12 1", xsec_12_re, "DATA"

' Process: Tabulate Area (12)...
gp.TabulateArea_sa wet_veg, "ID_num", xsec_12_re, "VALUE", xsec_area_12,
"0.17"

' Process: Join Field (12)...
gp.JoinField_management xsec_area_12, "ID_NUM", wet_veg, "ID_num", "MEAN"

' Process: Add Field (13)...
gp.AddField_management xsec_area_12__2_, "xsec_code", "SHORT", "", "", "",
"", "NON_NULLABLE", "NON_REQUIRED", ""

' Process: Calculate Field (14)...
gp.CalculateField_management xsec_area_12__3_, "XSEC_CODE", "12", "VB", ""

' Process: Reclassify (12)...
gp.Reclassify_sa xsec_11, "Value", "11 1", xsec_11_re, "DATA"

' Process: Tabulate Area (11)...
gp.TabulateArea_sa wet_veg, "ID_num", xsec_11_re, "VALUE", xsec_area_11,
"0.17"

' Process: Join Field (11)...
gp.JoinField_management xsec_area_11, "ID_NUM", wet_veg, "ID_num", "MEAN"

' Process: Add Field (12)...
gp.AddField_management xsec_area_11__2_, "xsec_code", "SHORT", "", "", "",
"", "NON_NULLABLE", "NON_REQUIRED", ""

' Process: Calculate Field (13)...

```

```

gp.CalculateField_management xsec_area_11__3_, "XSEC_CODE", "11", "VB", ""
' Process: Reclassify (11)...
gp.Reclassify_sa xsec_10, "Value", "10 1", xsec_10_re, "DATA"
' Process: Tabulate Area (10)...
gp.TabulateArea_sa wet_veg, "ID_num", xsec_10_re, "VALUE", xsec_area_10,
"0.17"
' Process: Join Field (10)...
gp.JoinField_management xsec_area_10, "ID_NUM", wet_veg, "ID_num", "MEAN"
' Process: Add Field (11)...
gp.AddField_management xsec_area_10__2_, "xsec_code", "SHORT", "", "", "",
"", "NON_NULLABLE", "NON_REQUIRED", ""
' Process: Calculate Field (12)...
gp.CalculateField_management xsec_area_10__3_, "XSEC_CODE", "10", "VB", ""
' Process: Reclassify (10)...
gp.Reclassify_sa xsec_9, "Value", "9 1", xsec_9_re, "DATA"
' Process: Tabulate Area (9)...
gp.TabulateArea_sa wet_veg, "ID_num", xsec_9_re, "VALUE", xsec_area_9, "0.17"
' Process: Join Field (9)...
gp.JoinField_management xsec_area_9, "ID_NUM", wet_veg, "ID_num", "MEAN"
' Process: Add Field (10)...
gp.AddField_management xsec_area_9__2_, "xsec_code", "SHORT", "", "", "", "",
"NON_NULLABLE", "NON_REQUIRED", ""
' Process: Calculate Field (11)...
gp.CalculateField_management xsec_area_9__3_, "XSEC_CODE", "9", "VB", ""
' Process: Reclassify (9)...
gp.Reclassify_sa xsec_8, "Value", "8 1", xsec_8_re, "DATA"
' Process: Tabulate Area (8)...
gp.TabulateArea_sa wet_veg, "ID_num", xsec_8_re, "VALUE", xsec_area_8, "0.17"
' Process: Join Field (8)...
gp.JoinField_management xsec_area_8, "ID_NUM", wet_veg, "ID_num", "MEAN"
' Process: Add Field (9)...
gp.AddField_management xsec_area_8__2_, "xsec_code", "SHORT", "", "", "", "",
"NON_NULLABLE", "NON_REQUIRED", ""
' Process: Calculate Field (10)...
gp.CalculateField_management xsec_area_8__3_, "XSEC_CODE", "8", "VB", ""
' Process: Reclassify (8)...
gp.Reclassify_sa xsec_7, "Value", "7 1", xsec_7_re, "DATA"
' Process: Tabulate Area (7)...
gp.TabulateArea_sa wet_veg, "ID_num", xsec_7_re, "VALUE", xsec_area_7, "0.17"

```

```

' Process: Join Field (7)...
gp.JoinField_management xsec_area_7, "ID_NUM", wet_veg, "ID_num", "MEAN"

' Process: Add Field (8)...
gp.AddField_management xsec_area_7__2_, "xsec_code", "SHORT", "", "", "", "",
"NON_NULLABLE", "NON_REQUIRED", ""

' Process: Calculate Field (9)...
gp.CalculateField_management xsec_area_7__3_, "XSEC_CODE", "7", "VB", ""

' Process: Reclassify (7)...
gp.Reclassify_sa xsec_6, "Value", "6 1", xsec_6_re, "DATA"

' Process: Tabulate Area (6)...
gp.TabulateArea_sa wet_veg, "ID_num", xsec_6_re, "VALUE", xsec_area_6, "0.17"

' Process: Join Field (6)...
gp.JoinField_management xsec_area_6, "ID_NUM", wet_veg, "ID_num", "MEAN"

' Process: Add Field (7)...
gp.AddField_management xsec_area_6__2_, "xsec_code", "SHORT", "", "", "", "",
"NON_NULLABLE", "NON_REQUIRED", ""

' Process: Calculate Field (8)...
gp.CalculateField_management xsec_area_6__3_, "XSEC_CODE", "6", "VB", ""

' Process: Reclassify (6)...
gp.Reclassify_sa xsec_5, "Value", "5 1", xsec_5_re, "DATA"

' Process: Tabulate Area (5)...
gp.TabulateArea_sa wet_veg, "ID_num", xsec_5_re, "VALUE", xsec_area_5, "0.17"

' Process: Join Field (5)...
gp.JoinField_management xsec_area_5, "ID_NUM", wet_veg, "ID_num", "MEAN"

' Process: Add Field (6)...
gp.AddField_management xsec_area_5__2_, "xsec_code", "SHORT", "", "", "", "",
"NON_NULLABLE", "NON_REQUIRED", ""

' Process: Calculate Field (7)...
gp.CalculateField_management xsec_area_5__3_, "XSEC_CODE", "5", "VB", ""

' Process: Reclassify (5)...
gp.Reclassify_sa xsec_4, "Value", "4 1", xsec_4_re, "DATA"

' Process: Tabulate Area (4)...
gp.TabulateArea_sa wet_veg, "ID_num", xsec_4_re, "VALUE", xsec_area_4, "0.17"

' Process: Join Field (4)...
gp.JoinField_management xsec_area_4, "ID_num", wet_veg, "ID_num", "MEAN"

' Process: Add Field (5)...
gp.AddField_management xsec_area_4__2_, "xsec_code", "SHORT", "", "", "", "",
"NON_NULLABLE", "NON_REQUIRED", ""

```

```

' Process: Calculate Field (6)...
gp.CalculateField_management xsec_area_4__3_, "XSEC_CODE", "4", "VB", ""

' Process: Reclassify (4)...
gp.Reclassify_sa xsec_3, "Value", "3 1", xsec_3_re, "DATA"

' Process: Tabulate Area (3)...
gp.TabulateArea_sa wet_veg, "ID_num", xsec_3_re, "VALUE", xsec_area_3, "0.17"

' Process: Join Field (3)...
gp.JoinField_management xsec_area_3, "ID_NUM", wet_veg, "ID_num", "MEAN"

' Process: Add Field (4)...
gp.AddField_management xsec_area_3__2_, "xsec_code", "SHORT", "", "", "", "", "NON_NULLABLE", "NON_REQUIRED", ""

' Process: Calculate Field (5)...
gp.CalculateField_management xsec_area_2__6_, "XSEC_CODE", "3", "VB", ""

' Process: Reclassify (3)...
gp.Reclassify_sa xsec_2__2_, "Value", "2 1", xsec_2_re, "DATA"

' Process: Tabulate Area (2)...
gp.TabulateArea_sa wet_veg, "ID_num", xsec_2_re, "VALUE", xsec_area_2, "0.17"

' Process: Join Field (2)...
gp.JoinField_management xsec_area_2, "ID_NUM", wet_veg, "ID_num", "MEAN"

' Process: Add Field (3)...
gp.AddField_management xsec_area_2__1_, "xsec_code", "SHORT", "", "", "", "", "NON_NULLABLE", "NON_REQUIRED", ""

' Process: Calculate Field (4)...
gp.CalculateField_management xsec_area_2__3_, "XSEC_CODE", "2", "VB", ""

' Process: Reclassify (2)...
gp.Reclassify_sa xsec_1, "Value", "1 1", xsec_1_re, "DATA"

' Process: Tabulate Area...
gp.TabulateArea_sa wet_veg, "ID_num", xsec_1_re, "VALUE", xsec_area_1, "0.17"

' Process: Join Field...
gp.JoinField_management xsec_area_1, "ID_NUM", wet_veg, "ID_num", "MEAN"

' Process: Add Field...
gp.AddField_management xsec_area_1__4_, "xsec_code", "SHORT", "", "", "", "", "NON_NULLABLE", "NON_REQUIRED", ""

' Process: Calculate Field (3)...
gp.CalculateField_management xsec_area_1__5_, "XSEC_CODE", "1", "VB", ""

' Process: Select Layer By Attribute (13)...
gp.SelectLayerByAttribute_management comm_centroids, "NEW_SELECTION",
""""VALUE"" =14"

' Process: Trend (13)...

```

```

gp.Trend_sa comm_centroids__15_, "VALUE", xsec_14, "0.17", "1", "LINEAR",
Output_RMS_file__13_

' Process: Reclassify (14)...
gp.Reclassify_sa xsec_14, "Value", "14 1", xsec_14_re, "DATA"

' Process: Tabulate Area (13)...
gp.TabulateArea_sa wet_veg, "ID_num", xsec_14_re, "VALUE", xsec_area_14,
"0.17"

' Process: Join Field (13)...
gp.JoinField_management xsec_area_14, "ID_NUM", wet_veg, "ID_num", "MEAN"

' Process: Add Field (2)...
gp.AddField_management xsec_area_14__2_, "xsec_code", "SHORT", "", "", "",
"", "NON_NULLABLE", "NON_REQUIRED", ""

' Process: Calculate Field (2)...
gp.CalculateField_management xsec_area_14__3_, "XSEC_CODE", "14", "VB", ""

'Merges all of the vegetation community tables containing the area and ID
numbers together
' Process: Merge...
gp.Merge_management "'C:\Users\Candice\Documents\AOE\Survey
Files\GIS\xsec_area_13';'C:\Users\Candice\Documents\AOE\Survey
Files\GIS\xsec_area_12';'C:\Users\Candice\Documents\AOE\Survey
Files\GIS\xsec_area_11';'C:\Users\Candice\Documents\AOE\Survey
Files\GIS\xsec_area_10';'C:\Users\Candice\Documents\AOE\Survey
Files\GIS\xsec_area_9';'C:\Users\Candice\Documents\AOE\Survey
Files\GIS\xsec_area_8';'C:\Users\Candice\Documents\AOE\Survey
Files\GIS\xsec_area_7';'C:\Users\Candice\Documents\AOE\Survey
Files\GIS\xsec_area_6';'C:\Users\Candice\Documents\AOE\Survey
Files\GIS\xsec_area_5';'C:\Users\Candice\Documents\AOE\Survey
Files\GIS\xsec_area_4';'C:\Users\Candice\Documents\AOE\Survey
Files\GIS\xsec_area_3';'C:\Users\Candice\Documents\AOE\Survey
Files\GIS\xsec_area_2';'C:\Users\Candice\Documents\AOE\Survey
Files\GIS\xsec_area_1';'C:\Users\Candice\Documents\AOE\Survey
Files\GIS\xsec_area_14'", xsec_areas_dbf, "ID_NUM 'ID_NUM' true true false 4
Long 0 0 ,First,#,C:\Users\Candice\Documents\AOE\Survey
Files\GIS\xsec_area_1,ID_NUM,-1,-1,C:\Users\Candice\Documents\AOE\Survey
Files\GIS\xsec_area_11,ID_NUM,-1,-1,C:\Users\Candice\Documents\AOE\Survey
Files\GIS\xsec_area_9,ID_NUM,-1,-1,C:\Users\Candice\Documents\AOE\Survey
Files\GIS\xsec_area_7,ID_NUM,-1,-1,C:\Users\Candice\Documents\AOE\Survey
Files\GIS\xsec_area_5,ID_NUM,-1,-1,C:\Users\Candice\Documents\AOE\Survey
Files\GIS\xsec_area_3,ID_NUM,-1,-1,C:\Users\Candice\Documents\AOE\Survey
Files\GIS\xsec_area_4,ID_NUM,-1,-1,C:\Users\Candice\Documents\AOE\Survey
Files\GIS\xsec_area_12,ID_NUM,-1,-1,C:\Users\Candice\Documents\AOE\Survey
Files\GIS\xsec_area_10,ID_NUM,-1,-1,C:\Users\Candice\Documents\AOE\Survey
Files\GIS\xsec_area_6,ID_NUM,-1,-1,C:\Users\Candice\Documents\AOE\Survey
Files\GIS\xsec_area_2,ID_NUM,-1,-1,C:\Users\Candice\Documents\AOE\Survey
Files\GIS\xsec_area_8,ID_NUM,-1,-1,C:\Users\Candice\Documents\AOE\Survey
Files\GIS\xsec_area_13,ID_NUM,-1,-1,C:\Users\Candice\Documents\AOE\Survey
Files\GIS\xsec_area_14,ID_NUM,-1,-1;VALUE_1 'VALUE_1' true true false 8
Double 0 0 ,First,#,C:\Users\Candice\Documents\AOE\Survey
Files\GIS\xsec_area_1,VALUE_1,-1,-1,C:\Users\Candice\Documents\AOE\Survey
Files\GIS\xsec_area_11,VALUE_1,-1,-1,C:\Users\Candice\Documents\AOE\Survey

```

```

Files\GIS\xsec_area_9,VALUE_1,-1,-1,C:\Users\Candice\Documents\AOE\Survey
Files\GIS\xsec_area_7,VALUE_1,-1,-1,C:\Users\Candice\Documents\AOE\Survey
Files\GIS\xsec_area_5,VALUE_1,-1,-1,C:\Users\Candice\Documents\AOE\Survey
Files\GIS\xsec_area_3,VALUE_1,-1,-1,C:\Users\Candice\Documents\AOE\Survey
Files\GIS\xsec_area_4,VALUE_1,-1,-1,C:\Users\Candice\Documents\AOE\Survey
Files\GIS\xsec_area_12,VALUE_1,-1,-1,C:\Users\Candice\Documents\AOE\Survey
Files\GIS\xsec_area_10,VALUE_1,-1,-1,C:\Users\Candice\Documents\AOE\Survey
Files\GIS\xsec_area_6,VALUE_1,-1,-1,C:\Users\Candice\Documents\AOE\Survey
Files\GIS\xsec_area_2,VALUE_1,-1,-1,C:\Users\Candice\Documents\AOE\Survey
Files\GIS\xsec_area_8,VALUE_1,-1,-1,C:\Users\Candice\Documents\AOE\Survey
Files\GIS\xsec_area_13,VALUE_1,-1,-1,C:\Users\Candice\Documents\AOE\Survey
Files\GIS\xsec_area_14,VALUE_1,-1,-1;MEAN 'MEAN' true true false 4 Float 0 0
,First,#,C:\Users\Candice\Documents\AOE\Survey Files\GIS\xsec_area_1,MEAN,-
1,-1,C:\Users\Candice\Documents\AOE\Survey Files\GIS\xsec_area_11,MEAN,-1,-
1,C:\Users\Candice\Documents\AOE\Survey Files\GIS\xsec_area_9,MEAN,-1,-
1,C:\Users\Candice\Documents\AOE\Survey Files\GIS\xsec_area_7,MEAN,-1,-
1,C:\Users\Candice\Documents\AOE\Survey Files\GIS\xsec_area_5,MEAN,-1,-
1,C:\Users\Candice\Documents\AOE\Survey Files\GIS\xsec_area_3,MEAN,-1,-
1,C:\Users\Candice\Documents\AOE\Survey Files\GIS\xsec_area_4,MEAN,-1,-
1,C:\Users\Candice\Documents\AOE\Survey Files\GIS\xsec_area_12,MEAN,-1,-
1,C:\Users\Candice\Documents\AOE\Survey Files\GIS\xsec_area_10,MEAN,-1,-
1,C:\Users\Candice\Documents\AOE\Survey Files\GIS\xsec_area_6,MEAN,-1,-
1,C:\Users\Candice\Documents\AOE\Survey Files\GIS\xsec_area_2,MEAN,-1,-
1,C:\Users\Candice\Documents\AOE\Survey Files\GIS\xsec_area_8,MEAN,-1,-
1,C:\Users\Candice\Documents\AOE\Survey Files\GIS\xsec_area_13,MEAN,-1,-
1,C:\Users\Candice\Documents\AOE\Survey Files\GIS\xsec_area_14,MEAN,-1,-
1;XSEC_CODE 'XSEC_CODE' true true false 2 Short 0 0
,First,#,C:\Users\Candice\Documents\AOE\Survey
Files\GIS\xsec_area_1,xsec_code,-1,-1,C:\Users\Candice\Documents\AOE\Survey
Files\GIS\xsec_area_11,xsec_code,-1,-1,C:\Users\Candice\Documents\AOE\Survey
Files\GIS\xsec_area_9,xsec_code,-1,-1,C:\Users\Candice\Documents\AOE\Survey
Files\GIS\xsec_area_7,xsec_code,-1,-1,C:\Users\Candice\Documents\AOE\Survey
Files\GIS\xsec_area_5,xsec_code,-1,-1,C:\Users\Candice\Documents\AOE\Survey
Files\GIS\xsec_area_3,xsec_code,-1,-1,C:\Users\Candice\Documents\AOE\Survey
Files\GIS\xsec_area_4,xsec_code,-1,-1,C:\Users\Candice\Documents\AOE\Survey
Files\GIS\xsec_area_12,xsec_code,-1,-1,C:\Users\Candice\Documents\AOE\Survey
Files\GIS\xsec_area_10,xsec_code,-1,-1,C:\Users\Candice\Documents\AOE\Survey
Files\GIS\xsec_area_6,xsec_code,-1,-1,C:\Users\Candice\Documents\AOE\Survey
Files\GIS\xsec_area_2,xsec_code,-1,-1,C:\Users\Candice\Documents\AOE\Survey
Files\GIS\xsec_area_8,xsec_code,-1,-1,C:\Users\Candice\Documents\AOE\Survey
Files\GIS\xsec_area_13,xsec_code,-1,-1,C:\Users\Candice\Documents\AOE\Survey
Files\GIS\xsec_area_14,XSEC_CODE,-1,-1"

```

'Adds and calculates a field containing the width of each vegetation community along each centroid

' Process: Add Field (16)...

```
gp.AddField_management xsec_areas_dbf, "Sec_len", "DOUBLE", "", "", "", "", "NON_NULLABLE", "NON_REQUIRED", ""
```

' Process: Calculate Field (17)...

```
gp.CalculateField_management xsec_areas_dbf__2_, "Sec_len", "[VALUE_1]/0.17", "VB", ""
```

'Adds and calculates a field containing the cross sectional area of each vegetation community along each centroid

' Process: Add Field (17)...

```

gp.AddField_management xsec_areas_dbf__8_, "sec_area", "DOUBLE", "", "", "",
"", "NON_NULLABLE", "NON_REQUIRED", ""

' Process: Calculate Field (18)...
gp.CalculateField_management xsec_areas_dbf__4_, "sec_area", "[Sec_len] *
[MEAN]", "VB", ""

'Calculates the total wet cross sectional area along each centroid
' Process: Summary Statistics...
gp.Statistics_analysis xsec_areas_dbf__6_, xsec_areas_sum_dbf, "sec_area
SUM", "XSEC_CODE"

'Joins the total cross sectional area to the cross sectional area table by
community
' Process: Join Field (15)...
gp.JoinField_management xsec_areas_dbf__6_, "XSEC_CODE", xsec_areas_sum_dbf,
"XSEC_CODE", "XSEC_CODE;SUM_sec_ar"

'Calculates the proportion of the total flow area for each vegetation
community
' Process: Add Field (18)...
gp.AddField_management xsec_areas_dbf__5_, "proportion", "DOUBLE", "", "",
"", "", "NON_NULLABLE", "NON_REQUIRED", ""

'Joins the width, area, and proportion variables to the new inundated
vegetation community polygon shapefile
' Process: Calculate Field (19)...
gp.CalculateField_management xsec_areas_dbf__9_, "proportion", "[sec_area] /
[SUM_sec_ar]", "VB", ""

' Process: Make Table View...
gp.MakeTableView_management xsec_areas_dbf__7_, xsec_areas_View, ""ID_NUM""
= ""XSEC_CODE"", "", "ID_NUM ID_NUM VISIBLE NONE;VALUE_1 VALUE_1 VISIBLE
NONE;MEAN MEAN VISIBLE NONE;XSEC_CODE XSEC_CODE VISIBLE NONE;'Sec_len' 'Sec_
len' VISIBLE NONE;sec_area sec_area VISIBLE NONE;XSEC_CODE XSEC_CODE VISIBLE
NONE;SUM_sec_ar SUM_sec_ar VISIBLE NONE;proportion proportion VISIBLE NONE"

' Process: Join Field (16)...
gp.JoinField_management wet_veg, "ID_num", xsec_areas_View, "XSEC_CODE",
"Sec_len;sec_area;SUM_sec_ar;proportion"

```

File Creator Step 3

```

' -----
' step 3.vbs
' Created on: Fri Mar 12 2010 09:31:45 AM
' (generated by ArcGIS/ModelBuilder)
' -----

' Create the Geoprocessor object
set gp = WScript.CreateObject("esriGeoprocessing.GPDispatch.1")

' Load required toolboxes...

```

```

gp.AddToolbox "C:/Program Files (x86)/ArcGIS/ArcToolbox/Toolboxes/Data
Management Tools.tbx"

' Creates the temporary files used in the processes
' Local variables...
wet_veg = "wet_veg"
wet_veg__25_ = "wet_veg"
wet_veg__23_ = "wet_veg"
Hedge_veg_data_csv = "Hedge veg data.csv"
wet_veg_tester__3_ = "wet_veg"
wet_veg__6_ = "wet_veg"
wet_veg__7_ = "wet_veg"
wet_veg__24_ = "wet_veg"
wet_veg__5_ = "wet_veg"
wet_veg__11_ = "wet_veg"
wet_veg__9_ = "wet_veg"
wet_veg__10_ = "wet_veg"
wet_veg__13_ = "wet_veg"
wet_veg__12_ = "wet_veg"
wet_veg__14_ = "wet_veg"
wet_veg__18_ = "wet_veg"
wet_veg__15_ = "wet_veg"
wet_veg__17_ = "wet_veg"
wet_veg__19_ = "wet_veg"
wet_veg__20_ = "wet_veg"
wet_veg__16_ = "wet_veg"
wet_veg__21_ = "wet_veg"
wet_veg__22_ = "wet_veg"
wet_veg__2_ = "wet_veg"
wet_veg__4_ = "wet_veg"
wet_veg__8_ = "wet_veg"
communities = "communities"
communities__2_ = "communities"
comm_out_shp = "C:\Users\Candice\Documents\AOE\Survey Files\GIS\comm_out.shp"

'Calculates the velocity in each community based on the proportion of the
cross-sectional area
' Process: Add Field...
gp.AddField_management wet_veg__2_, "Velocity", "DOUBLE", "", "", "", "",
"NON_NULLABLE", "NON_REQUIRED", ""

' Process: Calculate Field...
gp.CalculateField_management wet_veg, "Velocity", "[proportion] *0.0673",
"VB", ""

'Adds empty fields for maa-d, average d, Restem, f, and K
' Process: Add Field (2)...
gp.AddField_management wet_veg__25_, "MAAd", "DOUBLE", "", "", "", "",
"NON_NULLABLE", "NON_REQUIRED", ""

' Process: Add Field (3)...
gp.AddField_management wet_veg__6_, "avg_d", "DOUBLE", "", "", "", "",
"NON_NULLABLE", "NON_REQUIRED", ""

' Process: Add Field (4)...

```

```

gp.AddField_management wet_veg__7_, "Restem", "DOUBLE", "", "", "", "",
"NON_NULLABLE", "NON_REQUIRED", ""

' Process: Add Field (5)...
gp.AddField_management wet_veg__19_, "K", "DOUBLE", "", "", "", "",
"NON_NULLABLE", "NON_REQUIRED", ""

' Process: Add Field (6)...
gp.AddField_management wet_veg__20_, "f", "DOUBLE", "", "", "", "",
"NON_NULLABLE", "NON_REQUIRED", ""

'Joins the vegetation data table to the inundated vegetation community
shapefile
' Process: Add Join...
gp.AddJoin_management wet_veg__22_, "Comm_ID", Hedge_veg_data_csv, "Comm_ID",
"KEEP_ALL"

'Selects communities with average depths less than 10 cm
' Process: Select Layer By Attribute...
gp.SelectLayerByAttribute_management wet_veg__23_, "NEW_SELECTION",
"" "wet_veg.MEAN" >= 0 AND "" "wet_veg.MEAN" <0.1"

'Calculates maa-d and average d for communities with average depths less than
10 cm
' Process: Calculate Field (2)...
gp.CalculateField_management wet_veg_tester__3_, "wet_veg.MAAd",
"[MAAd_0_01]", "VB", ""

' Process: Calculate Field (3)...
gp.CalculateField_management wet_veg__24_, "wet_veg.avg_d", "[d_0_01]", "VB",
""

'Selects communities with average depths less than 20 cm and greater than 10
cm
' Process: Select Layer By Attribute (2)...
gp.SelectLayerByAttribute_management wet_veg__5_, "NEW_SELECTION",
"" "wet_veg.MEAN" >=0.1 AND "" "wet_veg.MEAN" <0.2"

'Calculates maa-d and average d, for communities with average depths less
than 20 cm and greater than 10 cm
' Process: Calculate Field (4)...
gp.CalculateField_management wet_veg__11_, "wet_veg.MAAd", "[MAAd_01_02]",
"VB", ""

' Process: Calculate Field (5)...
gp.CalculateField_management wet_veg__9_, "wet_veg.avg_d", "[d_01_02]", "VB",
""

'Selects communities with average depths less than 30 cm and greater than 20
cm
' Process: Select Layer By Attribute (3)...
gp.SelectLayerByAttribute_management wet_veg__10_, "NEW_SELECTION",
"" "wet_veg.MEAN" >=0.2 AND "" "wet_veg.MEAN" <0.3"

'Calculates maa-d and average d, for communities with average depths less
than 30 cm and greater than 20 cm

```

```

' Process: Calculate Field (6)...
gp.CalculateField_management wet_veg__13_, "wet_veg.MAAAd", "[MAAd_02_03]",
"VB", ""

' Process: Calculate Field (7)...
gp.CalculateField_management wet_veg__12_, "wet_veg.avg_d", "[d_02_03]",
"VB", ""

'Selects communities with average depths less than 40 cm and greater than 30
cm
' Process: Select Layer By Attribute (4)...
gp.SelectLayerByAttribute_management wet_veg__14_, "NEW_SELECTION",
"" "wet_veg.MEAN" >=0.3"

'Calculates maa-d and average d, for communities with average depths less
than 40 cm and greater than 30 cm
' Process: Calculate Field (8)...
gp.CalculateField_management wet_veg__18_, "wet_veg.MAAAd", "[MAAd_03p]",
"VB", ""

' Process: Calculate Field (9)...
gp.CalculateField_management wet_veg__15_, "wet_veg.avg_d", "[d_03_04]",
"VB", ""

'Selects communities with average depths greater than 40 cm
' Process: Select Layer By Attribute (5)...
gp.SelectLayerByAttribute_management wet_veg__17_, "NEW_SELECTION",
"" "wet_veg.MEAN" >0"

'Calculates maa-d and average d, for communities with average depths greater
than 40 cm
' Process: Calculate Field (10)...
gp.CalculateField_management wet_veg__4_, "wet_veg.Restem",
"[wet_veg.Velocity] * [wet_veg.avg_d] /0.000001", "VB", ""

'Calculates f and K
' Process: Calculate Field (11)...
gp.CalculateField_management wet_veg__16_, "wet_veg.f", "95499.2586 *
[wet_veg.MAAAd]^0.47 * [wet_veg.Restem]^-1.52", "VB", ""

' Process: Calculate Field (12)...
gp.CalculateField_management wet_veg__21_, "wet_veg.K", "8*9.81*
[wet_veg.MEAN]/( [wet_veg.f]* [wet_veg.Velocity])", "VB", ""

' Process: Add Join (2)...
gp.AddJoin_management communities__2_, "Comm_ID", wet_veg__8_,
"wet_veg.Comm_ID", "KEEP_ALL"

'Copies new calculations to a new shapefile called Comm_out
' Process: Copy Features...
gp.CopyFeatures_management communities, comm_out_shp, "", "0", "0", "0"

```

File Creator Step 4

```
' -----  
' step 4.vbs  
' Created on: Fri Mar 12 2010 09:32:02 AM  
'   (generated by ArcGIS/ModelBuilder)  
' Usage: step 4 <ksat_surf_txt> <vcont_txt> <wet_depth> <lay_1_head>  
<shead_L1__TXT> <shead_L2__TXT> <lay_2_head> <drain_head>  
' -----  
  
' Create the Geoprocessor object  
set gp = WScript.CreateObject("esriGeoprocessing.GPDispatch.1")  
  
' Check out any necessary licenses  
gp.CheckOutExtension "spatial"  
  
' Load required toolboxes...  
gp.AddToolbox "C:/Program Files (x86)/ArcGIS/ArcToolbox/Toolboxes/Spatial  
Analyst Tools.tbx"  
gp.AddToolbox "C:/Program Files (x86)/ArcGIS/ArcToolbox/Toolboxes/Conversion  
Tools.tbx"  
  
' Set the Geoprocessing environment...  
gp.extent = "3524437.24588055 2161618.16159737 3524481.74588055  
2161695.16159737"  
gp.cellSize = "0.5"  
  
' Script arguments...  
ksat_surf_txt = wscript.arguments.item(0)  
if ksat_surf_txt = "#" then  
  ksat_surf_txt = "C:\Users\Candice\Documents\AOE\Survey Files\GIS\ASCII  
Outputs\ksat_surf.txt" ' provide a default value if unspecified  
end if  
  
vcont_txt = wscript.arguments.item(1)  
if vcont_txt = "#" then  
  vcont_txt = "C:\Users\Candice\Documents\AOE\Survey Files\GIS\ASCII  
Outputs\vcont.txt" ' provide a default value if unspecified  
end if  
  
wet_depth = wscript.arguments.item(2)  
if wet_depth = "#" then  
  wet_depth = "wet_depth" ' provide a default value if unspecified  
end if  
  
lay_1_head = wscript.arguments.item(3)  
if lay_1_head = "#" then  
  lay_1_head = "initial_ws" ' provide a default value if unspecified  
end if  
  
shead_L1__TXT = wscript.arguments.item(4)  
if shead_L1__TXT = "#" then
```

```

    shead_L1__TXT = "C:\Users\Candice\Documents\AOE\Survey Files\GIS\ASCII
Outputs\shead_L1_.TXT" ' provide a default value if unspecified
end if

shead_L2__TXT = wscript.arguments.item(5)
if shead_L2__TXT = "#" then
    shead_L2__TXT = "C:\Users\Candice\Documents\AOE\Survey Files\GIS\ASCII
Outputs\shead_L2_.TXT" ' provide a default value if unspecified
end if

lay_2_head = wscript.arguments.item(6)
if lay_2_head = "#" then
    lay_2_head = "head_l2" ' provide a default value if unspecified
end if

drain_head = wscript.arguments.item(7)
if drain_head = "#" then
    drain_head = "C:\Users\Candice\Documents\AOE\Survey Files\GIS\drain_head" '
provide a default value if unspecified
end if

' Creates the temporary files used in the processes
' Local variables...
surface_K = "C:\Users\Candice\Documents\AOE\Survey Files\GIS\surface_K"
vcont = "C:\Users\Candice\Documents\AOE\Survey Files\GIS\vcont"
comm_out = "comm_out"
vcont_div1 = "C:\Users\Candice\Documents\AOE\Survey Files\GIS\vcont_div1"
thkns_L2 = "C:\Users\Candice\Documents\AOE\Survey Files\GIS\thkns_L2"
bottom_l2 = "bottom_l2"
vcont_div2 = "C:\Users\Candice\Documents\AOE\Survey Files\GIS\vcont_div2"
ksat_lay2 = "ksat_lay2"
vcont_div = "C:\Users\Candice\Documents\AOE\Survey Files\GIS\vcont_div"
Input_raster_or_constant_value_1__2_ = "2"
L1_isnull = "C:\Users\Candice\Documents\AOE\Survey Files\GIS\L1_isnull"
shead_L1 = "C:\Users\Candice\Documents\AOE\Survey Files\GIS\shead_L1"
IsNull_vcont = "C:\Users\Candice\Documents\AOE\Survey Files\GIS\IsNull_vcont"
vcont_l2 = "C:\Users\Candice\Documents\AOE\Survey Files\GIS\vcont_l2"
Input_raster_or_constant_value_1 = "1"
vcont_L1 = "C:\Users\Candice\Documents\AOE\Survey Files\GIS\vcont_L1"
drain_loc = "drain_loc"

'Converts the polygons to a raster coverage of K
' Process: Polygon to Raster...
gp.PolygonToRaster_conversion comm_out, "wet_veg_K", surface_K,
"CELL_CENTER", "NONE", "0.5"

'Converts the raster K coverage to an ASCII file for input to MODFLOW
' Process: Raster to ASCII...
gp.RasterToASCII_conversion surface_K, ksat_surf_txt

'Calculates vcont based on the K and thickness of layers 1 and 2
' Process: Divide...
gp.Divide_sa wet_depth, surface_K, vcont_div1

' Process: Minus...
gp.Minus_sa lay_2_head, bottom_l2, thkns_L2

```

```

' Process: Divide (3)...
gp.Divide_sa thkns_L2, ksats_L2, vcont_div2

' Process: Plus (2)...
gp.Plus_sa vcont_div1, vcont_div2, vcont_div

' Process: Divide (2)...
gp.Divide_sa Input_raster_or_constant_value_1__2_, vcont_div, vcont

' Process: Is Null (2)...
gp.IsNull_sa vcont, IsNull_vcont

' Process: Divide (4)...
gp.Divide_sa Input_raster_or_constant_value_1, vcont_div2, vcont_L2

' Process: Con (2)...
gp.Con_sa IsNull_vcont, vcont, vcont_L1, vcont_L2, "VALUE =0"

'Converts the raster vcont coverage to an ASCII file for input to MODFLOW
' Process: Raster to ASCII (2)...
gp.RasterToASCII_conversion vcont_L1, vcont_txt

'Creates shead raster for layer 1
' Process: Is Null...
gp.IsNull_sa lay_1_head, L1_isnull

' Process: Con...
gp.Con_sa L1_isnull, lay_1_head, shead_L1, lay_2_head, "VALUE = 0"

'Converts the raster shead1 coverage to an ASCII file for input to MODFLOW
' Process: Raster to ASCII (3)...
gp.RasterToASCII_conversion shead_L1, shead_L1__TXT

'Converts the raster shead2 coverage to an ASCII file for input to MODFLOW
' Process: Raster to ASCII (4)...
gp.RasterToASCII_conversion lay_2_head, shead_L2__TXT

```